

# Application of a non-linear temperature forecast post-processing technique for the optimization of powdery mildew protection on strawberry

Emanuele Eccel<sup>1</sup>, Stefano Fratton<sup>1</sup>, Luca Ghielmi<sup>1</sup>, Andrea Tizianel<sup>1</sup>, Dani Shtienberg<sup>2</sup>, Ilaria Pertot<sup>1</sup>

**Abstract:** Strawberry powdery mildew, caused by the fungus *Podosphaera aphanis*, is a dangerous disease in warm and dry climates as well as in greenhouses or plasticulture. Plant protection against *P. aphanis* is mainly based on chemical fungicides. More than ten chemical treatments for each growing cycle are often applied in tunnel strawberry production in northern Italy. SafeBerry is a decision support system, which optimises, and often reduces, the use of chemicals against this disease. The system is based on a correct fungicide application based on the disease risk level in each tunnel and on the specific action mechanism of the fungicides. The level of risk is based on crop and environmental parameters. The temperature assessment and its forecast represent two key points in the system. The decision-making procedure uses day-time temperatures forecasted for the three following days. They were calculated by post-processing of the operational weather model output (Model Output Statistics, MOS). MOS was carried out for three sites with a "machine learning", multivariate, non-linear technique ("Random Forest"), which uses many meteorological predictors. With this system in 2007 we obtained a strong reduction in the number of treatments (up to 60%).

**Keywords:** pesticide, fungicide, integrated pest management, MOS, temperature downscaling

**Riassunto:** L'oidio della fragola, causato dal fungo *Podosphaera aphanis* è una malattia molto dannosa in climi caldi e asciutti o nella coltivazione protetta in tunnel o in serra. La difesa nei confronti di *P. aphanis* si ottiene principalmente con l'uso di fungicidi chimici. Nelle colture in tunnel dell'Italia settentrionale, sono effettuati spesso anche più di dieci trattamenti per ciclo produttivo. SafeBerry è un sistema di supporto alle decisioni per l'agricoltore che permette l'ottimizzazione e, spesso, la riduzione dei fungicidi antiodioidici. Si basa su una loro corretta applicazione in funzione del livello di rischio di malattia nel singolo tunnel e del meccanismo d'azione dello specifico fungicida. Il livello di rischio è stimato sulla base di alcuni parametri culturali ed ambientali. Il rilievo della temperatura, come la sua previsione, rappresentano due punti chiave del sistema. La procedura decisionale impiega le temperature medie diurne attese per i tre giorni successivi; queste sono state calcolate mediante post-elaborazione (Model Output Statistics - MOS) di output di modello meteorologico operativo. Il MOS è stato condotto per tre località con una tecnica non lineare multivariata di "machine learning" del tipo "foresta stocastica" ("Random Forest") prendendo in considerazione molti predittori meteorologici. Con l'uso del sistema nel 2007 si è potuto avere una consistente riduzione dei trattamenti (fino al 60%).

**Parole chiave:** agrofarmaci, fungicidi, lotta integrata, MOS, downscaling di temperatura

## INTRODUCTION

Powdery mildew (PM) of strawberry, caused by *Podosphaera aphanis*, is a dangerous disease in the Mediterranean climate or greenhouses and polyethylene tunnels. The pathogen can attack all the aerial part of the plant, flowers and fruits included, and cause high economic losses especially on the most susceptible cultivars (Amsalem *et al.*, 2006). Plant protection is based on the application of chemical fungicides. In northern Italy (Trentino region) strawberries are mainly produced in high polyethylene tunnels on peat in suspended pots. Under tunnel conditions up to 10-12 fungicide treatments are often applied by growers in order to

protect plants. A reduction of pesticides can be obtained with an optimization of their use, which consists in applying them when they can reach the highest efficacy and in the selection of the most suitable fungicide according to its mechanism of action against the disease (Pertot *et al.*, 2008). Decision support systems may help in optimizing treatments in agriculture (Madden and Ellis, 1988). We developed a decision support system (SafeBerry) based on plant, pathogen, efficacy and mechanism of action of fungicides and both on past (measured) and future (forecasted) temperature. In order to make available a calibrated temperature forecast for the sites involved in this work, we applied a "Model Output Statistics" (MOS) to the meteorological model output. Indeed, local topography is ill-represented by general circulation models, due to the coarse grid used (scores of km). Hence, in an Alpine territory, orography strongly affects the goodness of

\* Corresponding author e-mail: emanuele.eccel@iasma.it

<sup>1</sup> Fondazione Edmund Mach – Centro Ricerca e Innovazione, S. Michele all'Adige (TN) Italy.

<sup>2</sup> Department of Plant Pathology, The Volcani Center, Bet Dagan, Israel.

the representation of true elevation of sites, with errors up to 1000 m at some model grid points, resulting in errors as large as 4–6 °C in temperature forecasts, the latter figures representing mean biases of estimation. This effect is particularly evident in the case of deep valleys such as Adige Valley, which is one of the largest in the Alps in terms of both length and depth.

Several approaches have been proposed to downscale temperature predictions from the raw (direct) model output (DMO) to the calibrated values. Not only do such algorithms allow to cope with the different elevation of sites with respect to the model orography, but they also improve the forecast by post-processing DMO with many predictors, other than the predicted temperature itself. The problem can be simply tackled by use of univariate methods as, for example, the application of site-specific offsets (fixed or seasonal) or Kalman filter techniques (Homleid, 1995; Galanis and Anadranistakis, 2002; Anadranistakis *et al.*, 2004; Cane *et al.*, 2004). Although univariate methods have been well tested, multivariate methods have the potential for modelling the influence of both properties of the site and prognostics provided by meteorological models. Among these techniques, non-linear, "machine learning" algorithms, proved suitable for this task (Schizas *et al.*, 1991; Abdel-Aal and Elhadidy, 1994; Robinson and Mort, 1997; Arca *et al.*, 1998; Verdes *et al.*, 2000; Basili *et al.*, 2006). Experiences in Trentino have shown that non-linear, multivariate techniques, namely "Random Forest" algorithm, do improve temperature forecast with respect to univariate methods (Eccel *et al.*, 2007). The main objective of this work was to test the goodness of the coupling of a 3-day temperature forecast method to the application of SafeBerry.

## MATERIALS AND METHODS

### The decision support system

The decision-making procedure in SafeBerry is comprised of three major steps: the determination of the risk of disease outbreak, the suitability of temperature to the disease and the recommendation of action. The potential risk index for the disease is the result of the integration of a basic risk index, which includes the risk factors that do not vary in the season, and the daily risk index, which includes the risk factors that vary on daily base. The risk factors were identified and quantified by interviewing growers and technicians and by searching literature. Each risk factor was rated in levels and risk points were empirically attributed to each level. The risk factors included in the basic risk index are: cultivar

susceptibility, presence of disease at less than 50 or 10 m at planting day, incidence of PM in the nursery where plants were grown, type of sprayer, overhead irrigation (sprinkler-cooling), tunnel height, density of plants per meter, mulching with black plastic. The risk factors included in the daily risk index are: phenological stage of the plants, disease incidence in the tunnel, time of disease onset, presence of disease in less than 10 m, time since last treatment, presence of runners.

Even in cases where the level of potential risk is high, its realization depends on the existence of a disease-conducive environment. We used a model that describes the relationship between day-time temperature (DTT; average between 5:00 and 17:00) and the rate of PM development (daily disease increase) and it is based on data collected in experiments in Trentino (northern Italy) from 1999 to 2003. Suitability of the weather to PM development is divided into three categories: low suitability (LS;  $DTT \leq 18^{\circ}C$  or  $DTT > 26^{\circ}C$ ) when temperature is expected to limit PM development; medium suitability (MS;  $18^{\circ}C < DTT \leq 20^{\circ}C$  or  $25^{\circ}C < DTT \leq 26^{\circ}C$ ) when temperature is suitable for PM development; and high suitability (HS;  $20^{\circ}C < DTT \leq 25^{\circ}C$ ) when temperature is highly conducive for PM development. The daily disease increase is based on DTT in the previous six days (measured) and in the next three days (forecasted).

In the last step of SafeBerry, the potential risk and the likelihood of its realization (suitability of the temperature to the disease) are integrated by taking into account the phenological stage of the crop and finally a recommendation for action is given. The possible recommendations for action are: "Do not spray today," and "Spray as soon as possible." In the latter case, a list of preferable fungicides is recommended according their mechanism of action, risk of developing resistance to the pathogen and restriction on time of application before harvest.

### The investigation area

The pilot area for this investigation is located in Trentino region, northern Italy. Three locations were chosen in the neighbourhood of meteorological stations within important strawberry growing areas; two are located in the lowest part of Valsugana valley (Pergine Valsugana, 460 m a.s.l. and Borgo, 420 m a.s.l.) while a third (Baselga di Pinè) is in a highland, at 950 m a.s.l.

SafeBerry was evaluated in five experiments carried out in 2007 at the same three locations (Baselga, Pergine1, Pergine2, Borgo1 and Borgo2). The

cultivar was Elsanta, which is the most widely used by strawberry growers in this area and is highly susceptible to PM. Strawberry plants were planted in peat, in suspended pots in rows in walk-in plastic tunnels and treated according to SafeBerry recommendation. Untreated control was included. Treatments were arranged in a randomized complete block design with four replicates. Each plot contained 24 potted plants (six plants/pot  $\times$  four pots). The fungicides were applied using a gun sprayer. To avoid any drift to adjacent plots, untreated plots were covered with polyethylene film during spraying. Plants in untreated plots were inspected visually starting at planting and continuing at three to five day intervals until disease onset, after which point disease was assessed in all plots on a weekly basis. 40 randomly chosen leaves were inspected per replicate. For each replicate, disease incidence on leaves (percentage of infected leaves) was determined. Incidence was arcsin-transformed before ANOVA to obtain homogeneity of variance (Levene's test). Statistical analyses were performed using the Statistica software 6.0 (Statsoft, Tulsa, OK, USA).

### **Downscaling temperature prediction**

A MOS approach was used to downscale temperature forecast, which is available daily from the meteorological model. In the MOS approach, relationships are obtained by using the model outputs as predictors (*e.g.*, temperature forecasts at different grid points at a given lead time), and measured quantities as predictands – in this case, temperature at the chosen sites at the same times. This approach also takes into account offsets that are intrinsic to the model itself, by applying non-linear functions to correct systematic, grid-point-specific biases.

For temperature forecast processing ECMWF's operational meteorological model "T511 L60" was used (60 vertical levels,  $0.5^\circ$  horizontal resolution). The nine grid points surrounding the target area were chosen. The operational run at 00 UTC was chosen in the 6-hourly outputs (at daily times 00, 06, 12 and 18) till +72 hours from issue. The absence of a suitable calibration period for the present operational release of ECMWF's model ("T799 L91" - 91 vertical levels,  $0.25^\circ$  horizontal resolution) lead us to develop the MOS with the previous version, even considering that previous grid points are available also in the latest version. In a previous experience in the same area, using the same model outputs as predictors, different approaches were tested for temperature prediction, limited to morning minimum at 06 UTC (Eccel *et*

*al.* 2007). The investigation had pointed out that non-linear methods, as artificial neural networks or Random Forest, performed better than simple bias corrections or linear models for output post-processing. The latter experience suggested to apply Random Forest to perform the MOS of GCM output. The freeware R (package "RandomForest"; Liaw and Wiener, 2005) was used. Some features of RF algorithm are given; for more details, refer to the abovementioned work and to Breiman (2001). RF model is a non-linear, multivariate regressive method that can be comprised in the "machine learning" category of algorithms, to which "artificial neural networks" also belong. It is only moderately prone to overfitting (Breiman, 2001) and, under this aspect, it is preferable to neural networks. RF model yields an ensemble processing, pooling several variables for the calculation of the predictands. In detail, having identified an optimal set of predictors (by means of a selection of an even high number of potential variables), RF performs the MOS by running a series of decision trees. A regression tree (Breiman *et al.*, 1984) consists of a set of nodes that branch out from a root node. Each node contains a question with several possible answers, each leading either to another node or a "leaf" (a terminal node with an associated prediction). At each branch in every tree the values of prediction variables are considered and consequently the direction of the "decision flux" is determined, based on the fulfilment (or not) of given logical conditions on predictors, and according to the conformation taken by each individual tree during the "training" stage. At every node, the vector of predictors drives the choice through different branches to the final result (a "leaf"); such operation is carried out on each tree in the same way. In general, the prediction stemming by individual trees is strongly inaccurate; on the contrary, the value obtained averaging results from all trees (1000 in this application) yields a stable prediction, with a limited variance (Geman *et al.*, 1992). In this application a RF model was created and calibrated for every lead time (00, 06, 12, 18).

### **Obtaining day-time values**

Having obtained the predictions for the four synoptic lead times, hourly values are calculated via interpolation after a refined version of the "TM" model (Cesaraccio *et al.*, 2001). The latter needs fixing expected times of occurrences of maximum and minimum temperatures; these parameters were set with a preliminary analysis. Curves are traced with four analytical functions, each one valid in a

	Mean	Mean Apr.–Sept.	Max (+)	Max (-)	25 <sup>th</sup> percent.	75 <sup>th</sup> percent.
Baselga di Piné	0.15	0.27	6.3	-3.3	-0.6	0.8
Pergine	0.72	0.63	6.5	-2.4	0.0	1.4
Borgo	0.84	0.63	5.9	-2.9	0.1	1.5

**Tab. 1** – Statistics of errors for the day-time temperature predictions over three days. Values in °C. Mean: mean of errors. Mean Apr.-Sept.: mean limited to the period April – September. Max (+): maximum of positive errors. Max (-): maximum of negative errors. 25<sup>th</sup> (75<sup>th</sup>) percent.: values of the 25<sup>th</sup> (75<sup>th</sup>) percentile.

*Tab. 1 – Statistica degli errori per la previsione delle temperature diurne su tre giorni. Valori in °C. Mean: media degli errori. Mean Apr.-Sept.: media limitata al periodo aprile – settembre. Max (+): massimo degli errori positivi. Max (-): massimo degli errori negativi. 25<sup>th</sup> (75<sup>th</sup>) percent.: valori del 25° (75°) percentile.*

given time range. Being  $H_{\min}$  and  $H_{\max}$  times when minimum and maximum temperatures are expected, respectively, the functions are defined in the following ranges:

1. from 00 UTC to  $H_{\min}$  – parabolic
2. from  $H_{\min}$  to  $H_{\max}$  – sinusoidal
3. from  $H_{\max}$  to 18 – sinusoidal
4. from 18 UTC to 24 UTC - parabolic.

Details on the equations of the interpolating curves are given in the Appendix.

The routine calculates hourly values until time +72 h, by an iterative application of the equations valid for the first 24 hours. Then, hourly values are averaged between 05 and 17 of every day to get day-time values, which are used by SafeBerry.

### Comparison of temperatures suitable to the disease in the next three days (measured vs. forecasted)

Temperatures suitable for the disease in the following three days were calculated and rated according to three classes: HS, MS and LS, both on measured and forecasted temperatures, and the two series compared. Differences were expressed as ± 1-2 classes of distance.

## RESULTS

### Temperature MOS

Implementation of RF required the set-up of the maximum number of predictors for each tree; in general, the total number of predictors is high, while the algorithm is optimised with a limited number of predictors at once, chosen at random from the pool. Usually, the improvement becomes negligible with more than 10 - 20 predictors. The latter were selected, in each trial, from a larger set. The routines available in the package RandomForest were used to select the relative importance of variables and hence the set of predictors. Beyond the output of meteorological model, in each of the grid points, the following variables were taken into account:

- temperatures at 00, 06, 12, and 18 UTC of the previous day;
- forecast errors of the previous three days, for every grid point;
- night length.

The potentially useful variables, for every lead time (00, 06, 12 e 18 UTC), are:

- ECMWF's output (24), for each of 9 grid points;
- temperature measured at every station in the following day;
- forecast errors for every grid point for each of the previous days;
- night length (only for prediction of temperature at 06 UTC).

As a whole, predictors had to be chosen among 245 variables, over a time span of +3 days from every weather forecast issue, and identically replicating in the following three days for every synoptic lead time. The most impacting variables proved to be (beyond the trivial DMO of temperature at 2 m): temperatures predicted for the previous day at the same times, dew temperatures, night length (for forecast at 06 UTC), temperature at different atmospheric levels (geopotential heights), and humidity at 850 hPa. The presence of the temperature forecast at 2 m for more than one grid point among the predictors, shows their independent contributions.

The accuracy of forecast was assessed with conventional error statistics. Errors arise from the sum of a meteorological forecast error (in turn, sum of a meteorological model error and a MOS error) and one due to the hourly interpolation. For the single day-time averages over the three-day forecast period, in about one year of simulations errors were assessed in the range of ± 0.1°C (mean error), 1.5°C-1.7°C (standard error, or RMSE), and 1.1°C-1.3°C (mean absolute error). Errors ranged between -3.3°C (Baselga) and +6.5°C (Pergine). The latter values are rather high; however, the cases with large errors are restricted to limited periods, and they occurred mostly in the first part of the trial



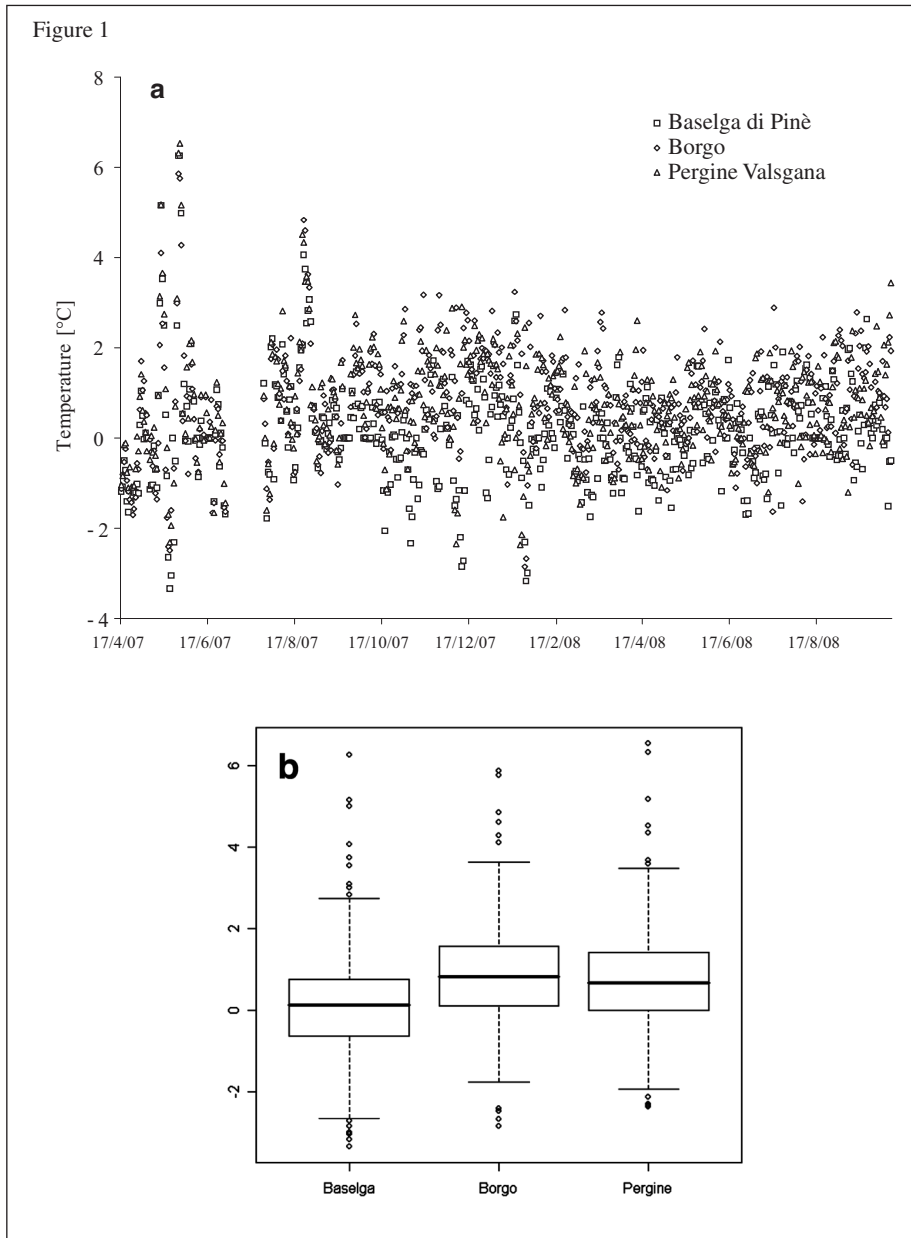


**Fig. 1 –** Errors of estimate of temperature by the meteorological model downscaled to sites by MOS technique: daily difference between predicted and measured temperature, day-time means (05 AM – 05 PM solar time). a) time series. b) boxplot.

*Fig. 1 – Errori di stima della temperatura da parte del modello meteorologico post-elaborato con tecnica MOS: differenza giornaliera tra temperatura prevista e misurata, medie diurne (ore 05 – 17 solari). a) serie temporale. b) boxplot.*

(Fig. 1), while in general the inter-quantile range of errors (IQR) is lower than 1.6°C (Pergine), with mean errors lower than 0.9°C (Tab. 1).

#### Temperature suitable for powdery mildew

The highest number of measured days with temperature suitable for the disease during the growing cycle was in Pergine1 (48.9%) followed by Baselga (33.8%), Borgo1 (21.2%), Borgo2 (17.6%) and Pergine2 (14.7%) (Fig. 2). These results indicate that in 2007 between June and July, which is the central part of the growing season in Trentino, temperature was highly conducive to PM. Therefore strawberry

growing cycles starting at the end of June- beginning of July had a high component in the risk of infection related to the weather. In Baselga and Pergine1 the suitability of the measured temperature to the disease was initially low, then increased in the last part of the growing cycle; the disease incidence increased very quickly in the period with temperatures highly suitable for the disease. In the last part of the season a low suitability of temperature was related to a steady disease development in the late stage. In fact in Pergine2 and Borgo2 the suitability of temperature to the disease was initially high and then became low for the second part of the growing cycle; the disease

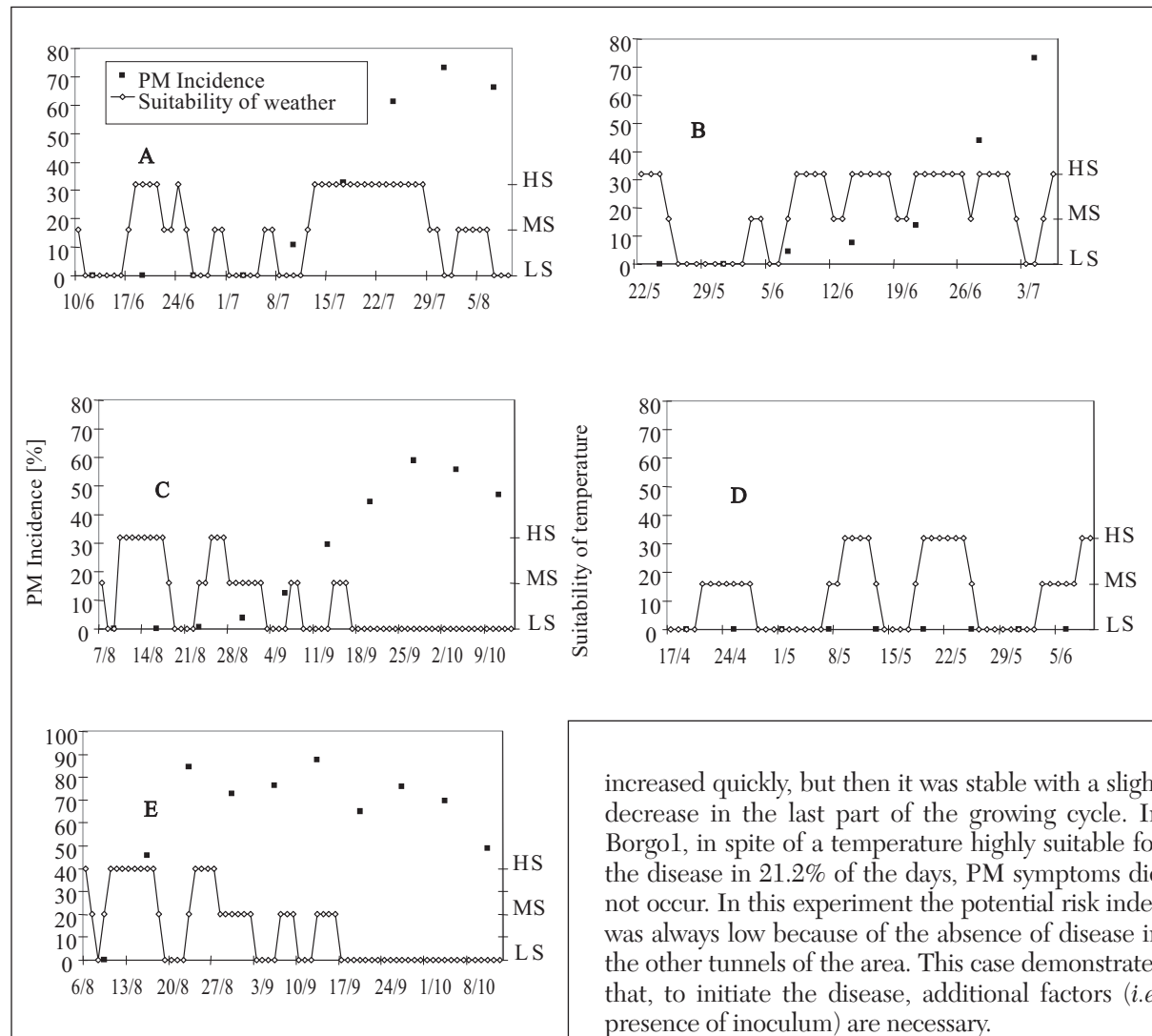


**Fig. 2** – Powdery mildew (PM) incidence (percentage of infected leaves) on untreated strawberry leaves in 2007 in five experiments (four replicates/each) in Trentino region: Baselga (A), Pergine1 (B), Pergine2 (C), Borgo1 (D) and Borgo2 (E). 40 randomly chosen leaves per replicate were assessed weekly. Suitability of temperature was calculated for each day, based on average temperature measured between 05 AM and 05 PM solar time, and ranked in three classes (low, medium, high - DTT  $\leq$  18°C or DTT  $>$  26°C = LS; 18°C < DTT  $\leq$  20°C or 25°C < DTT  $\leq$  26°C = MS; 20°C < DTT  $\leq$  25°C = HS).

Fig. 2 – Attacchi oidici (percentuale di foglie infette) su foglie di fragola non trattata nel 2007 in cinque esperimenti (quattro repliche ognuno) in Trentino: Baselga (A), Pergine1 (B), Pergine2 (C), Borgo1 (D) e Borgo2 (E). Per ogni replica sono state scelte a caso settimanalmente 40 foglie. Il potenziale ai fini infettivi della temperatura è stato calcolato giornalmente, in base alla temperatura media misurata tra le 5 e le 17 (ora solare) e classificato in tre livelli: basso, medio e alto (DTT  $\leq$  18°C o DTT  $>$  26°C = LS; 18°C < DTT  $\leq$  20°C o 25°C < DTT  $\leq$  26°C = MS; 20°C < DTT  $\leq$  25°C = HS)

increased quickly, but then it was stable with a slight decrease in the last part of the growing cycle. In Borgo1, in spite of a temperature highly suitable for the disease in 21.2% of the days, PM symptoms did not occur. In this experiment the potential risk index was always low because of the absence of disease in the other tunnels of the area. This case demonstrates that, to initiate the disease, additional factors (*i.e.* presence of inoculum) are necessary.

The suitability of temperature to the disease based on forecasted DTT compared to measured DTT was satisfactory: in Baselga di Pinè the forecasted DTT was correct in 89.9% of the days; it was overestimated by two and one level respectively in 1.3 and 8.7% of the days (17<sup>th</sup> April – 31<sup>st</sup> October 2007) and underestimated by one level in 8.1% of the days. In Pergine Valsugana the forecasted DTT was correct in 74.7% of the days; it was overestimated by two and one level respectively in 4.4 and 14.6% of the days, and underestimated by one level in 6.3% of the days. In Borgo the forecasted DTT was correct in 71.1% of the days; it was overestimated and underestimated by one level in 12.0 and 16.9% of the days, respectively (Fig. 3).

#### Optimization of treatments with SafeBerry

No symptoms of the disease were seen in Borgo1 during the growing cycle. In all the other experiments the incidence of the disease on leaves was significantly

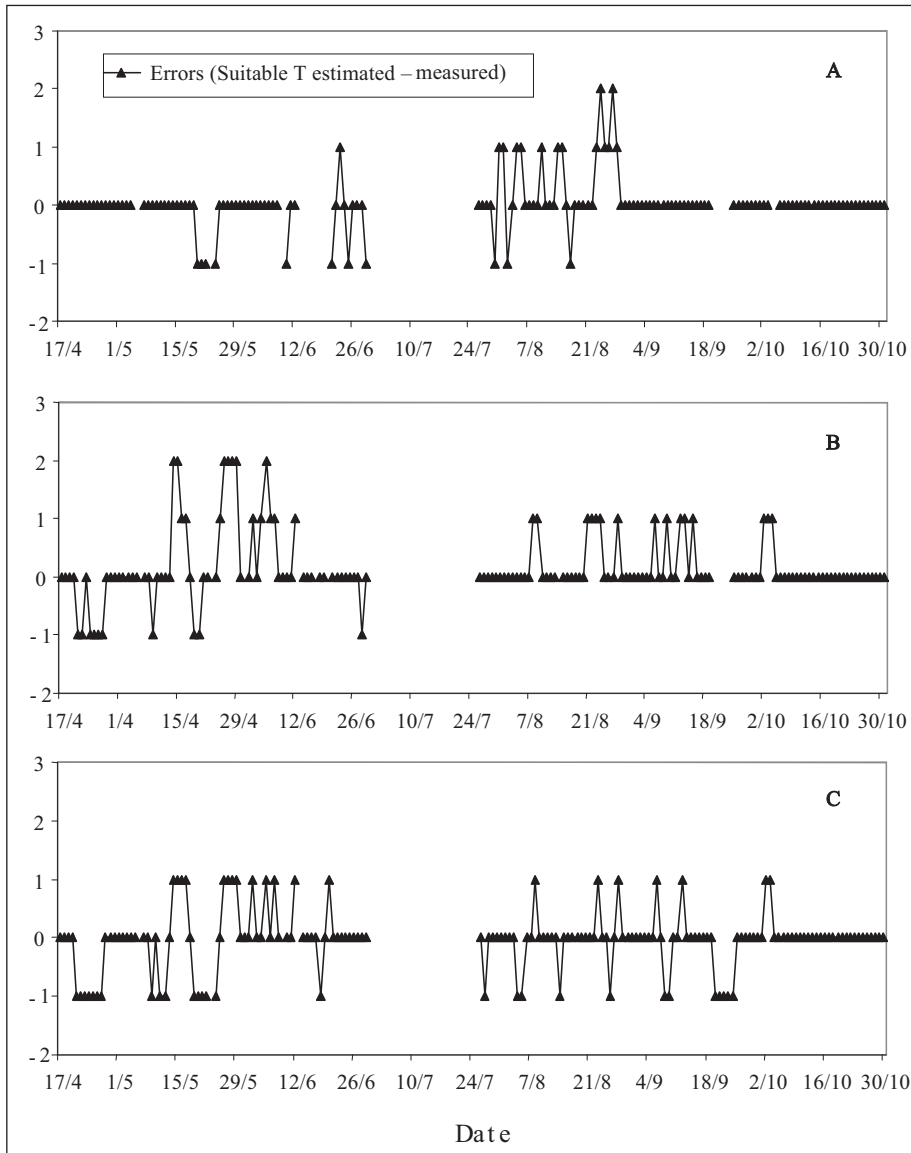


**Fig. 3 – Errors calculated as difference between levels of suitability of temperature ( $T$ ) to powdery mildew calculated on forecasted and measured day-time temperature in the three locations of meteorological downscaling and measurement in Trentino region in 2007: Baselga di Piné (A), Pergine Valsugana (B), Borgo (C).**

**Fig. 3 – Errori calcolati come differenza tra livelli di temperatura ( $T$ ) favorevoli o meno allo sviluppo dell'oidio valutate su temperatura diurna prevista e misurata nei tre siti di previsione meteorologica (downscalata) e misura del Trentino nel 2007: Baselga di Piné (A), Pergine Valsugana (B), Borgo (C).**

reduced in plots managed according to SafeBerry's recommendation compared to the untreated control (Tab. 2). The number of sprays applied according to SafeBerry's recommendations was reduced in all experiment (by 3 to 6 sprays) compared to the number applied according to the common practice of growers in the area.

## DISCUSSION

The method used to forecast temperature gave a satisfactory level of accuracy and resulted in an acceptable level of over/underestimation of the component of risk related to the suitability of temperature to strawberry PM. The central part of summer, at least in 2007, is the period in which temperatures are most suited to the disease, while

late spring and autumn are less suited. The decision support system allowed a reduction of 43.2% (3.8 sprays, on the average) in the number of fungicide treatments compared to the common practice in the area and a reduction of the disease if compared to the untreated. This reduction, combined to a satisfactory level of disease control, demonstrated that in Trentino some treatments currently applied to protect strawberry against PM are unnecessary. Further experiments under commercial conditions will be necessary to confirm these experimental results.

## ACKNOWLEDGEMENTS

This research was supported by SafeCrop Centre, funded by Autonomous Province of Trento. Thanks

Location	PM incidence (% $\pm$ SE) <sup>1</sup>			Fungicide treatments (No.)	
	SafeBerry	Untreated	P value <sup>2</sup>	SafeBerry	Common practice
Baselga	44.2 $\pm$ 3.0	66.3 $\pm$ 10.3	0.020	5	8
Pergine1	36.7 $\pm$ 3.6	73.1 $\pm$ 8.3	0.001	7	10
Pergine2	23.3 $\pm$ 4.4	53.3 $\pm$ 12.3	0.023	6	9
Borgo1	0.0	0.0	-	4	8
Borgo2	34.1 $\pm$ 5.5	46.9 $\pm$ 2.9	0.028	3	9

<sup>1</sup>Four replicates of 24 plants each

<sup>2</sup>ANOVA

**Tab. 2** - Powdery mildew (PM) incidence (percentage of infected leaves  $\pm$  standard error) in 2007 in five experiments in Trentino region on strawberry plants treated according to the recommendations of the decision support system SafeBerry or untreated; number of treatments applied according SafeBerry or the common practice of growers in the area.

*Tab. 2 - Incidenza dell'oidio (PM; percentuale di foglie infette  $\pm$  errore standard) nel 2007 in cinque esperimenti condotti in Trentino su piante di fragola trattate secondo le indicazioni del sistema di supporto alle decisioni SafeBerry o non trattate; numero di trattamenti effettuati secondo SafeBerry o nella pratica comune adottata dagli agricoltori della zona.*

are due to growers and advisors of APA Sant'Orsola and FEM-CTT.

where:

$$S_{06} = 0.5 \cdot \sin \left[ \frac{(30 - H_{\min})}{(H_{\max} - H_{\min})} \cdot \pi - \frac{\pi}{2} \right]$$

$$S_{12} = 0.5 \cdot \sin \left[ \frac{(36 - H_{\min})}{(H_{\max} - H_{\min})} \cdot \pi - \frac{\pi}{2} \right]$$

Under the hypothesis 2 an average of two functions is carried out:

$$T_{\min} = \left\{ \frac{\left[ T_{06} \cdot (S_{06} - S_{12}) - (T_{06} - T_{12}) \cdot S_{06} \right]}{(S_{06} - S_{12})} + T_{06} - \frac{(T_{12} - T_{06})}{(S_{12} - S_{06})} \cdot (0.5 + S_{06}) \right\} \cdot \frac{1}{2}$$

$$T_{\max} = \left\{ \frac{\left[ T_{06} \cdot (1 - S_{12}) + T_{12} \cdot (S_{06} - 1) \right]}{(S_{06} - S_{12})} + T_{06} - (T_{12} - T_{06}) \cdot \frac{(S_{06} - 0.5)}{(S_{12} - S_{06})} \right\} \cdot \frac{1}{2}$$

where:

$$S_{06} = \sin \left[ \frac{(30 - H_{\min})}{(H_{\max} - H_{\min})} \cdot \frac{\pi}{2} \right]$$

$$S_{12} = \sin \left[ \frac{(36 - H_{\min})}{(H_{\max} - H_{\min})} \cdot \frac{\pi}{2} \right]$$

## 1. Determining $T_{\min}$ and $T_{\max}$

In the first part  $T_{\min}$  and  $T_{\max}$  are determined via sinusoidal functions calibrated by forcing the passage through points already calculated by the MOS -  $T_{06}$  and  $T_{12}$ , and with the values of  $H_{\min}$  and  $H_{\max}$ , calculated from the statistical analysis (mode value) of individual temperature series at each station, generally different month by month. Such values express the time (hour) in which minimum and maximum values are expected to occur, counting from time 00 at the beginning of the simulation of the meteorological model. For instance, 36 indicates 12 UTC of the day following the issue of ECMWF's "run 00" forecast.

Under the hypothesis 1:

$$T_{\min} = T_{06} - \frac{(T_{12} - T_{06})}{(S_{12} - S_{06})} \cdot (0.5 + S_{06})$$

$$T_{\max} = T_{06} - (T_{12} - T_{06}) \cdot \frac{(S_{06} - 0.5)}{(S_{12} - S_{06})}$$



## 2. Hourly interpolation

The following equations are applied for each of the three days along which forecast is given. Term  $t$  indicates time in hours.

From 00 to  $H_{\min}$ :

$$T(t) = T_{00} + \left[ \frac{(T_{\min} - T_{00})}{(H_{\min} - 00)^{0.5}} \right] \cdot (t - 00)^{0.5}$$

From  $H_{\min}$  to  $H_{\max}$ :

- Hypothesis 1:

$$T(t) = T_{\min} + \frac{(T_{\max} - T_{\min})}{2} \cdot \left[ 1 + \sin \left( \pi \frac{t - H_{\min}}{H_{\max} - H_{\min}} - \frac{\pi}{2} \right) \right]$$

- Hypothesis 2:

$$T = \left\{ T_{\min} + (T_{\max} - T_{\min}) \cdot \sin \left( \frac{(t - H_{\min})}{(H_{\max} - H_{\min})} \cdot \frac{\pi}{2} \right) + T_{\min} + \frac{(T_{\max} - T_{\min})}{2} \cdot \left[ 1 + \sin \left( \pi \frac{t - H_{\min}}{H_{\max} - H_{\min}} - \frac{\pi}{2} \right) \right] \right\} \cdot \frac{1}{2}$$

From  $H_{\max}$  to 18:

$$T(t) = T_{18} - (T_{\max} - T_{18}) \cdot \sin \left[ \frac{\pi}{2} \cdot \left[ 1 + \frac{(t - H_{\max})}{(18 - H_{\max})} \right] \right]$$

From 18 to 24:

$$T(t) = T_{18} + \frac{(T_{24} - T_{18})}{\sqrt{6}} \cdot (t - 18)^{0.5}$$

## REFERENCES

- Abdel-Aal R.E. and Elhadidy M.A., 1994. A machine-learning approach to modelling and forecasting the minimum temperature at Dharan, Saudi Arabia. Energy, 19: 739-749.
- Anadreanistakis M., Lagouvardos K., Kotroni V., and Eleftheriadis, H., 2004. Correcting temperature and humidity forecasts using Kalman filtering: Potential for agricultural protection in Northern Greece. Atmospheric Research, 71: 115-125.
- Amsalem L., Freeman S., Rav-David D., Nitzani Y., Sztejnberg A., Pertot I., Elad Y., 2006. Effect of climatic factors on powdery mildew caused by *Sphaerotheca macularis* f. sp. *fragariae* on strawberry. Eur. J. Plant Path., 114: 283-292.
- Arca B., Benincasa F., De Vincenzi M., and Fasano G., 1998. A neural model to predict the daily minimum of air temperature. Proceedings of the 7th International Congress For Computer Technology in Agriculture, Computer technology in agricultural management and risk prevention. Florence, Italy, 15 – 18 November 1998: 485-493.
- Basili P., Bonafoni S. and Biondi R., 2006. Analisi e previsione di temperature minime e di gelate sul bacino del Trasimeno. Rivista Italiana di Agrometeorologia, 2006(1): 46-50.
- Breiman L., 2001. Random Forests. Machine Learning, 45: 5-32.
- Breiman L., Friedman J. H., Olshen R.A., and Stone, C.J. 1984. Classification and regression trees. Wadsworth International Group, Belmont, California (USA), 368 pp.
- Cane D., Milelli M., and Gandini D., 2004. Improvement of the meteorological parameters forecasts for the XX Olympic winter games venue. Geophysical Research Abstracts, Vol. 6, 03637.
- Cesaraccio C., Spano D., Duce P., Snyder R.L., 2001. An improved model for determining degree-day values from daily temperature data. Int. J. Biometeorol, 45: 161-169.
- Eccel E., Ghielmi L., Granitto P., Barbiero R., Grazzini, F., and Cesari, D., 2007. Prediction of minimum temperatures in an alpine region by linear and non-linear post-processing of meteorological models. Nonlinear Proc. Geoph., 14: 211-222.
- Galanis G., and Anadreanistakis M., 2002. A one-dimensional Kalman filter for the correction of near surface temperature forecasts. Meteorological Applications, 9: 437-441.
- Geman S., Bienenstock E., and Doursat R. 1992. Neural Networks and the Bias/Variance Dilemma. Neural Computation, 4: 1-58.
- Homleid M., 1995. Diurnal corrections of short-term surface temperature forecasts using the Kalman filter. Weather and Forecasting, 10: 689-707.
- Liaw A. and Wiener M., 2005. Breiman and Cutler's random forests for classification and regression. R-Package "randomForest": <http://stat-www.berkeley.edu/users/breiman/RandomForests>
- Madden L.V., Ellis M.A., 1988. How to develop a

- plant disease forecaster. In: J. Kranz and J. Rotem, eds. *Experimental Techniques in Plant Disease Epidemiology*. Springer-Verlag, New York: 191-208.
- Pertot I., Zasso R., Amsalem L., Baldessari M., Angeli G., Elad Y., 2008. Integrating biocontrol agents in strawberry powdery mildew control strategies in high tunnel growing systems. *Crop Protection*, 27: 622-631.
- Robinson C. and Mort C., 1997. A neural network system for the protection of citrus crop from frost damage. *Computers and Electronics in Agriculture*, 16: 177-187.
- Schizas C.N., Michaelides S., Pattichis C.S., and Livesay R.R., 1991. Artificial networks in forecasting minimum temperature. *Institution of Electrical Engineers*, 349: 112-114.
- Verdes P.F, Granitto P.M., Navone H.D., and Ceccatto H.A., 2000. Frost Prediction with Machine Learning Techniques. *Proceedings of the VI Argentine Congress on Computer Science*: 1423-1433.

# Dinamica temporale della volatilizzazione dell'ammoniaca da terreni agricoli: misure micrometeorologiche su liquami e urea

Ferrara Rossana Monica<sup>1\*</sup>

**Abstract:** Anthropogenic activities are altering the nitrogen (N) cycle, causing accumulation of reactive forms of N in ecosystems with consequent environmental issues. Among reactive forms, ammonia ( $\text{NH}_3$ ) is lost by agriculture sector following spreading of organic and inorganic N fertilizers. Nevertheless,  $\text{NH}_3$  measurements in the continuum soil-plant-atmosphere is extremely complex due to the reactive and sticky nature of this compound. Moreover,  $\text{NH}_3$  volatilization is strongly affected by many factors such as meteorological conditions, then applied measurement methods do not have to modify microclimate. Among available methods, the micrometeorological ones match this requirement, but their application to  $\text{NH}_3$  needs specific studies. In particular, scientific community is working on double front for  $\text{NH}_3$  monitoring: the development of new sensors, applicable on wide scale for monitoring in different conditions, and the applicability of direct and advance methods like eddy covariance (EC). In this study, by means of micrometeorological methods, the  $\text{NH}_3$  volatilization process was investigated following (i) slurry spreading on bare soil (aerodynamic gradient method) and urea application on irrigated cropland (EC method). The dynamics of  $\text{NH}_3$  volatilization are presented, highlighting the differences in term of duration and timetable.

**Keywords:** eddy covariance, Mediterranean environment, aerodynamic gradient method.

**Riassunto:** Le attività antropogeniche hanno alterato il ciclo dell'azoto (N), determinando un accumulo di forme reattive dell'N negli ecosistemi con conseguenti problematiche ambientali. Tra le forme reattive, l'ammoniaca ( $\text{NH}_3$ ) viene prevalentemente persa nel settore agricolo in seguito all'applicazione di fertilizzanti azotati organici e di sintesi. Tuttavia, la natura particolarmente reattiva di tale gas rende la misura dei suoi flussi nel continuo suolo-pianta-atmosfera estremamente complessa. Inoltre, la dipendenza del processo di volatilizzazione dell' $\text{NH}_3$  da molteplici fattori, tra cui le condizioni meteorologiche, impone l'utilizzo di metodi di misura che non alterino il microclima. Tra i metodi attualmente disponibili, quelli micrometeorologici rispondono a tale esigenza, ma la loro applicazione all' $\text{NH}_3$  richiede studi mirati. In particolare, la comunità scientifica sta lavorando su un duplice fronte per il monitoraggio dell' $\text{NH}_3$ : quello dello sviluppo di nuovi sensori, che possono essere applicati su ampia scala in modo da monitorare diverse realtà, e quello dell'applicabilità di metodi diretti e avanzati come l'eddy covariance (EC). In questo studio, mediante l'utilizzo di metodi micrometeorologici, si è indagato il processo di volatilizzazione dell' $\text{NH}_3$  in seguito all'applicazione di (i) liquame su suolo nudo (metodo gradiente aerodinamico) e di (ii) urea su coltura irrigata (metodo EC). Le dinamiche della volatilizzazione dell' $\text{NH}_3$  vengono presentate, evidenziandone le differenze in termini di durata e tempistica.

**Parole chiave:** eddy covariance, ambiente mediterraneo, metodo gradiente aerodinamico.

## INTRODUZIONE

A partire dagli inizi del XX secolo, grazie alla scoperta del processo di Haber-Bosch che permette di convertire azoto (N) atmosferico non reattivo in ammoniaca ( $\text{NH}_3$ ) reattiva, si è aumentato l'utilizzo di fertilizzanti azotati in grado di incrementare la produzione agricola a parità di superfici coltivate (Galloway *et al.*, 2003). Tuttavia, si stima che solo il 50% dell'N applicato venga effettivamente utilizzato dalle piante (FAO, 2001). L'eccesso di input azotati rispetto alle necessità effettive degli ecosistemi determina alterazioni del ciclo dell'N con accumulo di forme reattive ( $\text{N}_r$ ) quali l' $\text{NH}_3$ , l'ammonio ( $\text{NH}_4^+$ ), gli ossidi di azoto ( $\text{NO}_x$ ), l'acido nitrico ( $\text{HNO}_3$ ), l'o-

sido nitroso ( $\text{N}_2\text{O}$ ) e composti organici come urea e proteine (Galloway *et al.*, 2004). Molteplici sono le conseguenze negative sull'ambiente attribuibili a tali accumuli. Galloway *et al.* (2003) parla di effetto a cascata (*N cascade*). Ad esempio, nel caso dell' $\text{NH}_3$ , una catena di processi fa sì che un atomo di N rilasciato in atmosfera come  $\text{NH}_3$  contribuisca attivamente alla formazione di aerosol e, quindi,  $\text{PM}_{10}$  con conseguenze sulla salute e sulla visibilità; inoltre, lo stesso atomo una volta depositato al suolo, può incrementare l'acidità del suolo, influenzare la biodiversità e intervenire nei processi di eutrofizzazione delle acque (Erisman *et al.*, 2003). Di qui la necessità di investigare sui processi di perdita dell'N per via gassosa che, per quanto riguarda l' $\text{NH}_3$ , vedono il settore agricolo e zootecnico quale fonte primaria di emissione (FAO, 2001). Si stima che a livello globale il 23% e il 14% delle emissioni di  $\text{NH}_3$  siano

\* Corresponding author e-mail: rossana.ferrara.entecri.it

<sup>1</sup> CRA - Unità di Ricerca per i sistemi culturali degli ambienti caldo-aridi (SCA), Bari (Italia).

imputabili rispettivamente all'uso di liquami e fertilizzanti sintetici (Bouwman *et al.*, 2002), attraverso il processo di volatilizzazione dell' $\text{NH}_3$ . Si tratta di un fenomeno durante il quale l' $\text{NH}_3$  si trasferisce dall'aria in contatto con la soluzione ammoniacale associata a liquami animali e fertilizzanti azotati dissolti in acqua, dove l' $\text{NH}_4^+$  è in equilibrio dinamico con l' $\text{NH}_3$  gassosa, all'aria libera sovrastante. Tale processo è guidato da molteplici fattori, spesso interagenti. Diversi studi hanno dimostrato la dipendenza del fenomeno dalla temperatura, dalla concentrazione di  $\text{NH}_4^+$ , dal pH del mezzo, dal tasso di evaporazione, dalla formazione della rugiada e dal trasporto turbolento (ad es. Sommer e Hutchings, 2001; Søgaard *et al.*, 2002; Sommer *et al.*, 2003). Inoltre, la quantità di  $\text{NH}_3$  emessa e la durata del processo di volatilizzazione dipendono dal tipo di fertilizzante, dal metodo di applicazione, dal tipo di suolo, dalle condizioni meteorologiche e dal tipo di copertura vegetale (Søgaard *et al.*, 2002; Huijsmans *et al.*, 2003; Sommer *et al.*, 2004).

Le operazioni di misura dell' $\text{NH}_3$  in atmosfera sono particolarmente complesse a causa del fatto che è un gas altamente reattivo, molto solubile in acqua e portato ad essere adsorbito da diversi materiali come le comuni plastiche (Harper, 2005). Nonostante queste difficoltà, negli ultimi decenni molti miglioramenti sono stati fatti nel settore della misura e dello sviluppo di nuove tecniche. Occorre fare una distinzione tra misure di concentrazione e di flussi di  $\text{NH}_3$ . Attualmente, molti sensori sono disponibili per fare misure di concentrazione dell' $\text{NH}_3$  (Phillips *et al.*, 2001). Si passa dalle semplici e economiche trappole secche per monitoraggi su lunghe scale temporali (Sutton *et al.*, 2001), alle trappole a diffusione (*denuders*) a effluente liquido usate nel sistema AMANDA (ECN, Petten, NL) (Wyers *et al.*, 1993), fino ad arrivare ai sofisticati analizzatori basati sulla spettroscopia infrarossa con sorgenti laser a cascata quantica, i cosiddetti QC-TILDAS (*Quantum Cascade Tunable Infrared Laser Differential Absorption Spectroscopy*) in grado di acquisire 10 dati al secondo (Zanhiser *et al.*, 2005). Per quanto riguarda le misure dei flussi di  $\text{NH}_3$ , si è passati dai metodi basati sul bilancio di N nel suolo, in cui non si faceva alcuna misura diretta di perdite di  $\text{NH}_3$ , ai metodi micrometeorologici e delle camere. La necessità di non perturbare i fattori da cui la volatilizzazione dipende, rende i metodi micrometeorologici particolarmente adatti (Denmead, 1983; Kaimal e Finnigan, 1994).

La volontà di creare una rete di monitoraggio dei composti azotati analoghi a quanto già esiste per l'anidride carbonica ( $\text{CO}_2$ ), rende necessaria la messa a punto di sistemi non eccessivamente costosi, ma suf-

ficientemente robusti da poter essere utilizzati in svariate condizioni. Di qui, il moltiplicarsi di studi finalizzati anche alla realizzazione di nuove apparecchiature, con il supporto di progetti di portata internazionale (ad es. [www.nitroeurope.eu](http://www.nitroeurope.eu)). Se da un lato si vogliono consolidare tecniche semplificate per aumentare il grado di utilizzabilità, dall'altro si cerca di approfondire metodologie sofisticate che diano risposte certe e descrivano rigorosamente i processi in gioco. Mentre alcuni metodi micrometeorologici, quali il gradiente aerodinamico (AGM), vengono ritenuti facilmente adoperabili per la misura dell' $\text{NH}_3$  e si sta lavorando sullo sviluppo di nuovi sensori di misura, l'applicazione del metodo *eddy covariance* (EC) al monitoraggio dell' $\text{NH}_3$  è considerata un obiettivo ambizioso e una sfida dalla comunità scientifica. Solo grazie allo sviluppo dei QC-TILDAS si è potuto applicare tale tecnica all' $\text{NH}_3$ , ma poca è la letteratura attualmente presente sull'argomento a conferma delle numerose difficoltà che riguardano l'abbinamento EC –  $\text{NH}_3$  (Shaw *et al.*, 1998; Famulari *et al.*, 2005; Whitehead *et al.*, 2008; Brouder *et al.*, 2009). Altro elemento che emerge dalla letteratura è il limitato numero di studi sull' $\text{NH}_3$  in ambiente mediterraneo dove, comunque, le alte temperature in gioco dovrebbero creare le condizioni ideali per il processo di volatilizzazione dell' $\text{NH}_3$  (Rana e Mastrorilli, 1998; Sanz-Cobena *et al.*, 2008). In tale ambito si è sviluppato questo studio, in cui i flussi di  $\text{NH}_3$  a seguito di (i) spargimento di liquami in ambiente umido - temperato e (ii) applicazione di urea in ambiente semi-arido sono stati misurati mediante l'approccio micrometeorologico. Qui viene presentato un confronto sulla dinamica della volatilizzazione di  $\text{NH}_3$  nei due casi studio sopramenzionati, dando indicazioni sulle tecniche di misura applicate, soprattutto per ciò che concerne alcune novità e difficoltà incontrate. Il lavoro rientra nello studio condotto nell'ambito di un dottorato di ricerca (Ferrara, 2008).

## MATERIALI E METODI

### Siti sperimentali

Le due campagne sperimentali sono state condotte in ambiente umido-temperato (**Exp I**) e semi-arido (**Exp II**) rispettivamente in nord Europa (vicino Parigi) e sud Italia (vicino Bari).

Durante la campagna **Exp I** si sono monitorati i flussi di  $\text{NH}_3$  a seguito dello spandimento superficiale di liquame bovino interrato dopo due giorni a circa 10 cm di profondità. Il campo sperimentale di circa 20 ettari era coltivato a mostarda che è stata sfalciata e sminuzzata il giorno prima che iniziasse lo spandimento, il 18 aprile 2008. La quantità totale di azoto applicato era di circa 76 kgNha<sup>-1</sup>.



Campagna sperimentale	Velocità del vento	Direzione del vento	Temperatura dell'aria	Umidità relativa	Temperatura superficiale infrarossa	Radiazione globale incidente	Radiazione netta	Radiazione fotosinteticamente attiva incidente	Precipitazioni
	m s <sup>-1</sup>	deg / N	°C	%	°C	W m <sup>-2</sup>	W m <sup>-2</sup>	W m <sup>-2</sup>	mm
<b>Exp I</b>	Anemometro a coppe (MCB, Courbevoie, France)	Banderuola potenziometrica W200P (Campbell Sci. Inc., USA)	Termocoppie ventilate 0.25 mm (T-type, copper-constantan)	Termostrofometro HMP-35 (Vaisala, FI)		Albedometro CM6 and CM11 (Kipp & Zonen, NL).	Net radiometro (NR LITE, Kipp & Zonen, NL)	Quantum sensor Li-190 (Licor, USA)	Pluviometro (Campbell Sci. Inc., USA)
<b>Exp II</b>	Anemometro a coppe (A100, Vector Inst., USA)	Banderuola potenziometrica W200P (Campbell Sci., Shepshed, UK)	termoigrometro (M100, Rotronic, USA)	termoigrometro (M100, Rotronic, USA)	sensore temperatura infrarossa (IRR PN, Apogee Ins., USA)	Albedometro (Li-200, LI-COR, USA)	net radiometro (Q*6, REBS, USA)	Quantum sensor Li-190 (Licor, USA)	Pluviometro (ARG100, Campbell Sci., Shepshed, UK)

**Tab. 1** - Variabili meteorologiche monitorate durante le due campagne sperimentale: prova su liquame in ambiente umido-temperato (Exp I) e su urea in ambiente semi-arido (Exp II). I relativi strumenti di misura adoperati vengono indicati. Tutte le variabili, tranne la pioggia, sono state monitorate a 2 m dal suolo.

*Tab. 1 - Meteorological variables monitored during the two experimental campaigns: trial on slurry in humid-temperate climate (Exp I) and on urea in semi-arid climate (Exp II). The relative measurement devices are indicated. All variables, except rainfall, were monitored at 2 m above soil.*

La campagna **Exp II** è stata svolta durante l'estate 2008 su un campo di circa 2 ettari coltivato a sorgo irrigato con un sistema ad aspersione. Urea per circa 240 kgNha<sup>-1</sup> è stata applicata in tre *tranche*. La quantità di fertilizzante adoperato è stata maggiorata rispetto alle comuni pratiche agricole della zona al fine di poter essere sicuri di misurare flussi di NH<sub>3</sub> e, quindi, verificare il funzionamento di nuove apparecchiature di misura messe in campo. Campioni di suolo sono stati prelevati periodicamente al fine di monitorare il pH, il contenuto idrico a 20 e 40 cm e il contenuto di NO<sub>3</sub><sup>-</sup> e NH<sub>4</sub><sup>+</sup>.

In tabella 1 sono riportate le variabili meteorologiche monitorate durante le due sperimentazioni. In entrambe le prove tali variabili sono state misurate ad intervalli di 10 secondi e mediate su 30 minuti mediante un CR10X (Campbell Sci., Shepshed, UK).

### Strumenti e metodi di misura dell'NH<sub>3</sub>

In entrambi casi è stato scelto l'approccio micrometeorologico, rispondendo alla necessità di effettuare misure non invasive, su ampie aree (alcuni ettari) in maniera continuativa. In particolare, il metodo AGM e quello EC sono stati adoperati per **Exp I** e **Exp II**, rispettivamente. L'applicazione di tali metodi, tuttavia, richiede che siano soddisfatte delle condizioni: (1) stazionarietà dello scalare (es. gas, calore, vapore acqueo) o vettore (velocità del vento) che si vuole indagare, garantita scegliendo opportunamente i tempi di mediazione; (2) omogeneità su ampie superfici, per evitare gradienti e, quindi, trasporto lungo le direzioni orizzontali; (3) superfici in piano.

Il metodo AGM si basa sul concetto che il tra-

sporto verticale di un gas al disopra una superficie avviene attraverso un processo di diffusione turbolenta del gas lungo il suo gradiente di concentrazione. Risultano, quindi, necessarie misure dirette di concentrazione del gas a diverse altezze rispetto alla superficie e la conoscenza di un opportuno coefficiente di diffusione turbolenta (*K*) che può essere ricavato con diversi approcci, tra cui quello aerodinamico (Denmead, 1983). Quest'ultimo definisce il *K* mediante misure di velocità del vento e temperatura a più altezze, prendendo in considerazioni la stratificazione degli strati bassi dell'atmosfera mediante le correzioni di stabilità derivate dalla teoria di Monin-Obukhov (1954). L'approccio seguito in questo studio è quello sviluppato da Sutton *et al.* (1993), in cui il flusso del gas (*F<sub>x</sub>*) è dato da:

$$F_x = -u_* \chi_* \quad (1)$$

con *u<sub>\*</sub>* velocità di frizione e *χ<sub>\*</sub>* parametro di "scaling" per la concentrazione *χ*, dato da:

$$\chi_* = k \frac{\partial \chi}{\partial [\ln(z-d) - \Psi_H]} \quad (2)$$

Nell'equazione (2) *k* è la costante di von Karman (0.41), *z* e *d* sono l'altezza al di sopra della superficie e il piano di spostamento nullo, *Ψ<sub>H</sub>* la funzione di stabilità calcolata mediante la lunghezza di Monin-Obukhov. In questo studio, la concentrazione di NH<sub>3</sub> è stata misurata mediante un sistema graduato aerodinamico innovativo denominato ROSAA (RObust and Sensitive Ammonia Analyzer) (Loubet *et al.*, 2008), messo in campo per la prima volta pro-

prio durante la sperimentazione **Exp I**. Tale sistema è in grado di misurare flussi di NH<sub>3</sub> in condizione di elevate emissioni (maggiori di 1 µm<sup>-2</sup>s<sup>-1</sup>) e basse deposizioni (minor di 50 ngm<sup>-2</sup>s<sup>-1</sup>), autocalibrandosi. Il principio di base è quello dei *denuders* a effluente liquido con cattura dell'NH<sub>3</sub> mediante una soluzione acida che converte NH<sub>3</sub> in NH<sub>4</sub><sup>+</sup>; la concentrazione di quest'ultimo viene determinata mediante un dispositivo che fa misure di conducibilità elettrica, accoppiato a una membrana semi-permeabile (ECN, Netherlands). Il sistema è in grado di monitorare contemporaneamente la concentrazione dell'NH<sub>3</sub> a tre livelli dal suolo (0.3; 0.7 e 1.50 m) ogni 30 minuti. Dettagli relativi al sistema ROSAA, ai test di laboratorio e ai risultati sperimentali possono trovarsi in Personne *et al.* (2007) e Ferrara (2008).

Il metodo EC si basa sul concetto che il trasporto di uno scalare avviene attraverso il moto turbolento dell'atmosfera che sposta le particelle di aria da un livello ad un altro (Kaimal e Finnigan, 1994). Quindi, il trasporto verticale del gas si ottiene correlando il valore istantaneo della componente verticale della velocità del vento (*w*) e quello della concentrazione del gas ( $\chi$ ) che devono essere misurati ad una opportuna altezza. La densità di flusso verticale è data da:

$$F = \overline{w\chi} = \overline{w}\overline{\chi} + \overline{w'}\overline{\chi'} \quad (3)$$

dove alle due variabili si è applicata la decomposizione di Reynolds ( $a = \bar{a} + a'$ ). La barra sopra al prodotto rappresenta la media su un appropriato periodo di tempo (15 min – 1 ora), mentre l'indice ' indica la deviazione dalla media delle variabili considerate (varianza). Al flusso concorrono vortici (*eddy*) di varie dimensione e tempi di vita, quindi, per garantire la maggior parte possibile dello spettro della turbolenza efficace per il trasporto è necessario che le frequenze di campionamento siano elevate. È necessario disporre di sensori in grado di fare misure a frequenze dell'ordine di 5-10 Hz, sia per la componente vento (anemometri sonici) sia per lo scalare in questione. L'applicabilità di tale metodo, quindi, dipende dalla disponibilità di analizzatori veloci che, ad esempio, per il vapor acqueo (H<sub>2</sub>O) e la CO<sub>2</sub> sono presenti già da molti anni sul mercato. Se da un lato si può affermare che l'EC è ormai una tecnica consolidata per il monitoraggio di H<sub>2</sub>O e CO<sub>2</sub> (Baldoch, 2003), dall'altro le difficoltà di realizzazione di sensori veloci per l'NH<sub>3</sub> hanno tardato l'applicazione dell'EC a tale gas e molti sono ancora i problemi da risolvere. In particolare, confronti con altri metodi di misura dei flussi di NH<sub>3</sub>

	Rg max (Wm <sup>-2</sup> )	T (°C)	RH (%)	U (ms <sup>-1</sup> )
<b>Exp I</b>	<b>761</b>	<b>-0.5±15.0</b>	<b>32.2±96.4</b>	<b>0.4±10.2</b>
<b>Exp II</b>	<b>945</b>	<b>16.1±34.7</b>	<b>23.6±92.7</b>	<b>0.3±6.5</b>

**Tab. 2** - Valore massimo orario misurato della radiazione globale incidente (Rg max) e intervallo di valori osservati per la temperatura dell'aria (T), l'umidità relativa (RH) e la velocità del vento (u) a 2 metri dal suolo in entrambe le sperimentazioni: prova su liquame in ambiente umido-temperato (Exp I) e su urea in ambiente semi-arido (Exp II).

*Tab. 2 - Maximum hourly value of incident global radiation (Rg max) and range of observed values of air temperature (T), relative humidity (RH) e wind speed (u) at 2 m above soil during the two experimental campaigns: trial on slurry in humid-temperate climate (Exp I) and on urea in semi-arid climate (Exp II).*

hanno evidenziato sottostime, anche dell'ordine dell'80%, nei flussi misurati tramite EC sia in esperimenti in campo che in laboratorio (Whitehead *et al.*, 2008; Brodeur *et al.*, 2009). Tra i problemi da risolvere, si deve ricordare la forte limitazione dovuta all'adsorbimento dell'NH<sub>3</sub> sulle pareti del tubo di campionamento: quest'ultimo determina smorzamenti delle fluttuazioni del gas alle alte frequenze, con conseguente sottostima dei flussi che possono essere valutate (ad es. Massman, 2000). Il sistema EC utilizzato durante la prova **Exp II** era posto a 1.50 m dal suolo ed era costituito da un anemometro sonico Gill R2 (Gill Instruments Ltd, UK) e un analizzatore veloce per l'NH<sub>3</sub> sviluppato dall'Aerodyne, il compact QC-TILDAS-76 SN002-U (Aerodyne Research Inc, USA).

## Durata della sperimentazione

La durata effettiva della campagna sperimentale **Exp I** è stata di circa 10 giorni, ma le emissioni di NH<sub>3</sub> in seguito allo spandimento di liquame si sono esaurite nel giro di 3 giorni, portandosi a valori di concentrazione dell'NH<sub>3</sub> inferiori ai limiti di rilevabilità degli strumenti messi in campo.

La prova **Exp II** è durata 13 giorni (dal 17 al 29 luglio) ed è stata interrotta a causa di problemi tecnici del QC-TILDAS non rapidamente risolvibili. In particolare, si è verificato una riduzione dell'ampiezza del segnale in uscita dal QC-TILDAS causata da un disallineamento degli specchi del banco ottico e un accumulo di detriti all'interno della cella di campionamento. Le procedure di allineamento e pulizia della cella sono laboriose e non eseguibili direttamente in campo, quindi, si è dovuto rimuovere lo strumento dal sito sperimentale prima della fine della prova.

## RISULTATI E DISCUSSIONE

Le condizioni meteorologiche registrate durante le due campagne sperimentali sono riassunte in ta-

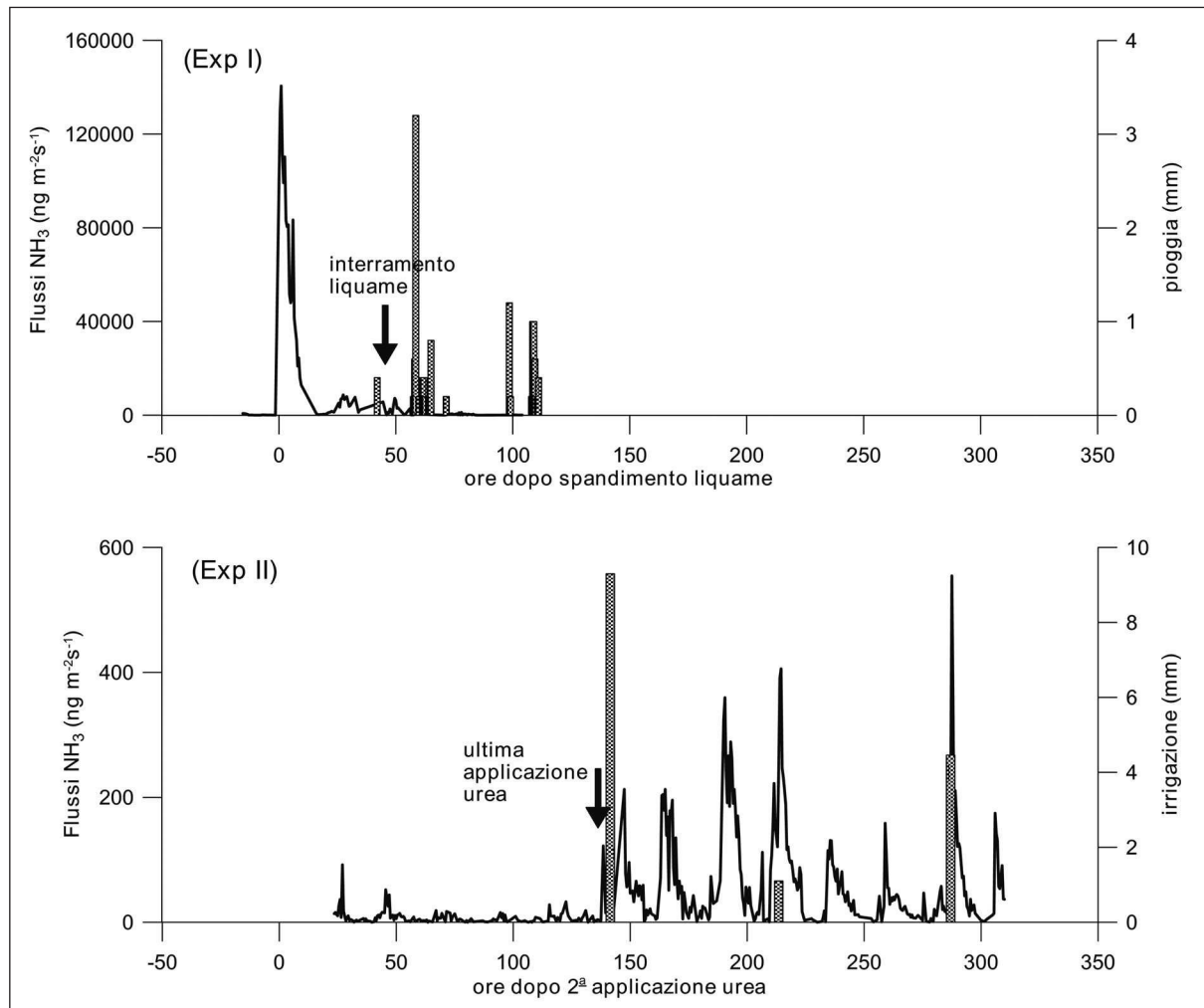
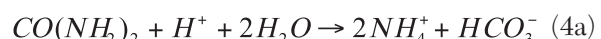


**Fig. 1** - Andamento dei flussi di ammoniaca ( $\text{NH}_3$ ) misurati durante le due campagne sperimentali in seguito all'applicazione di liquame (Exp I) e urea (Exp II). L'interramento del liquame è avvenuto dopo 48 ore dall'applicazione, mentre la terza e ultima applicazione di urea è avvenuta 7 giorni dopo la seconda. Le piogge e le irrigazioni sono indicate per Exp I e Exp II rispettivamente.

*Fig. 1 - Ammonia flux patterns ( $\text{NH}_3$ ) measured during the two experimental campaigns following slurry spreading (Exp I) and urea application (Exp II). Slurry was incorporated into the soil after 48 hours, while the third and last urea application was carried out 7 days after the second one. The rainfall and irrigation are indicated for Exp I and Exp II, respectively.*

bella 2 in cui sono riportati il valore massimo orario della radiazione globale e gli intervalli dei valori orari di: temperatura dell'aria, umidità relativa e velocità del vento. La campagna **Exp I** è stata caratterizzata da basse temperature, con cielo limpido il giorno dello spandimento, forte vento il giorno dopo e pioggia a partire dalla notte del giorno dell'interramento (12 mm) con effetti di abbattimento sulle emissioni di  $\text{NH}_3$ : il tutto si è esaurito nel giro di 3 giorni. La prova **Exp II** ha avuto una durata più lunga rispetto a **Exp I** legata alla diversa dinamica temporale del processo di volatilizzazione dell' $\text{NH}_3$  da fertilizzanti di sintesi quali l'urea. Infatti, quando applicata al suolo, l'urea viene idrolizzata dall'enzima ureasi in  $\text{NH}_4^+$  che, in funzione del pH

del suolo, può produrre  $\text{NH}_3$  che può volatilizzare tramite la seguente reazione:

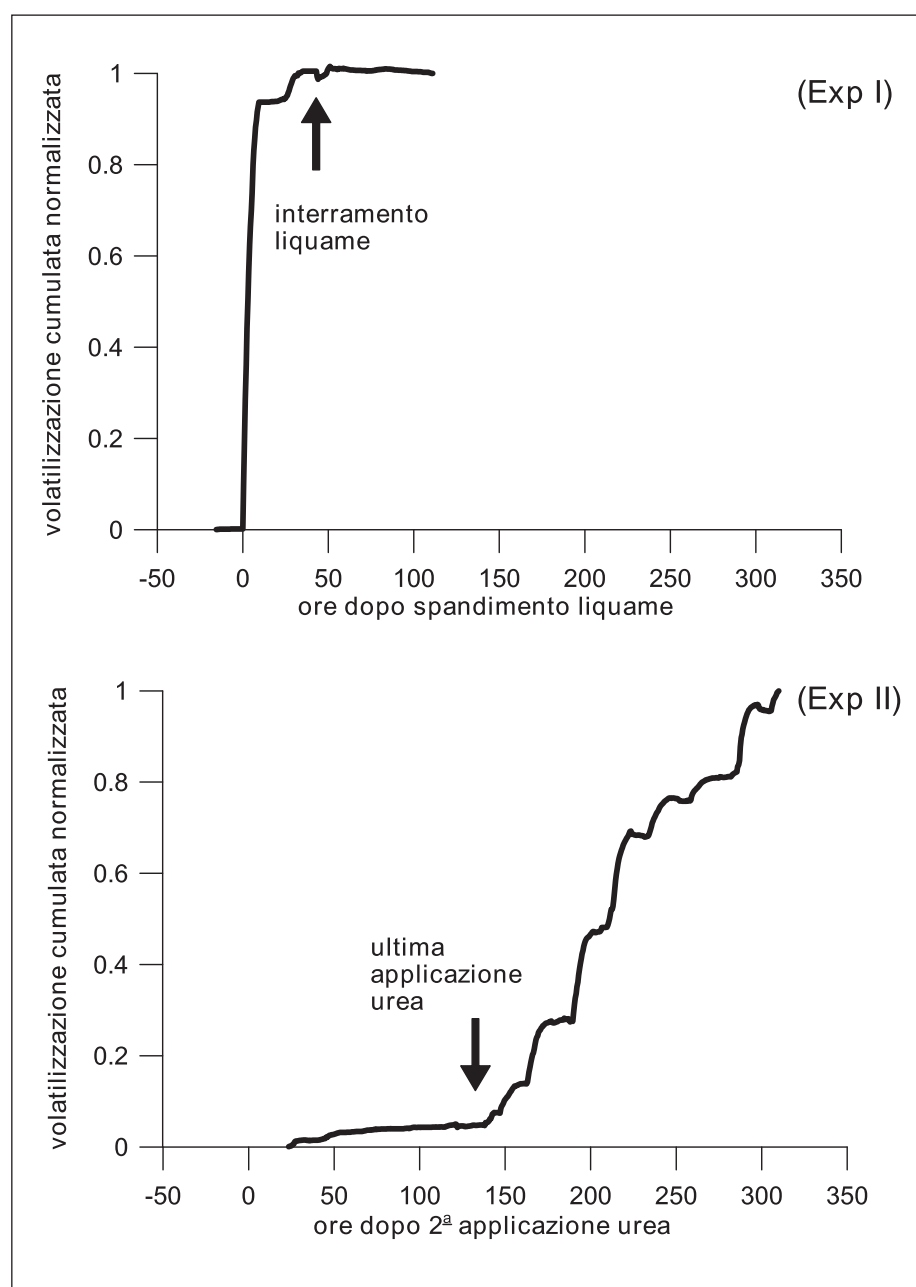


L' $\text{NH}_3$  viene persa in atmosfera in quanto l'aumento del pH muove l'equilibrio  $\text{NH}_4^+ - \text{NH}_3$  verso destra nella reazione (4b) (Van der Weerder and Jarvis, 1997). L'idrolisi dell'urea avviene rapidamente in suoli umidi e in presenza di elevate temperature, con la maggior parte dell'urea trasformata in  $\text{NH}_4^+$  nel giro di qualche giorno. Durante la prima settimana di misure della campagna **Exp II**, nonostante

le elevate temperature (si sono raggiunti anche valori orari di 54.6 °C al suolo), le condizioni particolarmente secche del suolo, per mancanza di pioggia e irrigazione, hanno inibito il processo di idrolisi dell'urea e di conseguenza le emissioni di NH<sub>3</sub>. Solo in seguito all'irrigazione e a brevi precipitazioni si sono iniziati ad osservare flussi di NH<sub>3</sub>.

Questa diversità nella dinamica temporale nel fenomeno di volatilizzazione dell'NH<sub>3</sub> da liquami e urea è mostrata in figura 1 in termini di andamenti dei flussi di NH<sub>3</sub> e in Figura 2 in termini di volatilizzazione cumulata normalizzata. Nel caso del liquame

(Fig. 1 – **Exp I**) il processo di idrolisi e la relativa volatilizzazione dell'NH<sub>3</sub> è già in corso al momento dell'applicazione del liquame e il tasso di volatilizzazione raggiunge il picco entro poche ore dalla spandimento, con esaurimento del fenomeno subito dopo l'interramento, coinciso anche con l'inizio delle precipitazioni che sono proseguiti nei giorni successivi. Per quanto riguarda l'urea granulare applicata nell'**Exp II**, invece, solo nel momento in cui si sono raggiunte le condizioni ideali di temperatura e umidità del suolo (irrigazione di 9.3 mm) si sono iniziati ad osservare le emissioni di NH<sub>3</sub> (vedi figura



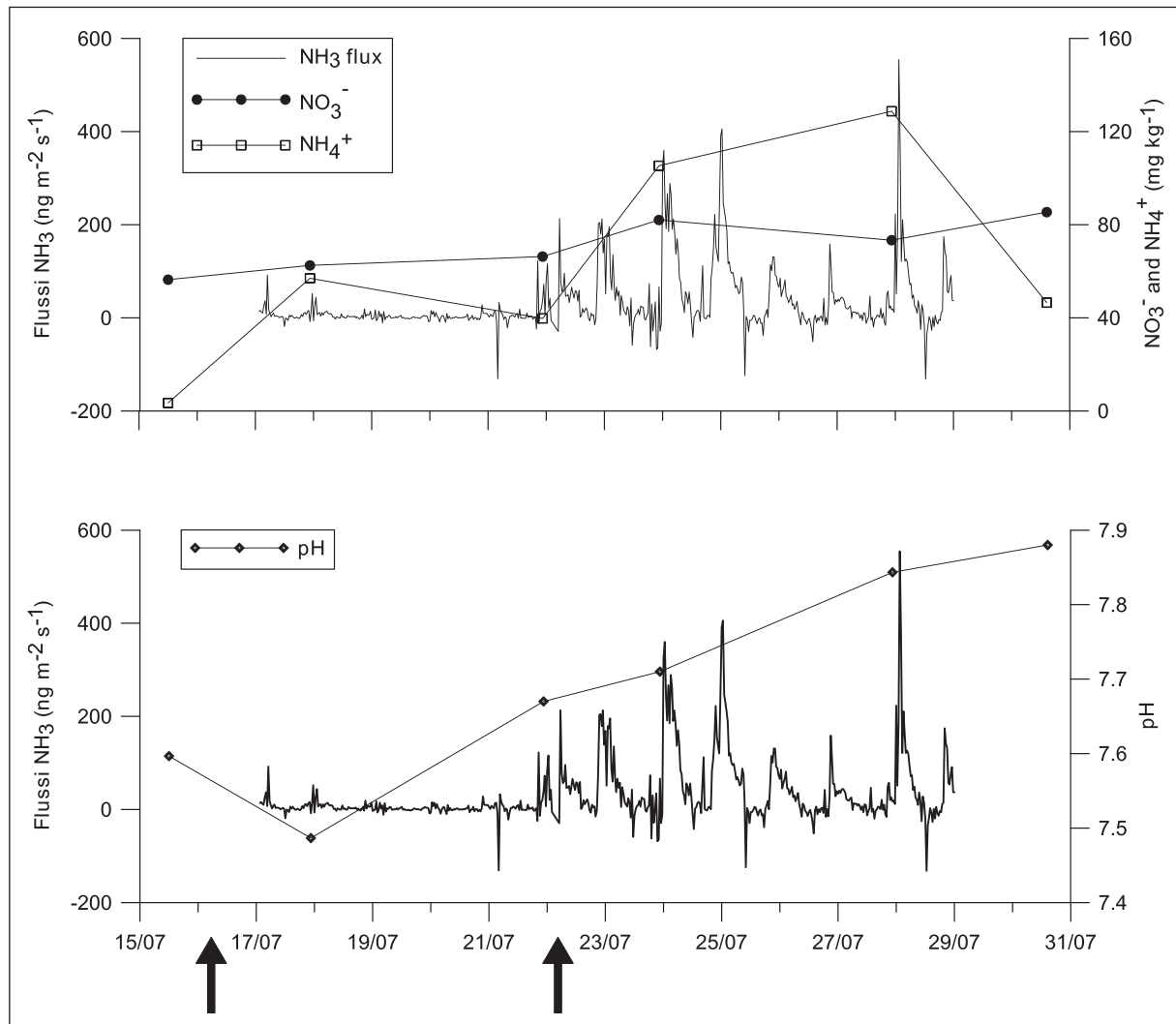


**Fig. 3** - Andamento dei flussi di ammoniaca ( $\text{NH}_3$ ), pH e concentrazioni di  $\text{NH}_4^+$  e  $\text{NO}_3^-$  nel suolo durante la sperimentazione su urea. Le frecce indicano i giorni di spandimento dell'urea.

*Fig. 3 - Ammonia ( $\text{NH}_3$ ) fluxes, pH and concentrations of  $\text{NH}_4^+$  and  $\text{NO}_3^-$  in the soil during the urea trial. The arrows indicate days of urea spreading.*

1 – **Exp II**). In particolare, dopo 7 giorni dalla seconda applicazione di urea, quando si è irrigato prima della terza e ultima applicazione, si sono iniziati a misurare emissioni di  $\text{NH}_3$ .

Per quanto riguarda la volatilizzazione cumulata normalizzata (Fig. 2), occorre specificare che la normalizzazione si è resa necessaria per una duplice motivazione riguardante la sperimentazione **Exp II**: (1) interruzione dell’acquisizione per i sindacati problemi tecnici del sistema QC-TILDAS prima che terminasse il processo di volatilizzazione di  $\text{NH}_3$  da urea; (2) riscontrata sottostima dei flussi misurati dal sistema EC, valutata mediante analisi spettrale. Quest’ultima è stata condotta secondo le indicazioni fornite da Ammann *et al.* (2006), basate sull’ipotesi di similarità tra i cross-spettri di tutti gli scalari: per-

dite a alte frequenze tra il 30 e il 60% sono state evidenziate. Nell’**Exp I**, il rapido svolgimento del fenomeno, con flussi importanti nelle prime ore dallo spandimento seguiti da una riduzione del tasso di volatilizzazione terminata essenzialmente dopo l’internamento del liquame, è mostrato dalla ripida risalita della curva immediatamente dopo lo spandimento (Fig. 2 - **Exp I**). Durante le prime 24 ore dallo spandimento si è verificato il 98% delle perdite totali, risultato confrontabile con quanto riportato da Klarenbeek *et al.*, (1993) e Wulf *et al.*, (2002) che parlano di 80% e 88% delle perdite totali, rispettivamente. Tuttavia, in letteratura sono presenti studi in cui il fenomeno ha avuto una dinamica più lenta: ad esempio Génermont *et al.*, (1998) trovano solo il 30% delle perdite totali durante il



primo giorno. Tali diversità si possono spiegare considerando i molteplici fattori da cui il processo dipende, tra cui le condizioni meteorologiche. In particolare, l'effetto del forte vento il giorno dopo lo spandimento (fino a  $10.2 \text{ ms}^{-1}$ ) dovrebbe aver ridotto le emissioni di  $\text{NH}_3$  rispetto al giorno dello spandimento per due motivi: (1) all'aumentare della velocità del vento, in condizioni di elevata radiazione globale, la temperatura superficiale si riduce e, quindi, si riduce la concentrazione di  $\text{NH}_4^+$  disponibile al processo di volatilizzazione alla superficie ammoniacale (Sommer *et al.*, 2003); (2) formazione di una crosta secca che ha aumentato la resistenza al trasporto dell' $\text{NH}_3$ , riducendo la quantità di  $\text{NH}_3$  disponibile alla volatilizzazione.

Nel caso dell'urea, invece, l'andamento tipico atteso per la volatilizzazione cumulata dovrebbe essere descritto da una sigmoide in grado di distinguere le seguenti tre fasi del processo: (1) fase iniziale di preparazione all'idrolisi dell'urea; (2) periodo di emissioni di  $\text{NH}_3$  crescenti descritto dalla risalita della curva; (3) fase finale di flussi decrescenti corrispondente al plateau della curva. Come si può osservare in figura 2 – **Exp II**, le prime due fasi sono state chiaramente colte dalla sperimentazione, mentre manca l'ultima fase di flussi decrescenti a causa dei problemi tecnici che hanno imposto il termine della campagna sperimentale prima del tempo. Con i dati a disposizione non si è in grado di stabilire rigorosamente se il fenomeno di volatilizzazione stesse volgendo a termine o fosse ancora nella fase di flussi crescenti. Infatti, misure analoghe in ambiente semi-arido sono state condotte da Sanz-Coben *et al.* (2008), i quali hanno trovato il picco massimo delle emissioni di  $\text{NH}_3$  dopo 4 giorni dall'applicazione di urea, con emissioni che sono andate avanti per 36 giorni (contro i nostri 13 giorni effettivi di misura). Tuttavia, pur non disponendo di dati di flussi di  $\text{NH}_3$ , si è cercato di dare una indicazione qualitativa sull'evoluzione del fenomeno, prendendo in considerazione l'andamento del pH e delle concentrazioni di  $\text{NO}_3^-$  e  $\text{NH}_4^+$  nel suolo (Fig. 3). Nel periodo tra la seconda e la terza applicazione di urea, l' $\text{NH}_4^+$  disponibile, non essendoci le condizioni ottimali per il processo di volatilizzazione dell' $\text{NH}_3$ , potrebbe aver subito un processo di nitrificazione che dovrebbe aver convertito l' $\text{NH}_4^+$  in  $\text{NO}_3^-$ . A partire dall'ultima applicazione di urea, essendosi create le condizioni ottimali per la volatilizzazione, si iniziano a osservare flussi significativi di  $\text{NH}_3$  abbinati ad un pH e una concentrazione di  $\text{NH}_4^+$  crescenti (reazioni 4a e 4b). Al termine della sperimentazione, nonostante il crescente andamento del pH, l'ultimo dato utile di  $\text{NH}_4^+$  mostra una riduzione drastica che potrebbe essere una indica-

zione di esaurimento del processo di volatilizzazione, a cui potrebbe essere subentrato un processo di nitrificazione dell' $\text{NH}_4^+$  in  $\text{NO}_3^-$ .

## CONCLUSIONI

L'approccio micrometeorologico è stato adoperato con successo per il monitoraggio della volatilizzazione dell' $\text{NH}_3$  da terreni agricoli in seguito all'applicazione di fertilizzanti azotati organici (liquame – **Exp I**) e di sintesi (urea – **Exp II**). Un nuovo sistema gradiente aerodinamico abbinato a denuders a effluente liquido, ROSAA, è stato messo in campo, consentendo misure dirette di flussi di  $\text{NH}_3$ . Inoltre, per la prima volta flussi di  $\text{NH}_3$  con la tecnica EC in ambiente semi-arido sono stati misurati. In quest'ultimo caso, le problematiche incontrate nella sperimentazione sono state molteplici, prima tra tutte il garantire la stabilità elettrica e termica dell'analizzatore veloce QC-TILDAS, le cui *performance* risentono fortemente delle condizioni al contorno. Tuttavia, la campagna sperimentale **Exp II** può considerarsi a tutti gli effetti la messa a punto di un banco di prova del sistema EC: molte migliorie sono state apportate alla luce dei risultati ottenuti. In particolare: un sistema di condizionamento dell'aria per assicurare una temperatura stabile di lavoro di circa  $20^\circ\text{C}$ , un sistema di riscaldamento del tubo di campionamento per evitare condensa all'interno e riduzione al minimo indispensabile della lunghezza del tubo di campionamento per ridurre le perdite a alta frequenza. Prescindendo dal valore assoluto dei flussi misurati, tuttavia, il sistema EC è stato in grado di cogliere la dinamica del fenomeno di volatilizzazione dell' $\text{NH}_3$  da urea, completamente differente rispetto a quello da liquame in termini di evoluzione temporale. Alla rapidità della volatilizzazione di  $\text{NH}_3$  da liquame, con esaurimento subito dopo l'interramento, si oppone un rilascio lento di  $\text{NH}_3$  da urea che richiede condizioni ottimali di temperatura e umidità del suolo perché si avvii il processo di idrolisi dell'urea e, quindi, tempi di osservazione molto più lunghi. In ogni caso, risulta necessario mettere a punto strumenti sufficientemente robusti da poter essere utilizzati in condizioni anche estreme, al fine di poter quantificare il totale delle perdite gassose di N e, quindi, ottimizzare l'uso dei fertilizzanti per limitarne gli impatti ambientali negativi.

## RINGRAZIAMENTI

Ringrazio il Dott. Gianfranco Rana per le interessanti discussioni e il costante supporto. Inoltre ringrazio: il Progetto AQUATER (D.M. n. 209/7303/05 - Coord: Dr. M. Rinaldi, finanziato da Ministero delle Politiche Agricole, Alimentari e Forestali);

NinE - ESF Research Networking Programme “Nitrogen in Europe”; ACCENT - Biaflux (Network of Excellence funded by EC, FP6, PRIORITY 1.1.6.3 Global Change and Ecosystems: subproject Biosphere-Atmosphere Exchange of Pollutants). Ringrazio infine Marcello Mastrangelo per le analisi di laboratorio.

## BIBLIOGRAFIA

- Ammann C., Brunner A., Spirig C. & Neftel A., 2006. Technical note: Water vapour concentration and flux measurements with PTR-MS. *Atmos. Chem. Phys.*, 6: 4643-4651.
- Baldocchi D.D., 2003. Assessing the eddy covariance technique for evaluating carbon dioxide exchange rates of ecosystems: past, present and future. *Glob. Change Biol.*, 9: 479-492.
- Bouwman A.F., Boumans L.J.M. and Batjes N.H., 2002. Estimation of global NH<sub>3</sub> volatilization loss from synthetic fertilizers and animal manure applied to arable lands and grasslands. *Global Biogeochem. Cycles*, 16 doi: 10.1029/2000GB001389.
- Brodeur J.J., Warland J.S., Staebler R.M., Wagner-Riddle C., 2009. Technical note: Laboratory evaluation of a tunable diode lasersystem for eddy covariance measurements of ammonia flux. *Agric. For. Meteorol.*, 149: 385-391.
- Denmead O.T., 1983. Micrometeorological methods for measuring gaseous losses of nitrogen in the field. In J.R. Freney and J.R. Simpson (Eds): Gaseous loss of nitrogen from plant-soil systems. Martinus Nijhoff/W. Junk, The Hague: 133-157.
- Erisman J.W., Grennfelt P., Sutton M., 2003. The European perspective on nitrogen emission and deposition. *Environ. Int.*, 29: 311 – 325.
- Famulari D., Fowler D., Hargreaves K., Milford C., Nemitz E., Sutton M., Weston K., 2005. Measuring eddy covariance fluxes of ammonia using tunable diode laser absorption spectroscopy. *Water Air Soil Pollut. Focus*, 4 (6): 151-158.
- FAO, 2001. Global estimates of gaseous emissions of NH<sub>3</sub>, NO and N<sub>2</sub>O from agricultural land. FAO, Rome (Italy), 106 pp.
- Ferrara R.M., 2008. Study of the Soil-Crop-Atmosphere continuum under Mediterranean climate: role of H<sub>2</sub>O, CO<sub>2</sub> and NH<sub>3</sub> emissions from arable land. Tesi di Dottorato di Ricerca, 135 pp.
- Galloway J.N., Aber J.D., Erisman J.W., Seitzinger S.P., Howarth R.W., Cowling E.B., Cosby B.J., 2003. The Nitrogen Cascade. *BioScience*, 53 (4): 341-356.
- Galloway J.N., Dentener F.J., Capone D.G., Boyer E.W., Howarth R.W., Seitzinger S.P., Asner G.P., Cleveland C.C., Green P.A., Holland E.A., Karl D.M., Michaels A.F., Porter J.H., Townsend A.R., Vörösmarty C.J., 2004. Nitrogen cycles: past, present, and future. *Biogeochemistry*, 70: 153–226.
- Génermont S., Cellier P., Flura D., Morvan T., Laville P., 1998. Measuring ammonia fluxes after slurry spreading under actual field conditions. *Atmos. Environ.*, 32 (3): 279-284.
- Harper L.A., 2005. Ammonia: measurement issues. In J.L. Hatfield, J.M. Baker and M.K. Viney (Eds): *Micrometeorology in Agricultural systems*. Agronomy Monograph, 47. ASA, CSSA and SSSA, Madison, Wisconsin, USA: 345-379.
- Huijsmans J.F.M., Hol J.M.G., Vermeulen G.D., 2003. Effect of application method, manure characteristics, weather and field conditions on ammonia volatilization from manure applied to arable land. *Atmos. Environ.*, 37: 3669-3680.
- Kaimal J.C., Finnigan J.J., 1994. *Atmospheric boundary layer flows – their structure and measurements*. Oxford University Press, Oxford, 289 pp.
- Klarenbeek J.V., Pain B.F., Phillips V.R., Lockyer D.R., 1993. A comparison of methods for use in the measurement of ammonia emissions following the application of livestock wastes to land. *Intern. J. Environ. Anal. Chem.*, 53: 205-218.
- Loubet B., Decuq C., Personne E., Ferrara R., Massad R.S., Fanucci O., Génermont S., 2008. A mini-wedd gradient system for measuring ammonia fluxes. In: Proc. Of NitroEurope IP, 3rd Annual Meeting & Open Science Conference “Reactive nitrogen and the European greenhouse gas balance”, Ghent (Belgio), 20-21/02/2008: 9.
- Massman W.J., 2000. A simple method for estimating frequency response corrections for eddy covariance systems. *Agric. For. Meteorol.*, 104 (3): 185-198.
- Personne E., Loubet B., Decuq C., Fanucci O., Ferrara R.M., Génermont S., 2007. ROSAA – Robust and Sensitive Ammonia Analyser. Rapport de synthèse \_ Projet Innovant 2006 – 2007, 26 pp.
- Phillips V.R., Lee D.S., Scholtens R., Garland J.A., Sneath R.W., 2001. A review of method for measuring emission rates of ammonia from livestock buildings and slurry or manure stores, part 2: monitoring flux rates concentrations and airflow rates. *J. Agr. Eng. Res.*, 78 (1): 1-14.
- Rana G., Mastrorilli M., 1998. Ammonia emissions from fields treated with green manure in Mediterranean climate. *Agr. Forest Meteorol.*, 90: 265-274.
- Sanz-Cobena A., Misselbrook T.H., Arce A., Mingot J.I., Diez J.A. & Vallejo A., 2008. An inhibitor of urease activity effectively reduces ammonia emissions from soil treated with urea under Mediterranean conditions. *Agric. Ecosyst. Environ.*, 126: 243-249.

- Shaw W.J., Spicer C.W. & Kenny D.V., 1998. Eddy correlation fluxes of trace gases using a tandem mass spectrometer. *Atmos. Environ.*, 32 (17): 2887-2898.
- Søgaard H.T., Sommer S.G., Hutchings N.J., Huijsmans J.F.M., Bussink D.W., Nicholson F., 2002. Ammonia volatilization from field-applied animal manure - the ALFAM model. *Atmos. Environ.*, 36: 3309-3319.
- Sommer S.G., Génermont S., Cellier P., Hutchings N.J., Olesen J.E., Morvan T., 2003. Processes controlling ammonia emission from livestock slurry in the field. *Eur. J. Agron.*, 19: 465 - 486.
- Sommer S.G., Hutchings N.J., 2001. Ammonia emission from field applied manure and its reduction: review. *Eur. J. Agron.*, 15: 1-15.
- Sommer S.G., Schjoerring J.K., Denmead O.T., 2004. Ammonia emission from mineral fertilizers and fertilized crops. *Adv. Agr.*, 82: 557-622.
- Sutton M.A., Pitcairn C.E.R., Fowler D., 1993. The exchange of ammonia between the atmosphere and plant communities. *Adv. Ecol. Rs.*, 24: 301-389.
- Sutton M.A., Tang Y.S., Miners B., Fowler D., 2001. A new diffusion denuder system for long-term, regional monitoring of atmospheric ammonia and ammonium. *Water Air Soil Pollut. Focus* (1):145-156.
- Van der Weerden T.J., Jarvis S.C., 1997. Ammonia emission factors for N fertilizers applied to two contrasting grassland soils. *Environ. Pollut.*, 95: 205-211.
- Whitehead J., Twigg M., Famulari D., Nemitz E., Sutton M.A., Gallagher M.W., Fowler, D., 2008. Evaluation of Laser Absorption Spectroscopic Techniques for Eddy covariance Flux Measurements of Ammonia. *Environ. Sci. Technol.*, 42: 2041-2046.
- Wulf S., Maeting M., Clemens, J., 2002. Application Technique and Slurry Co-Fermentation Effects on Ammonia, Nitrous Oxide, and Methane Emissions after Spreading: I. Ammonia Volatilization. *J. Environ. Qual.*, 31: 1789-1794.
- Wyers G.P., Otjes R.P., Slanina J., 1993. A continuous-flow denuder for the measurement of ambient concentrations and surface exchange fluxes of ammonia. *Atmos. Environ.*, 27A: 2085-2090.
- Zahniser M.S., Nelson D.D., McManus J.B., Shorter J.H., Herndon S., Jimenez R., 2005. Development of a Quantum Cascade Laser-Based Detector for Ammonia and Nitric Acid. Final Report, U.S. Department of Energy, SBIR Phase II, Grant No. DE-FG02-01ER83139.



# The use of crop coefficient approach to estimate actual evapotranspiration: a critical review for major crops under Mediterranean climate

Paola Lazzara<sup>1</sup>, Gianfranco Rana<sup>1</sup>

**Abstract:** The Mediterranean region is greatly affected by water problems; often it must be faced with scarcity, pollution, conservation, sanitation and management of resources. Presently, most of the countries of basin Mediterranean have to deal with major problems related to water shortage for agriculture. The misuse of water due to either low efficiency of irrigation or inadequate irrigation scheduling can lead to loss of water, resulting in higher production costs and/or negative environmental impacts. Matching water supply and demand are essential for productivity and sustainability in any irrigation scheme. Then, knowledge of crop-water requirements is crucial for water resources management and planning in order to improve water-use efficiency. The procedure most widely used by agronomists for the estimation of crop water requirements is the FAO-56 methodology that is based on the estimation of actual crop evapotranspiration ( $ET_c$ ) by evaluation of the reference grass evapotranspiration ( $ET_0$ ) and the estimation of crop coefficients ( $K_c$ ), by means the relation  $ET_c = K_c \times ET_0$ . The FAO 56 bulletin (1998) gives the values of crop coefficients to be used for many agricultural crops, both herbaceous and orchard. In this paper, we make a detailed analysis of the most important international scientific literature about  $K_c$ , experimentally measured as ratio between  $ET_c$  and  $ET_0$ , with the purpose of understand both the reliability and accuracy of this method for arid e semi-arid climate. We compared the experimental values of  $K_c$  obtained by the single or dual crop coefficient approach and the values given by the FAO 56 bulletin for the main spread crops in Mediterranean climate. From this review appears that there is an acceptable agreement between the  $K_c$  values measured and the ones tabulated only for specific cases; in many cases corrections is strongly necessary. Both the single and basal crop coefficient is affected by variability based on climate conditions and crop's management. Also, it was observed very important inter-annual variability explained by different weather conditions over years. Besides, the dual crop coefficient approach is not very frequent, because it requires the measurement or computation of more variables and processes. In conclusion, the  $K_c$  approach (single and dual) is a model that needs more improvement and more experimental data, in fact, it was evaluated for a few crops only in the 10% of the countries of Mediterranean area, in particular for herbaceous crop. Very few works are devoted to computation of the  $K_c$  for orchard and tall crops, the most profitable in this region.

**Keywords:** reference evapotranspiration, dual crop coefficient, arid climate, semi-arid climate, crop water requirements.

**Riassunto:** Nel bacino del Mediterraneo, da sempre afflitto da problemi di scarsità idrica, l'acqua rappresenta un problema in termini di approvvigionamento, gestione, controllo dell'inquinamento e risanamento. Ad oggi, l'agricoltura rappresenta il settore che risente maggiormente dei problemi legati alla risorsa idrica e alla sua scarsità. Una bassa efficienza dell'irrigazione e/o un'inadeguata programmazione possono comportare un uso improprio e perdite di acqua con conseguenti alti costi di produzione e negativi impatti sull'ambiente. In ogni schema irriguo l'incontro tra domanda e offerta e l'esatta conoscenza dei fabbisogni idrici delle colture risulta essenziale per una corretta gestione della risorsa idrica e per un miglioramento dell'efficienza d'uso dell'acqua che assicuri produttività e sostenibilità. Il metodo FAO 56, attualmente, è la procedura più ampiamente usata per la stima dei fabbisogni idrici delle colture agrarie. Esso è basato sulla stima dell'evapotraspirazione culturale effettiva ( $ET_c$ ), mediante la valutazione dell'evapotraspirazione di riferimento ( $ET_0$ ) e la stima del coefficiente culturale ( $K_c$ ) secondo la relazione:  $ET_c = K_c \times ET_0$ . Il quaderno FAO 56 (1998) riporta i valori del coefficiente culturale di un ampio numero di colture, erbacee ed arboree. Nel presente studio s'intende verificare l'affidabilità e l'accuratezza di questo metodo per il clima mediterraneo. A tale scopo sono stati confrontati i valori di  $K_c$  riportati nella letteratura scientifica internazionale, ottenuti sperimentalmente come rapporto tra  $ET_c$  e  $ET_0$  seguendo l'approccio del coefficiente culturale singolo o duale, e i valori riportati nel quaderno FAO 56 per le colture tipicamente coltivate in ambiente mediterraneo. Da questa analisi risulta che, solo in pochi casi, si può ritenere accettabile l'accordo tra i valori di  $K_c$  misurati e quelli tabellati; nella maggior parte delle situazioni sono necessarie delle correzioni. Per diverse culture, e sistemi culturali, è risultata una variabilità del coefficiente culturale singolo o duale dovuta sia alle condizioni climatiche sia alle pratiche culturali. È stata anche osservata un'interessante variabilità interannuale del  $K_c$  spiegata dalle differenti condizioni climatiche riscontrate negli anni. L'approccio del coefficiente culturale duale non risulta molto utilizzato, perché esso richiede il calcolo di molte variabili e processi. Va rilevato, infine, che la stima dell'evapotraspirazione basata sull'approccio del  $K_c$  (singolo o duale) necessita di ulteriori dati sperimentali, infatti, il coefficiente culturale è stato valutato in appena il 10% dei Paesi del Mediterraneo e per poche colture, la maggior parte delle quali erbacee. Risultano esigui, ancora, i lavori dedicati alla misura del  $K_c$  per le colture arboree da frutto, le più redditizie in questa regione.

**Parole chiave:** Evapotraspirazione di riferimento, coefficiente culturale duale, clima arido e semi-arido, fabbisogno idrico.

<sup>1</sup> Corresponding author e-mail: gianfranco.rana@entecra.it

<sup>1</sup> CRA- Research Unit for Agricultural in Dry Environments, Bari, Italy  
e-mail: paola.lazzara@entecra.it



## 1. INTRODUCTION

In Mediterranean region, submitted to arid and semi-arid climate, water is a limiting factor for worthwhile agriculture, in terms both of overall amount and intermittence and/or irregularity of rainfall events throughout crops' growing season. In this context, irrigation (full or supplementary) of the crops is needed for providing best level of production. However, water is a scarce natural resource and agriculture represents the major water consumption at global scale, thus, proper irrigation scheduling has to be employed by the producers for exploring water saving measures.

The misuse of water due to either low efficiency of irrigation or inadequate irrigation scheduling can lead to loss of water, resulting in higher production costs and negative environmental impacts. Matching water supply and demand are essential for productivity and sustainability in any irrigation scheme. Moreover, knowledge of crop water requirements is crucial for water resources management and planning in order to improve water use efficiency (i.a. Hamdy and Lacirignola, 1999; Katerji and Rana, 2008).

Crop water requirements vary during the growing period, mainly due to variation in crop canopy and climatic conditions, and related to both cropping technique and irrigation methods. About 99% of the water uptake by plants from soil is lost as evapotranspiration (ET), so, it can be stated that the measurement of actual crop evapotranspiration ( $ET_c$ ) for the whole vegetative cycle is equal to the water requirement of the given crop. Actual ET knowledge is necessary for sustainable development and environmentally sound water management in the Mediterranean region. However, overestimation of water consumption is very common practice in this region (Shideed *et al.*, 1995), causing both waste of water and harmful impacts on economic, social and environmental levels (Katerji and Rana, 2008). Then, a correct knowledge of  $ET_c$  allows improved water management by changing the volume and frequency of irrigation to meet the crop requirements and to adapt them to soil characteristics.

ET can be measured or modelled by more or less complex techniques. Usually, for practical purposes at local-field scale the evapotranspiration is estimated by models usable for the same crop in sites in the same region. The most known and used technique to estimate ET is the one based on the  $K_c$  approach (Allen *et al.*, 1998) where the  $ET_c$  is calculated by using standard agro-meteorological variables and a crop-specific coefficient, the crop coefficient  $K_c$ , which should take into account the relationship between atmosphere, crop physiology and agricultural practices (Katerji and Rana, 2006).

Since this method is really very used both at research and practical level and since there is a lot of papers (scientific and popular ones) on it, some questions arise: is this method really reliable to accurately determine  $ET_c$ ? Furthermore: are the  $K_c$  values site dependent? Are the  $K_c$  values weather dependent?

The present work, basically made by studying the huge literature about the  $K_c$ , tries to contribute to answer to the above questions. Here, we analyzed the  $K_c$  values found in literature for the main crops cultivated in countries submitted to Mediterranean climate. The main objective of this work is to compare the experimental  $K_c$  and the values given by the FAO 56 bulletin (Allen *et al.*, 1998) for the main spread crops in Mediterranean climate.

## 2. METHODS FOR CALCULATING ACTUAL EVAPOTRANSPIRATION WITH $K_c$ APPROACH

For operational and practical purposes, the water consumption of a crop ( $ET_c$ ) is evaluated as a fraction of the reference crop evapotranspiration ( $ET_o$ ):  $ET_c = K_c ET_o$ , where  $K_c$  is the "crop coefficient", which takes into account the differences existing between a standard crop taken as reference (as grass, alfalfa) and the real crop under study.

The reference evapotranspiration  $ET_o$  can be:

- Directly measured on a reference surface (well-watered grass meadow, free water in a standard pan);
- Estimated from a semi-empirical formulation based on an analytical approach;
- Estimated from empirical formulation based on a statistical approach.

In order to make procedures and results comparable worldwide, a well-adapted variety of clipped grass has been chosen to measure  $ET_o$ . It must be 8 to 16 cm in height, actively growing and in well-watered conditions, subject to the same weather as the crop for which the water consumption has to be estimated. The reference crop should be adequately extended to avoid the oasis effect. This effect is due to different climatic or moisture condition of reference crop with respect to surroundings, for example vegetation well watered in dry land. This condition has effect on radiative and energetic balance. Net radiation in excess of latent heat is converted into sensible heat that is advected toward the vegetation well watered, resulting in an increase of ET relative to the surrounding crop. This overestimation of ET could be particularly important under a high radiative climate, as in the Mediterranean region. Regard to  $K_c$  values, this should adjust by means of exact estimation of the wind velocity, relative humidity,



height of vegetation of interest and by parameters expressing the aridity of surrounding area.

$ET_o$  can be measured directly (by means of a weighing lysimeter) or indirectly measured with a micro-meteorological method (Rana *et al.*, 1994; Allen *et al.*, 1996; Steduto *et al.*, 1996; Ventura *et al.*, 1999; Todorovic, 1999; Howell *et al.*, 2000).

The difficulty of measuring directly  $ET_o$  in a grass meadow led to the use of evaporation pans, in this case we speak about reference evaporation  $E_o$ . It is easy to obtain the evaporation rate from those pans. The pan evaporation data routinely measured with simple equipment at meteorological stations (but, which requests maintenance and management accurate) are used to estimate reference  $E_o$ , using a simple proportional relationship:  $E_o = K_p E_{pan}$ , where,  $K_p$  is dependent on the type of pan involved and the pan environment in relationship to nearby surfaces and the climate.

Although the pan responds in a similar way to the same climatic factors affecting crop transpiration, several factors produce significant differences in loss of water from a water surface and from a cropped surface. The main shortcomings can be summarised as following (Riou, 1984): a) The heat exchange between pan and soil is not negligible; b) The underground pans are very sensitive to the surrounding environment; c) The need to maintain a sufficient edge can cause a wind break effect, which can disturb the evaporation in a way that is difficult to estimate; d) During the night the water usually gets cold on the surface, causing convective flows which can cause the warm water to rise to the surface with consequent possible evaporation.

Doorenbos and Pruitt (1977) provided detailed guidelines for using pan data of estimate reference  $E_o$  to obtain values of  $ET_o$ . These formulations are generally based on the physical laws concerning the energy balance and the convective exchange on a well irrigated grass surface. An empirical element is introduced in these formulations to facilitate their calculation, starting from data collected in standard agro-meteorological stations. These stations are usually situated so as to be representative of the catchment, i.e. an area of several kilometres in extension. The main formulas in this case are: 1. Penman formula and its by-product; 2. the Penman-Monteith formula proposed by Allen *et al.* (1998). The first approach generally is called "corrected Penman" and it includes several formulas. The most commonly used corrected formula is the one proposed by Doorenbos and Pruitt (1977). It was considered in the FAO 24 bulletin. The second approach was adopted in FAO 56 bulletin, it represent an upgrade of the Doorenbos and Pruitt

technique and nowadays it is widely used as the standard approach for estimating reference ET. The introduction of the atmometer can overcome the management problems of pan evaporimeters (refill of water, development of algae, interference of animals and so on) as recently stated by many authors (see for example Magliulo *et al.*, 2003).

The Penman-Monteith approach is a reliable, physically based method and it is a close, simple representation of the physical and physiological factors governing the evapotranspiration process.

Reference evapotranspiration concept was revised during the last decade resulting in the introduction of the standardized computational procedures by two groups of scientists: the FAO Expert Group on the Revision of FAO Methodologies for Crop Water Requirements, which published the FAO 56 bulletin (Allen *et al.*, 1994a; Allen *et al.*, 1994b; Allen *et al.*, 1998), and the ASCE-EWRI (American Society of Civil Engineers-Environmental Water Resources Institute) Task Committee on Standardization of Reference Evapotranspiration, which realized a report on standardized reference evapotranspiration (Allen *et al.*, 2005).

But the climate data required in the Penman-Monteith equation are not always available, especially in developing regions. Therefore, many simpler methods have been used and tested in some areas.

Blaney-Criddle (1950) and Hargreves-Samani (1982, 1985), for example, are empirical methods that require only temperature data.

The concept of  $K_c$  was introduced by Jensen (1968) and further developed by the other researchers (Doorenbos and Pruitt, 1975, 1977; Burman *et al.*, 1980a, Burman *et al.*, 1980b; Allen *et al.*, 1998). The crop coefficient is the ratio of the well watered crop evapotranspiration ( $ET_c$ ) to reference crop evapotranspiration ( $ET_o$ ) and it integrates the effects of characteristics that distinguish field crops from grass, like ground cover, canopy properties and aerodynamic resistance. The estimation of  $ET_c$  relies on the so called two steps approach, where  $ET_o$  is determined and  $ET_c$  is calculated as the product of  $ET_o$  and the  $K_c$  for the same day. Reference evapotranspiration is loss of water by a "standard" canopy that is a specific crop with fixed characteristics of height, ground cover and growing in well-watered conditions, subject to the same weather as the crop whose consumption is to be estimated. Instead, the crop coefficient accounts for crop characteristics and management practices (e.g., frequency of soil wetness). It is specific for each vegetative surface and it evolves in function of the development stage of the crop considered. Evapotranspiration varies in the



course of the season because morphological and eco-physiological characteristics of the crop do change over time.

The FAO and WMO (World Meteorological Organization) experts have summarised such evolution in the “crop coefficient curve” to identify the  $K_c$  value corresponding to the different crop development and growth stages (initial, middle and late, hence it has  $K_{c\text{ in}}$ ,  $K_{c\text{ mid}}$ ,  $K_{c\text{ end}}$ ) (Tarantino and Spano, 2001). Values of  $K_c$  for most agricultural crops increase from a minimum value at planting until a maximum  $K_c$  is reached at about full canopy cover. The  $K_c$  tends to decline at a point after a full cover is reached in the crop season. The declination extent primarily depends on the particular crop growth characteristics (Jensen *et al.*, 1990) and the irrigation management during the late season (Allen *et al.*, 1998), when it is often submitted to senescence. A  $K_c$  curve is the seasonal distribution of  $K_c$ , often expressed as a smooth continuous function.

For irrigation scheduling purposes, daily values of crop  $ET_c$  can be estimated from crop coefficient curves, which reflect the changing rates of crop-water use over the growing season, if the values of daily  $ET_o$  are available. FAO 56 bulletin (Allen *et al.*, 1998) presents a procedure to calculate  $ET_c$  using three  $K_c$  values that are appropriate for four general growth stages (in days) for a large number of crops. In the single crop coefficient approach, the effect of crop transpiration and soil evaporation are combined into a single  $K_c$  coefficient. The coefficient integrates differences in the soil evaporation and crop transpiration rate between the crop and the grass reference surface. As the soil evaporation may fluctuate daily as a result of rainfall or irrigation, the single crop coefficient express only the time-averaged (multi-day) effects of crop evapotranspiration. In the dual crop coefficient approach, the effect of specific wetting events on the value of  $K_c$  and  $ET_c$  is determined by splitting  $K_c$  into two separate coefficients: one for crop transpiration, i.e., the basal crop coefficient ( $K_{cb}$ ) representing the transpiration of the crop; and another for soil surface evaporation, the soil water evaporation coefficient ( $K_e$ ). The single  $K_c$  coefficient is replaced by  $E_q$ :  $K_c = K_{cb} + K_e$ .

The basal crop coefficient,  $K_{cb}$ , is defined as the ratio of  $ET_c$  and  $ET_o$  when soil water evaporation is minimal, but soil water availability remains non-limiting to plant transpiration. As the  $K_c$  values include averaged effects of evaporation from the soil surface, the  $K_{cb}$  values lie below the  $K_c$  values. The soil evaporation coefficient,  $K_e$ , describes the evaporation component from the soil surface.

To take account of water stress,  $K_{cb}$  or  $K_c$  are

multiplied by a coefficient  $K_s$  which is equal to 1.00 till half the available water is used up and which then declines linearly to zero when all the available water in the rooting zone has been used up. Hence,

$$ET_c = (K_c K_s) ET_0 \quad (1)$$

$$ET_c = (K_{cb} K_s + K_e) ET_0 \quad (2)$$

The terms in brackets in previous equations is called crop coefficient adjusting,  $K_{c\text{ adj}}$ . Because the water stress coefficient impacts only crop transpiration, rather than evaporation from the soil, the application using the equation (2) is generally more valid than application using the equation (1). Allen *et al.* (1998) reported that in situations where evaporation from soil is not a large component of  $ET_c$ , use of equation (1) will provide reasonable results.

In the FAO 56 bulletin are reported both  $K_c$  and  $K_{cb}$  values corresponding at the three grown stages for many crops. These latter values have been obtained by a limited number of experiments carried out in Arizona and Eastern Europe.

To make the use of  $K_c$  operational, research and experiments have been carried out worldwide, and they have led to determination of the average value that  $K_c$  may take in the course of the season over the years (Grattan *et al.*, 1998). It is worth highlighting that the  $K_c$  is affected by all the factors that influence soil water status, for instance, the irrigation method and frequency (Doorenbos and Pruitt, 1977; Wright, 1982), the weather factors, the soil characteristics and the agronomic techniques that affect crop growth (Stanghellini *et al.*, 1990; Tarantino and Onofrii, 1991; Cavazza, 1991; Annandale and Stockle, 1994). Consequently, the crop coefficient values reported in the literature can vary even significantly from the actual ones if growing conditions differ from those where the said coefficients were experimentally obtained (Tarantino and Onofrii, 1991).

Ko *et al.* (2009) and Piccinni *et al.* (2009) observe that  $K_c$  values can be different from one region to the other. It is assumed that the different environmental conditions between regions allow variation in variety selection and crop developmental stage which affect  $K_c$  (Allen *et al.*, 1998). Elevated air temperatures and water vapour pressure deficit over the growing seasons can cause temporal and transient leaf stomata closure (Baker *et al.*, 2007; Bruce, 1997; Cornic and Massassi, 1996), impeding plants to transpire at its full potential.

The use of  $K_c$  developed in other regions with respect to those where it is calculated will not meet accurate crop water requirement and it results in either increased production costs due to over-irrigation or

N.	Crops		N.	Crops	
1	Alfalfa	<i>Medicago sativa</i> L.	13	Melon	<i>Cucumis melo</i> L.
2	Broad bean	<i>Vicia faba</i> L.	14	Olive	<i>Olea Europea</i> L.
3	Cauliflower	<i>B. oleacea</i> L. var. <i>botrytis</i>	15	Onion	<i>Allium cepa</i> L.
4	Citrus	<i>Citrus</i> sp.	16	Peach	<i>Prunus persica</i> L.
5	Cotton	<i>Gossypium hirsutum</i> L.	17	Potato	<i>Solanum tuberosum</i> L.
6	Cowpea	<i>Vigna unguiculata</i> (L.) Walp.	18	Red Cabbage	<i>B. oleacea</i> L. var. <i>rubra</i>
7	Flax	<i>Linum usitatissimum</i> L.	19	Sorghum	<i>Sorghum bicolor</i> L.
8	Garlic	<i>Allium sativum</i> L.	20	Soybean	<i>Glycine max</i> L. Merrill
9	Grapevine	<i>Vitis vinifera</i> L.	21	Sweet pepper	<i>Capsicum annuum</i> L.
10	Green bean	<i>Phaseolus vulgaris</i> L.	22	Tomato	<i>Lycopersicon esculentum</i> , Mill.
11	Lettuce	<i>Lactuca sativa</i> L.	23	Watermelon	<i>Citrullus lanatus</i> L.
12	Maize	<i>Zea mays</i> L.	24	Wheat	<i>Triticum vulgare</i> L.

**Tab. 1** - Crops object of the review.

*Tab. 1 - Coltura oggetto della review.*

reduced profits due to deficit irrigation. However, the development of regionally based  $K_c$  could greatly help in irrigation management and furthermore provides precise water applications in those areas where high irrigation efficiencies should be achieved.

### 3. THE REVIEW OF $K_c$ VALUES

We started this study by reviewing the literature in order to investigate the variability of crop coefficient values of the more widespread crops in Mediterranean area compared to those reported in the FAO 56 bulletin. This research would highlight all the factors affecting the  $K_c$  experimental values, such as cultivar type, agronomics techniques (i.e. fertilizing, pruning, tillage, mulch and greenhouse), measurement or estimating methods of  $ET_c$  and  $ET_o$  and irrigation methods and management. We consulted the international (and a few national) recent scientific papers relative to areas of the world characterized by Mediterranean climate. This selection assures the reliability of the  $K_c$  values, but it limits the number of countries and of crops found. Table 1 reports the crops investigated (24); the countries involved in the study are: California, Chile, Italy, Jordan, Lebanon, Morocco, Portugal, Spain, Texas and Turkey.

The Table 1 shows that the number of investigated crops is quite adequate to draw important observations on use of  $K_c$  as practical tool for estimating water requirements. Moreover, Citrus, Tomato, Peach, Maize and Melon crops present the major number of variety and cultivars. Furthermore, all studied crops well represent the Mediterranean agriculture in terms of dates of transplanting, density and spacing of plantation, cover fraction, fertilization, pest and weed control, maximum height of the crops.

Spain (7 works) and Italy and California (5 works each) are the countries which have most scientific studies on crop ET and  $K_c$ , followed by Texas, Turkey and Portugal (3 works). All the countries are characterized by Mediterranean climate, varying from temperate to semi-arid and arid.

The studies show that for the more important crops in Mediterranean area the more used irrigation methods are drip (surface and subsurface) and sprinkler ones. This observation reflects the increasing sensitivity of the users towards police of saving water, since this irrigation method allows improving irrigation efficiency.

In all examined papers (34), several measure or estimate methods have been used by authors to determine  $ET_c$ ,  $ET_o$  and hence  $K_c$ . Also the temporal scale adopted changes from work to work, therefore  $K_c$  values obtained are relative to daily, monthly or seasonal interval for different crops. For this reason, the relationship between the empirical and FAO-56  $K_c$  values is not often easy and immediate, although the same authors provide useful information for the comparison.

The reference evapotranspiration in the most of cases is estimated by FAO-56 Penman-Monteith equation (40% of the cases). Other models of estimation, like those proposed in the FAO 24 bulletin (Blaney-Criddle (1950), radiation (Priestley and Taylor, 1972) and modified Penman), CIMIS Penman equation and ASCE Penman-Monteith equation are used in a few cases. Often, the reference evapotranspiration is measured. The most used methods are Class A pan and weighing lysimeter (40% and 26% of the all cases, respectively), then, other measurement methods occur rarely, like atmometer and evaporimeter. In these methods, when a reference surface is used, a

Crop	Type-variety	K <sub>c</sub>			N. years	Irrigation method	Country		Reference
		Initial	Middle	End			Season		
<b>a. Small vegetable</b>									
Cauliflower	<i>B. oleracea</i> L. var. botrytis				0.84	1	Ponding	Turkey	Erzurum
Red Cabbage	<i>B. oleracea</i> L. var. rubra				0.83	1			Sahin et al., 2009
<b>FAO-56</b>		1.05	0.95						
Garlic	cv. California Early	0.8	1.2-1.3	0.7		1	Center-pivot	Spain	Guadaluquivir V, (Cordoba, Ecia)
	cv. Chinese			0.91-0.94		1			Villalobos et al., 2004
<b>FAO-56</b>		1	0.7						
Lettuce	var. Capitata cv. XP 6256	0.3			0.6	1	Drip	Chile	Santiago
<b>FAO-56</b>		1		0.95		1			Manuel-Casanova et al., 2009
Orion	cv. Graniero	0.65	1.2	0.75		1	Sprinkler	Spain	Albacete
<b>FAO-56</b>		1	0.75						Lopez-Urrea et al., 2009
<b>b. Vegetables – Solanaceae (Solanaceae)</b>									
		0.6	1.15	0.8		2	Furrow	Chile	Maulé region
	cv. Pull	1.1	1.3	0.8		1	Drip	Italy	Puglia
	Hybrid FS 1296	0.8	1.2	0.9		1			Rinaldi and Rana, 2004
<b>Tomato</b>									
		0.81	0.44	0.47	0.7	2	Drip with mulch	Jordan	Jordan Valley
		0.83	0.47						Amayreh and Al-Abed, 2005
		0.36	0.77-1.2	0.74					
	Processing Tomato	0.19	0.99-1.08	0.6		4	Drip	Algeria	Bechar, Tamanrasset
		0.19	0.9-1.15	0.7		2	Drip with mulch	California	Hanson and May, 2005
<b>FAO-56</b>		1.15-1.2	0.7-0.9						Vazquez et al., 2005
Sweet pepper	cv. Drago Lanuayo type	0.2	1.3	0.9		2	Drip	Spain	Ebro Valley
<b>FAO-56</b>		1.05	0.9						
<b>c. Vegetables - Cucurbitaceae (Cucurbitaceae)</b>									
<b>Melon</b>	cv. Categoría (supported)	0.2	1.1	1		2	Drip	Spain	Almería
	cv. Eros Gallia type (not supp.)	0.2	1.3	1.1		1			Orgaz et al., 2005
	var. Inodorus, cv. Nabucco	0.1	0.75	0.5		2	Drip whit mulch	Italy	Basilicata
<b>FAO-56</b>		0.15	0.85	0.6					Lovelli et al., 2005
<b>Watermelon</b>	cv. Reina de Corazones	0.2	1.1	1		1	Drip	Spain	Almería
<b>FAO-56</b>		0.4	1	0.75					Orgaz et al., 2005
<b>d. Roots and Tubers</b>									
Potato	cv Desirée class AA1				0.87	2	Sprinkler	Portugal	Braganca
<b>FAO-56</b>		1.15	0.75		0.85				Ferreira and Carr, 2002
<b>e. Legumes</b>									
Cowpea	California Blackeye N.46		1.28			2	Subsurface drip	California	San Joaquin Valley
<b>FAO-56</b>		0.4	1.05	0.6-0.35					DeTar, 2009
Broad bean		0.37	1.05						
<b>FAO-56</b>		0.5	1.15	1.1					
Green bean	cv. Helda	0.2	1.4	1.2		2	Drip	Spain	Almería
<b>FAO-56</b>		0.5	1.05	0.9					Orgaz et al., 2005
Soybean	cv. Asgrow A-3803	0.62	1	0.66	0.7	2	Sprinkler -Drip	Lebanon	Bekaa Valley
<b>FAO-56</b>		0.4	1.15	0.5					Karam et al., 2005

**Tab. 2** - Crop coefficient, K<sub>c</sub>, values reported by the bibliographies and FAO-56 K<sub>c</sub> values.  
 Tab. 2 - Valori del coefficiente colturale, K<sub>c</sub>, riportati nella bibliografia consultata e nel quaderno FAO 56.

it follows

g. Fibre Crops							
<b>Flax</b>	cv. Mikael	0.4	0.9	0.2	1		Viterbo
<b>FAO-56</b>		0.35	1.1	0.25			Casa et al., 2000
<b>Cotton</b>	DP555	0.4-0.5	1.25	0.6-0.1	0.2-1.5	3	Sprinkler
		0.8	1.13			1	Texas
		0.1-0.9	0.5-1			2	Furrow, drip
<b>FAO-56</b>		0.35	1.15 - 1.2	0.7-0.5			Turkey
<b>i. Cereals</b>							
	cv. Juanita			0.88	2		
<b>Maize</b>	cv. Pioneer PR34N43	0.48	1.28	0.35		Sprinkler	
	0.59	1.27	0.35		2	Spain	Ebro River Valley
	32H39, 30G54	0.35	1.2	0.9		Texas	Uvalde
<b>FAO-56</b>		0.3	1.2	0.6-0.35			
<b>Wheat</b>	Ogallala, TAM203	0.53	1.1	0.4	3	Sprinkler	
<b>FAO-56</b>		0.7	1.15	0.25-0.4	Winter Wheat (with non-frozen soils)	Texas	Coastier plain
<b>Sorghum</b>	DKS54	0.4	0.8	0.75	2	Sprinkler	
<b>FAO-56</b>		0.3	1-1.10	0.55	Sorghum grain	Texas	Coastier plain
<b>m. Grapes and Berries</b>							
	cv. Tom. Seedless clone 2A	0.2	0.9-1.3		1		
<b>Grapevine</b>	cv. Thompson Seedless	0.87			Drip	California	S. Joaquin V.
		1.08					Williams and Ayars, 2005
		0.98			3		
<b>FAO-56</b>		0.3	0.7	0.45	Drip	California	S. Joaquin V.
<b>n. Fruit tree</b>							
	Mandarin	0.45	0.6	0.5	0.52	Drip	Marrakech
<b>Citrus</b>	Orange tree	0.58	0.55	0.6		Flood	
	Citrus reticulata Blanco			0.8	1	Micro-sprayers	Er-Raki et al., 2009
	Clementine	0.8	1.2	0.8		Italy	Barbagallo et al., 2009
<b>FAO-56</b>		0.75	0.7	0.75	0.44	2	Catania Plain
	(var. Maybelle)	0.65	0.6	0.65	0.43	3	Villalobos et al., 2009
<b>Peach</b>	cv. Silver King				Drip	Spain	
	cv. O'Henry	0.98-1.06				Mazagon	
<b>FAO-56</b>		0.55	0.9	0.65	1	Apulia	Rana et al., 2005
<b>Olive</b>	cv. Arbequino				0.6-0.5	1	
	Agdal	0.65	0.45	0.65	0.5	Drip	Aguas de Moura
<b>FAO-56</b>		0.65	0.7	0.7	3	Portugal	Ferreira et al., 1996
					2	Drip	Atalaia, Montijo
<b>Peach</b>	cv. Silver King						Pago et al., 2006
	cv. O'Henry	0.98-1.06			3	Drip	S. Joaquin V.
<b>FAO-56</b>		0.55	0.9	0.65		California	Ayars et al., 2003
<b>Olive</b>	cv. Arbequino				3	Drip	Testi et al., 2004
	Agdal	0.65	0.45	0.65	2	Flood	Cordoba
<b>FAO-56</b>		0.65	0.7	0.7		Spain	Marrakech
							Er-Raki et al., 2008

generic grass is considered and the management indicated by FAO 56 bulletin and following improvement of ASCE Standardized Reference Evapotranspiration Equation (Allen *et al.*, 2005) to distinguish  $ET_0$  for both short and tall reference crop are taken into account.

With regard to actual crop evapotranspiration, it is measured in the majority of cases. The more spread method is the micrometeorological technique eddy covariance (36% of the total), followed by both the weighing lysimeter and soil water balance methods (33% and 16% of the total respectively). Rarely, other micrometeorological approaches (Bowen ratio), plant physiology approach (sap flow technique) and surface energy balance by data of remote sensing and satellite are used (e.g. Barbagallo *et al.*, 2009; Er-Raki *et al.*, 2008). In our opinion and following many authors (see for a synthesis Rana and Katerji, 2000; Katerji and Rana, 2008), the micrometeorological methods present features able to measure evapotranspiration at plot scale with good accuracy. Punctual methods (as sap flow) can have good accuracy if a suitable scaling-up technique is used. While methods based on remote sensing satellite data for estimating ET at plot scale could be affected by big errors if a suitable downscaling technique is not used or the resolution of images is small.

In the majority of the studies, the  $K_c$  values are obtained by the single crop coefficient approach, where the effect of crop transpiration and soil evaporation are combined into a single  $K_c$  coefficient. In some cases (e.g. Amayreh and Al-Abed, 2003; Barabagallo *et al.*, 2009; Er-Raki *et al.*, 2009; Ferreira *et al.*, 1996; Paço *et al.*, 2006; Villalobos *et al.*, 2004) the FAO-56  $K_c$  values were corrected for specific climatic and weather condition, as recommended by Allen *et al.* (1998) in FAO 56 bulletin. Infrequently, the dual crop coefficient approach is used, where the effects of crop transpiration and soil evaporation are determined independently (Lopez-Urrea *et al.*, 2009; Casa *et al.*, 2000; Benli *et al.*, 2006; Er-Raki *et al.*, 2009; Paço *et al.*, 2006). Thus, their discussion will deal with in separate sections (section 4 and 5, respectively).

#### 4. COMMENTS ON THE $K_c$ VALUES BY THE SINGLE CROP COEFFICIENT APPROACH

Table 2 reports the experimental crop coefficient values and those presented by FAO 56 bulletin. In the table the crops are subdivided as within FAO 56 bulletin (see table 12 of this technical paper).

It seems to be clear that the variability of the  $K_c$

values is mainly related to irrigation methods, mulching practice, growth in greenhouse, indicators of the development of the crops, such as both leaf area (LAI) and ground cover (GC) indexes. In general, when LAI and GC factors were taken into account the estimate of  $K_c$  resulted more accurate. Regarding the  $K_c$  values as indicated by FAO 56 bulletin, these were both underestimated or overestimated with respect to the measured ones. In particular, underestimation of FAO-56  $K_c$  is clearly observed for cauliflower, red cabbage, lettuce, melon, broad bean, wheat and clementine crops, while overestimation can be noted for garlic, melon (one cultivar), cowpea, green bean, cotton, grape wine and peach crops. The same  $K_c$  values of FAO 56 bulletin were found by authors only for a few crops or cultivars, such as tomato crop grown in both Italy and Chile, mandarin crop grown in Morocco and flax in Italy. Some crops present the measured  $K_c$  values equal to FAO-56  $K_c$  only for a specific grown stage. Ko *et al.* (2009) and Piccinni *et al.* (2009), in fact, show as some of the  $K_c$  values for cotton, wheat, maize and sorghum crops corresponded and some did not correspond to those reported by FAO 56 bulletin. The Authors consider necessary the development of regionally based and growth-stage-specific  $K_c$ .

Crop coefficient values different with respect to the theoretical FAO-56 were found by Rinaldi and Rana (2005) for tomato crop in Southern Italy. In particular the  $K_c$  value corresponding to middle growth stage is greater than FAO-56  $K_c$  of 0.13 and 0.03 for two varieties of tomato crop respectively. Here, the Authors highlight that the use of single crop coefficient approach underestimates the water use of tomato crops of 58 mm in one irrigation season.

The influence of the irrigation system and the use of mulch on crop water requirement is underlined by Amayreh and Al-Abed (2005) and Lovelli *et al.* (2005). The first authors studied the behaviour of crop coefficient for field-grown tomato under drip irrigation system with black plastic mulch. This study reports measured  $K_c$  values far below the FAO-56 values by about 31% and 40% for  $K_{cmid}$  and  $K_{cend}$ , respectively. This means that there is a 36% reduction in the crop coefficient over the entire growing season, excluding initial stage, compared to the FAO-56 corresponding value. These low experimental  $K_c$  values reflect the effect of practicing both localized drip irrigation and plastic covering mulch which are common practices in the Jordan Valley agricultural area. On the other hands, these results are in accordance with the general FAO recommendation of reducing the FAO-56  $K_c$



values by 10–30% when using plastic mulches (Allen *et al.*, 1998).

Lovelli *et al.* (2005) check the latest update  $K_c$  values proposed by the FAO 56 bulletin to estimate evapotranspiration in the case of muskmelon crop, both with plastic mulches and no mulch. The procedures suggested in FAO 56 bulletin allows an accurate  $ET_c$  estimate in the case of muskmelon cultivated without plastic mulch. For the crop under mulch, a good agreement of the estimated  $K_c$  values with the measured ones is obtained only at the initial stage of the cycle, while at the stage of maximum canopy development the measured values are underestimated with respect to the FAO-56 crop coefficients.

The work by Ferreira and Carr (2002) is interesting because they show the effects of differential irrigation and fertiliser treatments on the water use of potatoes. Soil evaporation and crop transpiration were the major components of the daily soil water balance. Drainage was negligible. For well-fertilised, well-irrigated crops, transpiration was dominant, contributing 75–85% of seasonal  $ET_c$ . For the unfertilised crops, evaporation from the soil surface becomes important, representing up to 50%  $ET_c$  over the same time period. As result of this mutual compensation, the total  $ET_c$  was similar for fertilised and unfertilised crops when irrigated. The season  $K_c$  values reported by authors for fully (0.87–0.85) and partially irrigated (0.62–0.69) and unirrigated treatments (0.4–0.3) are all lower than FAO-56 ones for two years of the experiment, underlining the important effect of irrigation on daily rates of actual evapotranspiration.

Er-Raki *et al.* (2009) use the FAO-56 single crop coefficient approaches to estimate actual evapotranspiration over an irrigated citrus orchard under drip and flood irrigations in Marrakech (Morocco). The results shows that, by using crop coefficients suggested in the FAO 56 bulletin, the performance of both approaches was poor for two irrigation treatments. While, after the determination of the appropriate values of  $K_c$  based on  $ET_c$  measurements by eddy covariance, the performance of both approaches greatly improved. The locally obtained  $K_c$  values were lower than the FAO-56 values by about 20%. The lower obtained  $K_c$  values with respect to the FAO-56  $K_c$  reflect the effects of the drip irrigation practice for one field and the low value of cover fraction for the other field. Additionally, the efficiency of the irrigation practices was investigated by comparing the measured  $K_c$  for two fields. The results showed that a considerable amount of water was lost by direct soil evaporation from the citrus orchard irrigated by flooding technique.

Many researches were direct to study both the water use and development of the crop coefficients for crops grown in greenhouse. In Mediterranean areas, the seasonal  $ET$  of greenhouse horticultural crops is quite low when compared to that of irrigated crops in open air field. This is due, firstly, to a lower evaporative demand inside a plastic greenhouse, which is 30–40% lower than outdoors throughout the entire greenhouse cropping season (Fernandez, 2000). Secondly, greenhouse cultivation in the Mediterranean areas is mostly concentrated in periods of low evaporative demand (autumn, winter and spring), whereas irrigated crops outdoors are often grown during high evaporative demand periods. Orgaz *et al.* (2005) carried out an investigation on the major horticultural crops (melon, sweet pepper, green bean, watermelon) usually cultivated in plastic greenhouse in Spain. In this analysis,  $K_c$  values results to vary by crop, by development stage and by management. Thus, for melon and watermelon greenhouse crops, the mid-season  $K_c$  values proposed for outdoor crops (Allen *et al.*, 1998) appear reasonable. By contrast, mid-season  $K_c$  value for vertically supported greenhouse crops (melon, green bean and sweet pepper) was around 1.3. This  $K_c$  value is higher than those reported for the same crops in Italy (Rubino *et al.*, 1986) and California (Snyder *et al.*, 1987; Grattan *et al.*, 1998), and those proposed by Allen *et al.* (1998) for sub-humid climates, all grown outdoors. The higher  $K_c$  values of the vertically supported greenhouse crops, usually reaching 1.5–2 m in height, is probably due to greater net radiation absorption with respect to the short crops, because of the morphological features. Manuel-Casanova *et al.* (2009) for lettuce grown in greenhouse conditions in Chile report  $K_c$  values lower than those generally adopted for lettuce in field conditions. These differences are due to the complexity of the coefficient which integrates various functions (Katerji *et al.*, 1991; Testi *et al.*, 2004) such as aerodynamic factors linked to crop height, biological factors related to leaf growth and senescence, physical factors linked to soil evaporation, physiological factors of stomata response to the air vapour pressure deficit, and agronomic management factors like distance between rows and irrigation system. Furthermore, in greenhouse conditions, the differences in  $K_c$  can also be attributed to the size of the greenhouse and the substrate used.

Many studies highlight the greater accuracy in the compute of the crop coefficient curves as a function of variables related to crop development: LAI, percent canopy that shades the ground or thermal-



based index, expressed as cumulative growing degree days (GDD). This approach, in fact, is considered an improvement compared to guidelines from FAO 56 bulletin, that proposes to estimate the  $K_c$  values as only function of the length of the four phenological stages in which crop development is divided. Moreover, it is important to exactly estimate the length of each single growth stage since  $K_c$  pattern over time only depends on it (Lovelli *et al.*, 2005).

Other alternative approaches have been proposed over the last years to estimate  $K_c$  curves for annual crops as a function of time in terms of days after sowing (DAS) or month of the year. This method is easy to implement but, as with the FAO methodology, it does not take into account the influence of environmental and cultural factors on the rate of canopy development.

Linear relationships between  $K_c$  and LAI values are reported for green bean and melon by Orgaz *et al.* (2005); for grapevine by Williams *et al.* (2003) and for young olive orchard by Testi *et al.* (2004). In particular, the last authors find that the  $K_c$  values determined in late autumn, winter and spring is usually high, variable and relatively independent of LAI or ground cover; during the summer the soil evaporation decreases and the  $K_c$  is lower, far less variable and LAI-dependent. Since  $K_c$  values are linearly correlated to LAI or ground cover, the authors proposed a linear model to predict it. This model has shown great robustness despite their empirical nature.

Ayars *et al.* (2003) find that the  $K_c$  was a linear function of the amount of light intercepted by peach (*Prunus persica* L.) trees. It could be assumed that as leaf area increases so would the amount of solar radiation intercepted and the amount of  $ET_c$ .

Martinez-Cob (2007) obtains two crop coefficient equations as function of fraction of GDD for corn crop. The use of grown degree days to estimate  $K_c$  curves has the advantage that air temperature data is readily available and there is enough evidence of the influence of such variable on crop development (Ritchie and NeSmith, 1991). In their conclusions, for real time irrigation scheduling, the authors advise of avoid the use of the methodology FAO if it is possible to use GDD to estimate  $K_c$ , since the FAO methodology does not take into account the possible variations of corn development due to different climatic conditions.

DeTar (2009) uses a modified soil water balance method with two independent variables (grown degree days, GDD, and days after planting, DAP) to determine the crop coefficients and water use for cowpea grown in California. During the early part of

the season the crop coefficients were more closely related to DAP than to GDD, for the full season there was very little difference in the correlation for the various models using DAP vs. GDD.

When the study of the crop water requirement is carried out for many years, a variability over years in both measured  $K_c$  and  $ET_c$  values at different temporal scale (grown season, daily, monthly) is found (Williams *et al.*, 2003 for grapevine; Martinez-Cob, 2007 for maize; Ferreira and Carr 2002 for potato; Amayreh and Al-Abed, 2005 for tomato; Testi *et al.*, 2004 for olive orchard). By contrast, Villalobos *et al.* (2009) do not report significant differences for the seasonal  $K_c$  values relate to two years of measurement for citrus orchard grown in Spain.

DeTar (2009) for cowpea in California estimates the crop coefficient computing  $ET_o$  through two methods: P-M equation and Pan evaporation. He finds that the crop coefficients calculated using P-M equation for mid-season 2007 were significantly lower than for mid-season 2005, whereas, there was no significant difference with respect to the pan data for the same time periods.

## 5. COMMENTS ON THE $K_c$ VALUES BY THE DUAL CROP COEFFICIENT APPROACH

Although the studies on dual crop coefficient approach under Mediterranean climate are nowadays not many (Tab. 3), some important considerations can be made.

The dual crop coefficient consists of two coefficients: a basal crop coefficient  $K_{cb}$  and a soil evaporation coefficient  $K_e$ . This procedure, using the separate estimates of the plant and soil components of the crop coefficient, would allow an independent observation of both components and the comparison between them (Paço *et al.*, 2006).

A good evaluation of the amount of water lost by direct soil evaporation needs a partitioning of total evapotranspiration into soil evaporation and plant transpiration components. Therefore, separate and direct measurements of transpiration and soil evaporation are desirable (i.e. through sap flow or isotope measurements) (Williams *et al.*, 2004, Rana *et al.*, 2005). For this reason, the dual crop coefficient is mainly used in research, real-time irrigation scheduling for highly frequent water applications, supplemental irrigation, and detailed soil and hydrologic water balance studies (Allen *et al.*, 1998).

Some studies, carried out in different regions of the world, have compared the results obtained using the approach described by Allen *et al.* (1998) with those



Crop	Type-variety	K <sub>cb</sub>				N. years	Irr.method	Country	Reference
		Initial	Middle	End	Season				
<b>a. Small vegetable</b>									
Onion	cv. Granero	0.6	1	0.65		1	Sprinkler	Spain	Albacete
FAO-56			0.95	0.65					Lopez-Urrea et al., 2009
<b>g. Fibre Crops</b>									
Flax	cv. Mikael	0.7	1.1	0.2		1		Italy	Viterbo
FAO-56			1.05	0.2					Casa et al., 2000
<b>j. Forages</b>									
Alfalfa		0.71	1.78	1.51		3	Sprinkler	Turkey	Plateau Anatolian
FAO-56		0.3	1.15	1.1					Benli et al., 2006
<b>n. Fruit tree</b>									
Citrus	Mandarin	0.35	0.55	0.45			Drip	Morocco	Marrakech
		0.3	0.5	0.4			Flood		
FAO-56		0.6	0.55	0.6					
Peach	cv. Silver King		0.7		0.66	2	Drip	Portugal	Atalaia, Montijo
FAO-56		0.45	0.85	0.6					Paço et al., 2006

**Tab. 3** - Basal crop coefficient,  $K_{cb}$ , values reported in review and  $K_{cb}$  values reported in FAO 56 Bulletin.

Tab. 3 - Valori del coefficiente culturale basale  $K_{cb}$  riportati in bibliografia e nel quaderno FAO 56.

resulting from other methodologies. From this comparison it results that some limitations should be expected in the application of the dual crop coefficient FAO-56 approach. For example, Dragoni *et al.* (2004), measuring actual transpiration in an apple orchard in cool, humid climate (New York, USA), showed a significant overestimation (over 15%) of basal crop coefficients by the FAO-56 method compared to measurements by sap flow technique.

Also, the studies carried out in Mediterranean region showed contrasted results. Casa *et al.* (2000) and Lopez-Urrea *et al.* (2009) reported a good agreement. In particular, the second authors found, for onion crop grow under semiarid conditions, that the dual crop coefficient approach is more reliable than the single crop coefficient, since the high values of evaporative component existed during the entire crop cycle.

In contrast, Benli *et al.* (2006) and Paço *et al.* (2006) reported basal crop coefficients higher than those tabulated. The first authors attribute this difference probably to the difference between the climates. The seconds, for the young peach orchard, indicate a discrepancy between FAO-56 and measured values of  $K_c$  only for the transpiration component of canopy water losses, which would lead to an overestimation of water consumption by 30%. In this case, the soil evaporation component estimates in the crop coefficient were similar to the measured ones.

Er-Raki *et al.* (2009) show the performance of the FAO-56 approach for citrus orchard submitted a two different irrigation methods (drip and flood irrigation). The results suggest that the single crop coefficient approach can be used to derive a good estimate of water consumption of citrus orchards irrigated by the flooding technique with less frequent water applications, while the dual approach can be used for

real-time irrigation scheduling with highly frequent water applications, as in the case of the drip irrigated citrus orchards. These results are in agreement with the recommendations suggested in the FAO 56 bulletin by Allen *et al.* (1998). In general, the dual crop coefficients approach, however, for incomplete cover and/or drip irrigation, seem to be more suited since it is more flexible.

## 6. CONCLUSIONS AND PERSPECTIVES

The use of P-M model for the reference evapotranspiration  $ET_0$  combined with FAO-56 single crop coefficient approach to calculate crop actual evapotranspiration is very spread in the world. However, it was mainly studied and calculated for herbaceous crop; in fact, only few works was devoted to the  $K_c$  for orchard and tall crops. Nowadays, the calculation and the great availability of the data requested by this model are not the biggest problems. However, the comparison between calculated evapotranspiration by FAO 56 bulletin and measured one by different methods showed an acceptable agreement only for specific cases, in many cases corrections is strongly necessary.

Besides, the variability of the  $K_c$  values respect to those tabulated isn't negligible. In fact, from the present study it emerges that the  $K_c$  is crop- and climate-specific. The interaction between management practices and climate influence the behavior of  $K_c$  curves, such as the three characteristics values (initial, middle and late). Important differences, for example, lie with the length of stage in the crop growth or in the spacing and density of plantation. Moreover, further research is necessary to determine  $K_c$  corrections when plastic mulches are used, to avoid errors on the water consumptions.

In conclusions, for Mediterranean region determination



of regionally based  $K_c$  curves for the major crops is needed. The crop coefficient values, in fact, were calculated only in the 10% of the countries of this fundamental agricultural area.

Some authors have observed very important inter-annual variability of  $K_c$  values, this aspect is explained by the different climatic conditions over years and different growth rate of the crops (especially for tall crop and trees), hence it requires more improvement. In this context, we consider useful the effort of many scientists to use functional approach for modelling  $K_c$ , by linking it to vegetation indices, such LAI, GC and in particular GDD, that, better than other, can capture the crop development due to different climatic conditions for a particular year.

From this review appears that the dual crop coefficient approach results more accurate for estimation of crop water requirements respect to single crop coefficient (Er-Raki *et al.*, 2009 for example). But,  $K_c$  values reported by FAO 56 bulletin cannot be utilized in all climatic regions of the world. Furthermore, the basal crop coefficient is affected by variability due to climate conditions and crop management. The fact that in this method one can separately adjust the contribution of both the soil and vegetation, improves its performance and accuracy with respect to single crop coefficient. Even if it requires the measurement or computation of more variables and processes, by limiting the practical application.

Numerous scientists are going along with Lascano (2000). He sustains that, for an irrigated cotton crop, the FAO-56 method could not describe adequately daily ET, showing a certain lack of sensibility to capture the dynamic nature of the evaporation process. Recently Katerji and Rana (2006) came to the same conclusion on the  $K_c$  approach performance by comparing two methods of determining  $ET_c$  for six species cultivated in the Mediterranean region. The first method is direct and uses a model of  $r_c$  proposed by Katerji and Perrier (1983). The second one is indirect and adopted the approach proposed by Allen *et al.* (1998) in the FAO 56 bulletin. In all the analysed situations the direct method gave more accurate estimation of  $ET_c$ . The lower performance of the indirect FAO-56 approach was analysed the authors. They found that the accuracy of  $ET_c$  values indirectly determined depends on two factors. Firstly, it depends on the accuracy of the determination of  $ET_o$ ; then, on the accuracy of the  $K_c$  values used. On the other hands, the direct evaluation of  $ET_c$  uses the one step approach instead of the two steps approach. This one step approach, since it is based on lower number of computation steps and on a lower number of error sources, can provide a more accurate estimation of

$ET_c$ . For this reason the recent scientific literature underlines the interest of developing methods permitting the direct calculation of  $ET_c$  (Testi *et al.*, 2004; Orgaz *et al.*, 2005), where the climatic variables are directly measured above the crop.

However, the need of characterising the weather variables above the crop, starting from specific measurements not performed routinely for correctly applying this direct one step method is the main obstacle to its use. About this, Rana and Katerji (2009) proposed an operational version of a direct ET model based on the determination of the weather variables in the agro-meteorological standard stations and on its calibration to adapt these measurements to the crop under study. This calculation needs only the height of the crop. On the other hands, also the indirect method needs the crop height for choosing the most appropriate crop coefficient during the different growth stages of the crop. Therefore, this operational version of the model can be applied in routine and it can be easily made automatic. Even if this methodology is able to replace the weather variables measured above the crop with those measured in a standard agro-meteorological station, as occur also within all the models based on the Penman-Monteith approach, further researches are necessary to evaluate its performance.

## ACKNOWLEDGEMENTS

The work has been supported by the projects "AQUATER" founded by Italian Ministry for agricultural, food and forestry policies, MIPAF, (contract nr. 209/7303/05) and "Mediterranean Dialogue on Integrated Water Management – MELIA" founded by the European Union in the range of the Framework Program 6 (contract FP6-INCO-517612).

The authors are grateful to the directors of the projects for the support and realization of this present paper.

## REFERENCE

- Allen R.G., Walter I.A., Elliott R.L., Howell T.A., Itenfisu D., Jensen M.E., Snyder R.L., 2005. The ASCE Standardized Reference Evapotranspiration Equation. Am. Soc. Civil Eng., Reston, VA, 59 pp. (with supplemental appendices).
- Allen R.G., Smith M., Perrier A., Pereira L.S., 1994a. An update for the definition of reference evapotranspiration. ICID Bulletin 43 (2): 1–34.
- Allen R.G., Smith M., Perrier A., Pereira L.S., 1994b. An update for the calculation of reference evapotranspiration. ICID Bulletin 43 (2): 35–92.
- Allen R.G., Pereira L.S., Raes D., Smith M., 1998. Crop evapotranspiration. Guidelines for computing crop



- water requirements. Irrigation and Drainage Paper 56, Food and Agric. Organization of the United Nations, Rome, Italy, 300 pp.
- Allen R.G., Smith M., Pruitt W.O., Pereira L.S., 1996. Modification of the FAO crop coefficient approach. In: Camp, C.R., Sadler, E.J., Yoder, R.E. (Eds.), Evapotranspiration and Irrigation Scheduling. Proceedings of the International Conference, November 3–6, San Antonio, TX: 124–132.
- Amayreh J., Al-Abed N., 2003. Determination of actual evapotranspiration and crop coefficients of broad bean (*Vicia Faba* L.) grown under field conditions in the Jordan valley, Jordan. *Agron. Soil Sci.*, 49(6): 655-662.
- Amayreh J., Al-Abed N., 2005. Developing crop coefficients for field-grown tomato (*Lycopersicon esculentum* Mill.) under drip irrigation with black plastic mulch, *Agric. Wat. Manage.*, 73: 247-254.
- Annandale J.G., Stockle C.O., 1994. Fluctuation of crop evapotranspiration coefficients with weather. A sensitivity analysis, *Irrig. Sci.*, 15: 1-7.
- Ayars J.E., Johnson R.S., Phene C.J., Trout T.J., Clark D.A., Mead R.M., 2003. Water use by drip-irrigated late-season peaches. *Irrig. Sci.*, 22: 187-194.
- Baker J.T., Gitz D.C., Payton P., Wanjura D.F., Upchurch D.R., 2007. Using leaf gas exchange to quantify drought in cotton irrigated based on Canopy temperature measurements. *Agron. J.*, 99: 637-644.
- Barbagallo S., Consoli S., Russo A., 2009. A one-layer satellite surface energy balance for estimating evapotranspiration rates and crop water stress indexes. *Sensors*, 9.1.21.
- Benli B., Kodal S., Ilbeyi A., Ustun H., 2006. Determination of evapotranspiration and basal crop coefficient of alfalfa with a weighing lysimeter. *Agric. Wat. Manage.*, 81: 358-370.
- Beyazgül M., Kayam Y., Engelsman F., 2000. Estimation methods for crop water requirements in the Gediz Basin of western Turkey. *J. Hydrol.*, 229: 19-26.
- Blaney H.F., Ciddle W.D., 1950. Determining water requirements in irrigated areas from climatological and irrigation data. USDA/SCS, SCS-TP 96.
- Bruce J.A., 1997. Does transpiration control stomatal responses to water vapour pressure deficit?. *Plant Cell Environ.*, 20: 136–141.
- Burman R.D., Wright J.L., Nixon P.R., R.W. Hill, 1980a. Irrigation management-water requirements and water balance, In: Irrigation, Challenges of the 80's, Proc. of the Second National Irrigation Symposium. Am. Soc. Agric. Eng., St. Joseph, MI: 141–153.
- Burman, R.D., Nixon P.R., Wright J.L., Pruitt W.O., 1980b. Water requirements. In: Jensen, M.E. (Ed.), Design of Farm Irrigation Systems, ASAE Mono. Am. Soc. Agric. Eng., St. Joseph, MI: 189–232.
- Casa R., Russell G., Lo Cascio B., 2000. Estimation of evapotranspiration from a field of linseed in central Italy. *Agric. For. Meteorol.*, 104: 289-301.
- Cavazza L., 1991. Valutazione dell'evapotraspirazione delle colture. Evapotraspirazione: chiarimenti concettuali preliminari. In: Proceedings of the Meeting "Irrigazione e Ricerca": 97–102 (in Italian).
- Cornic G., Massassi A., 1996. Leaf photosynthesis under drought stress. In: Baker, N.R. (Ed.), Photosynthesis and the Environment. Kluwer Academic Publishers, The Netherlands.
- DeTar W.R., 2009. Crop coefficients and water use for cowpea in the San Joaquin Valley of California. *Agric. Wat. Manage.*, 96: 53-66.
- Doorenbos J., Pruitt W.O., 1975. Guidelines for predicting crop water requirements. Irrigation and Drainage Paper no. 24, FAO-ONU, Rome, Italy, 168 pp.
- Doorenbos J., Pruitt W.O., 1977. Guidelines for predicting crop water requirements. FAO-ONU, Rome, Irrigation and Drainage Paper no. 24 (rev.), 144 pp.
- Dragoni D., Lakso A.N., Piccioni R.M., 2004. Transpiration of an apple orchard in a cool humid climate: measurement and modelling. *Acta Horticulturae*, 664: 175–180.
- Er-Raki S., Chehbouni A., Hoedjes J., Ezzahar J., Duchemin B., Jacob F., 2008. Improvement of FAO-56 method for olive orchards through sequential assimilation of thermal infrared-based estimates of ET. *Agric. Wat. Manage.*, 95: 309-321.
- Er-Raki S., Chehbouni A., Guemouria N., Ezzahar J., Khabba S., Boulet G., Hanich L., 2009. Citrus orchard evapotranspiration: Comparison between eddy covariance measurements and the FAO-56 approach estimates. *Plant Biosystems*, 00(0): 1-8.
- Fernandez M.D., 2000. Necesidades hidricas y programacion de riegos en los cultivos horticos en invernadero y suelo enarenado de Almeria. Doctoral Thesis, Universidad de Almeria, Espana (in Spanish).
- Ferreira M.I., Valancogne C., Daudet F.A., Ameglio T., Michaelsen J., Pacheco C.A., 1996. Evapotranspiration and crop water relations in a peach orchard. In: C.R. Camp, E.J. Sadler and R.E. Yoder, Editors, Evapotranspiration and Irrigation Scheduling, ASE, San Antonio, TX (1996): 60–68.
- Ferreira T.C., Carr M.K.V., 2002. Responses of

- potatoes (*Solanum tuberosum* L.) to irrigation and nitrogen in a hot, dry climate I. Water use. *Field Crop Res.*, 78: 51-64.
- Grattan S.R., George W., Bowers W., Dong A., Snyder R.L., Carroll J., 1998. New crop coefficients estimate water use of vegetables row crops. *California Agriculture*, 52 (1): 16–20.
- Hamdy A., Lacirignola D., 1999. Mediterranean Water Resources: Major Challenges Toward 21st Century. CIHEAM-IAM Bari, Italy, p. 570.
- Hamidat A., Benyoussef B., Hartini T., 2002, Small-scale irrigation with photovoltaic water pumping system in Sahara regions. *Renewable Energy*, 28: 1081-1096.
- Hanson B.R., May D.M., 2005. Crop coefficients for drip-irrigated processing tomato. *Agric. Wat. Manage.*, 81: 381-399.
- Hargreaves G.H., Samani Z.A., 1982. Estimating potential evapotranspiration. *Journal of Irrigation and Drainage Engineering, ASCE*, 108(IR3): 223-230.
- Hargreaves G.H., Samani Z.A., 1985. Reference crop evapotranspiration from temperature. *Transaction of ASAE* 1(2): 96-99.
- Howell T.A., Evett S.R., Schneider A.D., Dusek D.A., Copeland K.S., 2000. Irrigated fescue grass ET compared with calculated reference grass ET. *Proc. "4<sup>th</sup> National Irrig. Symp., ASAE"*, Phenix, AZ, 228-242.
- Jensen M.E., Burman R.D., Allen R.G., 1990. Evaporation and irrigation water requirements. *ASCE Manuals and Reports on Eng. Practices No. 70*, Am. Soc. Civil Eng., New York, NY, 360 pp.
- Jensen, M.E., 1968. Water consumption by agricultural plants. In: Kozlowski, T.T. (Ed.), *Water Deficits and Plant Growth*, Vol. II. Academic Press, Inc., New York, NY, pp. 1–22.
- Karam F., Masaad R., Sfeir T., Mounzer O., Roushael Y., 2005. Evapotranspiration and seed yield of field grown soybean under deficit irrigation conditions. *Agric. Wat. Manage.*, 75: 226-244.
- Katerji N., Hamdy A., Raad A., Mastrorilli M., 1991. Conséquence d'une contrainte hydrique appliquée à différents stades phénologiques sur le rendement des plantes de poivron. *Agronomie* 11:679-687 (in French).
- Katerji N., Perrier A., 1983. A modélisation de l'évapotranspiration réelle d'une parcelle de luzerne: rôle d'un coefficient cultural. *Agronomie*, 3(6): 513-521 (in French).
- Katerji N., Rana G., 2006, Modelling evapotranspiration of six irrigated crops under Mediterranean climate conditions. *Agric. For. Meteorol.*, 138: 142-155.
- Katerji N., Rana G., 2008. Crop evapotranspiration measurement and estimation in the Mediterranean region. ISBN 978 8 89015 241 2.
- Ko J., Piccinni G., Marek T., Howell T., 2009. Determination of growth-stage-specific crop coefficients (Kc) of cotton and wheat. *Agric. Wat. Manage.*, 96: 1691-1697.
- Lascano R.J., 2000. A general system to measure and calculate daily crop water use. *Agron. J.*, 92: 821–832.
- Lopez-Urrea R., Martin de Santa Olalla F., Montoro A., Lopez-Fuster P., 2009, Single and dual crop coefficients and water requirements for onion (*Allium cepa* L.) under semiarid conditions. *Agric. Wat. Manage.*, 96: 1031–1036.
- Lovelli S., Pizza S., Caponio T., Rivelli A.R., Perniola M., 2005. Lysimetric determination of muskmelon crop coefficients cultivated under plastic mulches. *Agric. Wat. Manage.*, 72: 147-159.
- Magliulo V., d'Andria R., Rana G., 2003. Use of the modified atmometer to estimate reference evapotranspiration in Mediterranean environments. *Agric. Wat. Manage.*, 63(1), 1-14.
- Manuel Casanova P., Ingmar M., Abraham J., Alberto Canete M., 2009. Methods to estimate lettuce evapotranspiration in greenhouse conditions in the central zone of Chile. *Chilean Journal of Agricultural Research*, 69(1): 60-70.
- Martinez-Cob A., 2007. Use of thermal units to estimate corn crop coefficients under semiarid climatic conditions. *Irrig. Sci.*, 26(4): 335-345.
- Orgaz F., Fernandez M.D., Bonachela S., Gallardo M., Fereres E., 2005. Evapotranspiration of horticultural crops in an unheated plastic greenhouse. *Agric. Wat. Manage.*, 72: 81-96.
- Ortega-Farias S.O., Olioso A., Fuentes S., Valdes, 2006. Latent heat flux over a furrow-irrigated tomato crop using Penman-Monteith equation with a variable surface canopy resistance. *Agric. Wat. Manage.*, 82: 421-432.
- Paço T.A., Ferreira M.I., Conceição N., 2006. Peach orchard evapotranspiration in a sandy soil: comparison between eddy covariance measurements and estimates by FAO 56 approach. *Agric. Wat. Manage.*, 85: 305-313.
- Piccinni G., Ko J., Marek T., Howell T., 2009. Determination of growth-stage-specific crop coefficients (Kc) of maize and sorghum. *Agric. Wat. Manage.*, 96: 1698-1704.
- Priestley C.H.B., Taylor R.J., 1972. On the assessment of surface heat flux and evaporation using large-scale parameters. *Monthly Weather Review, AMS Journal*, 100: 81-82.
- Rana G., Katerji N., 2000. Measurement and estimation of actual evapotranspiration in the field

- under Mediterranean climate: a review. *Eur. J Agr.*, 13(2-3): 125-153.
- Rana G., Katerji N., 2009. Operational model for direct determination of evapotranspiration for well watered crops in Mediterranean region. *Theor. Appl. Climat.*, 97(3): 243-253.
- Rana G., Katerji N., De Lorenzi F., 2005. Measurement and modelling of evapotranspiration of irrigated citrus orchard under Mediterranean conditions. *Agric. For. Meteorol.*, 128: 199-209.
- Rana G., Katerji N., Mastrorilli M., El Moujabber M., 1994. Evapotranspiration and canopy resistance of grass in a Mediterranean region. *Theor. Appl. Climat.*, 50 (1-2): 61-71.
- Rinaldi M., Rana G., 2004. I fabbisogni idrici del pomodoro da industria in Capitanata. *Rivista Italiana di Agrometeorologia*, 1: 31-35 (in Italian).
- Riou C., 1984. Estimation de l'evapotranspiration potentielle. In: "les bases de la bioclimatologia. 1-bases physiques", Edition INRA-France: 105-113.
- Ritchie J.T., NeSmith D.S., 1991. Temperature and crop development. In: Modelling Plant and Soil Systems, Hanks J., Ritchie J.T. (eds.). Series Agronomy N° 31: 5-29. American Society of Agronomy, Crop Science Society of America, Soil Science Society of America, Madison, WI, USA.
- Rubino P., Tarantino E., Miglionico M., 1986. Distribuzione dei consumi idrici durante il ciclo culturale del fagiolo da sguisciare misurati con lisimetro a pesata. *Irrigazione*, 33 (2): 23-29 (in Italian).
- Sahin U., Kuslu Y., Tunc T., Kiziloglu F.M., 2009. Determining Crop and Pan Coefficients for Cauliflower and Red Cabbage Crops Under Cool Season Semiarid Climatic Conditions. *Agricultural Science in China*, 8(2): 167-171.
- Shideed K., Oweis T., Gabr. M., Osman M., 1995. Assessing on-farm water use efficiency: a new approach. ICARDA/ESCWA, Ed. Aleppo, Syria, 86 pp.
- Snyder R.L., Lanini B.J., Shaw D.A., Pruitt W.O., 1987. Using reference evapotranspiration (ET<sub>0</sub>) and crops coefficients to estimate crop evapotranspiration (ET<sub>c</sub>) for agronomic crops, grasses, and vegetable crops. University of California, Division of Agricultural and Natural Resources, Leaflet 21427, 12 pp.
- Stanghellini C., Bosma A.H., Gabriels P.C.J., Werkoven C., 1990. The water consumption of agricultural crops: how crop coefficient are affected by crop geometry and microclimate. *Acta Horticulturae*, 278: 509-516.
- Steduto P., Caliandro A., Rubino P., Ben Mechlia N., Masmoudi M., Martinez-Cob A., Jose Faci M., Rana G., Mastrorilli M., El Mourid M., Karrou M., Kanber R., Kirda C., El-Quosy D., El-Askari K., Ait Ali M., Zareb D., Snyder R.L., 1996. Penman-Monteith reference evapotranspiration estimates in the Mediterranean region. In: Camp, C.R., Sadler, E.J., Yoder, R.E. (Eds.), *Evapotranspiration and Irrigation Scheduling*. Proceedings of the International Conference, November 3-6, San Antonio, TX, 357-364 pp.
- Tarantino E., Spano D., 2001. La valutazione dei fabbisogni irrigui, *Rivista di Irrigazione e Drenaggio*, 48 (4): 21-35 (in Italian).
- Tarantino E., Onofri M., 1991. Determinazione dei coefficienti colturali mediante lisimetri, *Bonifica*, 7: 119-136 (in Italian).
- Testi L., Villalobos F.J., Orgaz F., 2004. Evapotranspiration of a young irrigated olive orchard in southern Spain. *Agric. Wat. Manage*, 121: 1-18.
- Todorovic M., 1999. Single-layer evapotranspiration model with variable canopy resistance. *J. Irrig. Drain. Eng.*, 125 (5): 235-245.
- Vazquez N., Pardo A., Suso M.L., Quemada M., 2005. Drainage and nitrate under processing tomato growth with drip irrigation and plastic mulching. *Agric. Ecosys. Environ.*, 122: 313-323.
- Ventura F., Spano D., Duce P., Snyder R.L., 1999. An evaluation of common evapotranspiration equations. *Irrig. Sci.*, 18: 163-170.
- Villalobos F.J., Testi L., Rizzalli R., Orgaz F., 2004. Evapotranspiration and crop coefficients of irrigated garlic (*Allium sativum*L.) in a semi-arid climate. *Agric. Wat. Manage.*, 64: 233-249.
- Villalobos F.J., Testi L., Moreno-Perez M.F., 2009. Evaporation and canopy conductance of citrus orchards. *Agric. Wat. Manage.*, 96: 565-573.
- Williams D.G., Cable W., Hultine K., Hoedjes J.C.B., Yepez E.A., Simonneaux V., 2004. Evapotranspiration components determined by stable isotope, sap flow and eddy covariance techniques. *Agric. For. Meteorol.*, 125: 241-258.
- Williams L.E., Phene C.J., Grimes D.W., Trout T.J., 2003. Water use of mature Thomson Seedless grapevines in California. *Irrig. Sci.*, 22: 11-18.
- Williams L.E., Ayars J.E., 2005. Grapevine water use and crop coefficient are linear functions of the shaded area measured beneath the canopy. *Agric. For. Meteorol.*, 132: 201-211.
- Wright J.L., 1982. New evapotranspiration crop coefficients. *J. Irrig. Drain. Div. ASCE* 108: 57-74.



# What we can ask to hourly temperature recording.

## Part I: Statistical vs. meteorological meaning of minimum temperature

Emanuele Eccel<sup>\*1</sup>

**Abstract:** When the lowest temperature in 24-hourly time-spans is attributed to the nocturnal minimum, a systematic underestimation of the latter takes place, due to the missing contribution of warm nights that precede colder ones. This study, illustrated over one station, assesses the incidence of such bias in more than 20% of the cases, with a difference of 0.3 °C between the “standard” way of measuring minima, and the one which restricts the search of minima to the early hours of the day. The application of filters on the time band of search of minima is often mandatory for some temperature data processing, including the matching with meteorological and climate models.

**Keywords:** minimum temperature, hourly recording

**Riassunto:** L'attribuzione della temperatura più bassa nell'arco delle 24 ore alla temperatura minima notturna porta ad una sistematica sottostima di tale grandezza, dovuta al mancato contributo di notti calde che precedono notti più fredde. Lo studio, esemplificato in una stazione, quantifica l'incidenza di tale scarto in oltre il 20% dei casi, con una differenza di 0.3 °C tra il modo “standard” di misurare la minima e quello che prevede un'attribuzione limitata alla fascia delle prime ore del giorno. Tale accortezza è un passo spesso necessario per alcune elaborazioni, incluse quelle che richiedano confronti con modelli meteo-climatici.

**Parole chiave:** temperatura minima, registrazione oraria

According to the World Meteorological Organization, minimum temperature is the “lowest temperature attained during a specific time interval” (WMO, 1992). This definition is rather trivial, but consequences are less obvious when the “specific time interval” is one day. In figure 1, temperatures recorded at the meteorological station of S. Michele (Trento, Italy) during a winter day (27<sup>th</sup> December 2009) and the following morning are represented. The day began with a cloudy sky, followed by clearings, allowing a temperature rise during daytime. After sunset, strong outgoing radiation resulted in temperature fall, which continued during night. The meteorological database of the Fondazione Edmund Mach (FEM), like many others, records minimum daily temperatures as the lowest temperatures reached in each day, whose first record is taken at 0 AM (local time) and the last at 11 pm, each hourly record referring to measures taken in the previous 60'. The result of this setting, taken as it is, may be undesirable: the lowest value in the 24 hours of the day may be attributed to the (presumed) coldest period of the day - the early hours -, irrespective of the real recording time. In the example of figure 1, the same night (from 27<sup>th</sup> to 28<sup>th</sup> Dec.) is

accounted for twice, once for each day: the first at about half of the progressive night cooling, at the latest conventional time of day 27<sup>th</sup> (11 PM), the second one on the day 28<sup>th</sup> at 7 AM. On the contrary, the night between 26<sup>th</sup> and 27<sup>th</sup> Dec. does not contribute at all.

It may be argued that the case just discussed is an example and that this mechanism can hardly affect a long record. In order to ascertain possible effects of offsetting the measurement of average minimum night temperature, a long period of hourly recording was analyzed (27 years from 1983 to 2009). For each day, the times of occurrence of the lowest temperatures in all the 24-hour periods from 0 AM to 11 PM were calculated. The result is reported in figure 2. It can be seen that the proportion of times (hours) at which the minimum temperature is recorded increases until 7 AM, then decreases to negligible values in the second part of the morning. But after sunset it increases again, due to the presence of cold nights following warmer ones, and it reaches considerable values at 11 PM (in almost 12% of the days).

Now, let's accept the idea that attributing low temperatures that fall in the second part of the day to a day's minimum is incorrect (we will come back on this later). If this is case, the sum of all the incorrect attributions accounts for a non-negligible 22% of the whole dataset. The relevant bias, for the case of S. Michele, 1983-2009, can be

<sup>\*</sup> Corresponding author: emanuele.eccel@iasma.it

<sup>1</sup> IASMA Research and Innovation Centre - Fondazione Edmund Mach - Environment and Natural Resources Area - S. Michele all'Adige (TN) - Italy

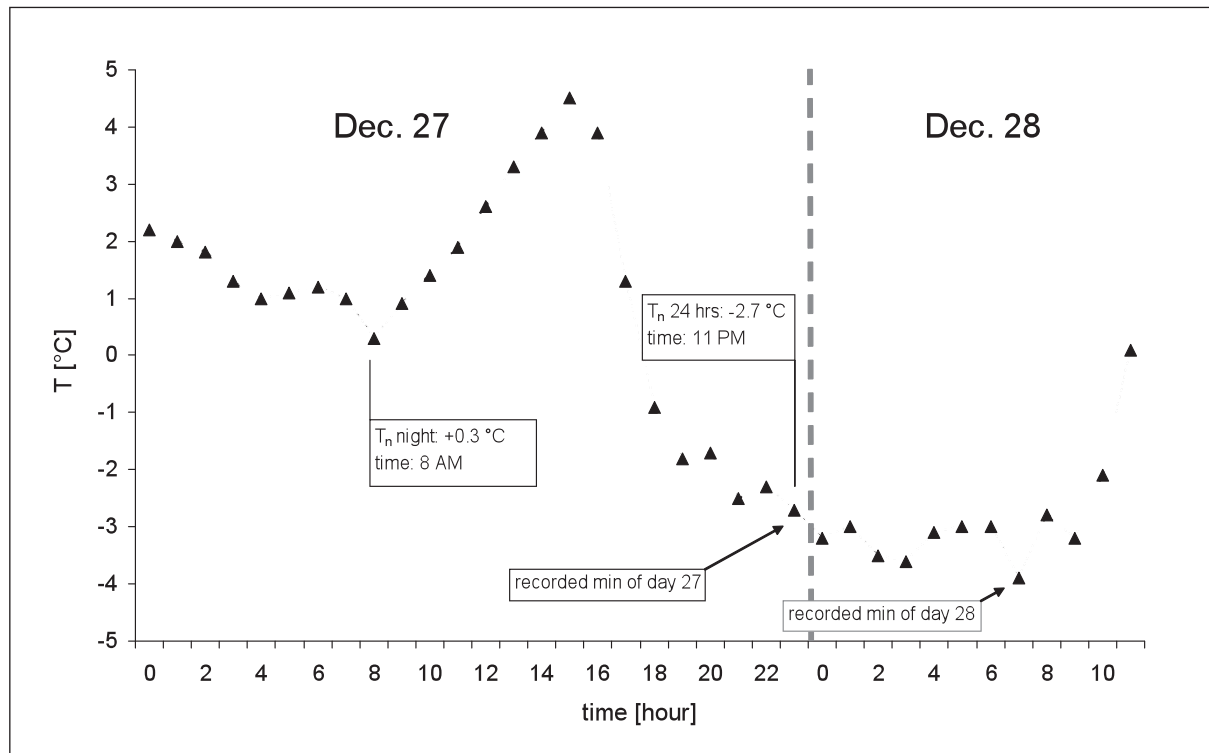


**Fig. 1** - Mean hourly temperatures at S. Michele, 27<sup>th</sup> – 28<sup>th</sup> December 2009.  
*Fig. 1 - Temperature medie orarie a S. Michele, 27 – 28 dicembre 2009.*

assessed in an average underestimation of minimum temperature of 0.3 °C. But single differences can be much larger, as shown in figure 3a, representing the departures from the “correct” estimation of minimum temperatures, that is, the

differences in minimum daily temperatures measured according to the two standards (search either over the whole 24-hour period or over early morning hours). The graph in figure 3a is quite impressive, even if it includes a few cases for which only a few hours of recording were available; the latter is the cause of an error of attribution of minimum daily temperatures, irrespective of the lack of recording during the expected cold band of hours in the day. The boxplot of differences (Fig. 3b) shows that the Inter-Quartile Range (IQR) of bias is flattened onto values little different from zero, even if it displays a good number of cases well below the lower IQR boundary.

The discussion above stems from the assumption that minimum temperatures should be measured on a meteorological (i.e., physical) ground, rather than just on a statistical one. Namely, they have to represent the lowest temperatures attained during the cold period of the day. Spotting the lowest record over a 24-hour period is formally (and statistically) correct, but it clashes against the purely conventional definition of a “day” as the period from 0 AM to 12 PM – a convention that is very useful for the sake of organizational aspects in human life, but not for measuring nocturnal,

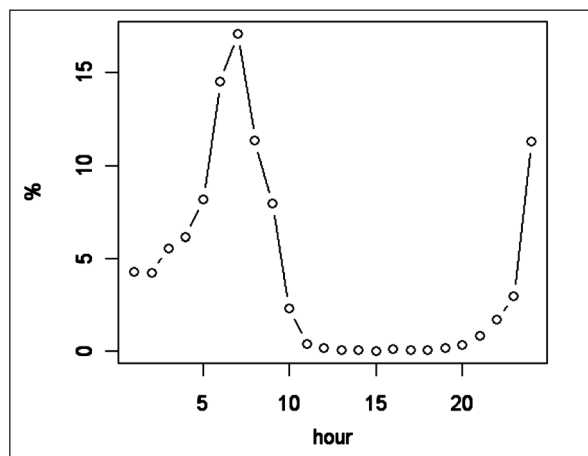


**Fig. 2** – Station of S. Michele: mean times of occurrence of the lowest daily temperature calculated over the fixed 24-hour periods “0 AM – 12 PM”, 1983-2009.

*Fig. 2 – Stazione di S. Michele: ore medie di registrazione della temperatura minima giornaliera calcolata su periodi prefissati di 24 ore “0 - 23”, 1983-2009.*

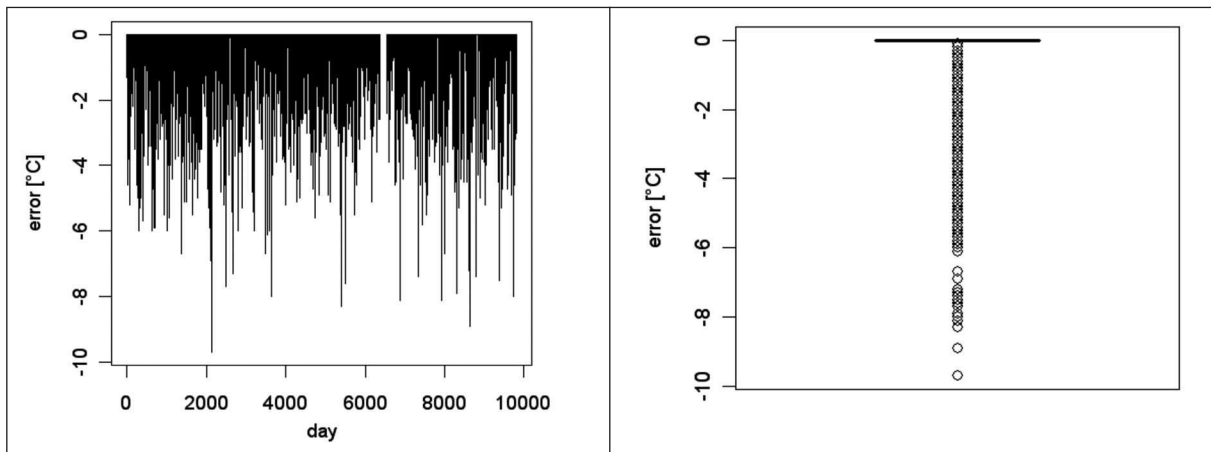


**Fig. 3** – Station of S. Michele, 1983-2009. Bias of estimation of minimum temperatures when no filtering on hours is carried out, compared to the estimation in which the search of the minimum is restricted to the early hours of the day. a) Daily time series. b) Boxplot of the bias.

*Fig. 3 – Stazione di S. Michele, 1983-2009. Scarto della stima della temperatura minima in assenza di filtri sulla fascia oraria, comparata con la stima in cui la ricerca della minima è limitata alle prime ore del giorno, 1983-2009. a) Serie giornaliera. b) Boxplot dell'errore.*

natural phenomena, where the night should be kept as an unbroken unit.

Moreover, it must be remembered that, before the introduction of thermographs, temperatures were measured twice a day, minimum daily temperatures being recorded at morning: whether the minimum had been reached in the late hours of the previous day, or in the early hours of the current day, remained unknown to the observer, but the case was excluded of a minimum temperature of the day falling after midday. In long climatic series, neglecting this aspect may lead to a systematic underestimation of minima since the instrumental change. Finally, the choice of a minimum temperature really representing the lowest value of the cold period of the day is

mandatory when measured values are compared with model outputs, as is the case of calibration of models based on the match between observed and modelled temperatures.

#### ACKNOWLEDGMENT

This study was carried out in the frame of the project ENVIROCHANGE, funded by the Autonomous Province of Trento.

Thanks to Piero Cau for his help in revising the manuscript.

#### REFERENCE

WMO, 1992. International meteorological vocabulary. Geneva (CH), 784 pp.

# What we can ask to hourly temperature recording.

## Part II: hourly interpolation of temperatures for climatology and modelling

Emanuele Eccel<sup>\*1</sup>

**Abstract:** Several applications in agrometeorology and in biological modelling make use of hourly time series. However, some difficulties arise in finding hourly series of acceptable length, resulting in a limited application of hourly models. In this work, an interpolation model is described which makes use of linear, parabolic and sinusoidal functions between daily maximum and minimum temperatures. Benefits coming from the use of simulated time series are discussed. The errors due to the reconstructed hourly series are small, especially when applications like thermal sums are considered, in which a compensation of single hourly errors takes place. The generation of hourly series allows a good correction of the error committed in mean temperature estimation, when it is calculated by the simple arithmetic average of daily maximum and minimum.

**Keywords:** temperature, interpolation

**Riassunto:** Le serie temporali orarie hanno diverse applicazioni in agrometeorologia e nella modellistica biologica. Esistono tuttavia difficoltà nel reperire serie orarie di sufficiente lunghezza, tanto che l'uso ne è limitato. Nel lavoro viene descritto un modello che impiega funzioni lineari, paraboliche e sinusoidali per interpolare valori orari a partire dai valori giornalieri di temperatura massima e minima. Vengono quindi discussi i benefici dell'uso delle serie orarie simulate. Gli errori determinati dall'uso di serie orarie ricostruite sono piccoli, specialmente quando si valutano applicazioni come le somme termiche, che consentono una compensazione dei singoli errori orari. La generazione di serie orarie permette anche di correggere in gran parte l'errore che si commette nella stima delle temperature medie effettuata con la semplice media algebrica di massime e minime giornaliere.

**Parole chiave:** temperatura, interpolazione

In spite of a widespread use of models that make use of daily meteorological values, there are many situations in which hourly resolution is advisable, or even required. This is the case of modelling infection precursors (for example: Rossi *et al.*, 2008; Gleason *et al.*, 1994; Blaeser and Weltzien, 1979); traditionally, chill requirements in phenological models has been expressed in (normalised) chill hours (Ashcroft and Richardson, 1977); Rea and Eccel (2006) found that phenological hourly models based on thermal sums performed better than the equivalent daily ones, even when hourly temperature series were artificially produced from daily maximum and minimum values. Worner (1988) warns about the errors coming from the use of daily values for thermal summations, instead of hourly ones; the author also presents a review of hourly interpolation algorithms developed starting from the sixties.

One problem with the use of hourly temperatures, at least in climate applications, is the limited availability of hourly series, often shorter than the period in which series of minima and maxima are available. In climatic

projections, hourly resolution is unavailable from both direct and downscaled model outputs. The present work shows the usefulness of implementing hourly interpolation models, proposing a simple and rapid algorithm. Equations were adapted from the "TM model" (Cesaraccio *et al.*, 2001); in particular, equation (2) was changed and equations (1) and (4) were split to account for possible linear interpolation stretches in the corresponding time bands.

The protocol consists of a first (optional) part of calibration, for the setting of monthly dawn times, hour of minimum, hour of maximum, and sunset times, and of the parameters "c" and "z". Hourly interpolation is carried out with four portions of curves (Fig. 1): parabola/line I, from 0 AM to dawn (same equation of the previous day, from sunset to 11 PM); sinusoid I, from dawn to time of maximum; sinusoid II, from maximum to sunset time; parabola/line II, from sunset to midnight (and continuing till dawn of the following day).

The four equations used are the following:

parab./line I:

$$T(t) = T_{s-1} + \Delta_I \cdot (t + 24 - H_s)^2 \quad (1)$$

$$0 \leq t \leq H_{\min}$$

<sup>\*</sup> Corresponding author: emanuele.eccel@iasma.it  
<sup>1</sup> IASMA Research and Innovation Centre - Fondazione Edmund Mach - Environment and Natural Resources Area - S. Michele all'Adige (TN) - Italy



sinus I:

$$T(t) = T_{min} + \frac{(T_{max} - T_{min})}{2} \cdot \left[ 1 + \sin\left(\pi \frac{t - H_{min}}{H_{max} - H_{min}} - \frac{\pi}{2}\right) \right] \quad (2)$$

$H_{min} \leq t \leq H_{max}$

sinus. II:

$$T(t) = T_s + (T_{max} - T_s) \cdot \sin\left\{ \frac{\pi}{2} \cdot \left[ 1 + \frac{(t - H_{max})}{(H_s - H_{max})} \right] \right\} \quad (3)$$

$H_{max} \leq t \leq H_s$

parab./line II:

$$T(t) = T_s + \Delta_{II} \cdot (t - H_s)^z \quad (4)$$

$H_s \leq t \leq 23$

with

$$T_s = T_{max} - c(T_{max} - T_{min+1}) \quad (5)$$

$$\Delta_I = \frac{T_{min} - T_{s-1}}{(H_{min} + 24 - H_s)^z} \quad (6a)$$

$$\Delta_{II} = \frac{T_{min+1} - T_s}{(H_{min} + 24 - H_s)^z} \quad (6b)$$

where  $H_{max}$ ,  $H_{min}$ ,  $H_s$  = times of maximum and minimum temperature and time of sunset, respectively;  $T_{max}$ ,  $T_{min}$ ,  $T_s$  = maximum, minimum and sunset temperature, respectively;  $c$ : coefficient;  $z$  = either 0.5 (parabola - case of “clear late/early

night”) or 1 (line - case of “cloudy late/early night”). Subscript “-1”: day before; subscript “+1”: day after. The discrimination between clear and cloudy late night (from midnight to the hour of morning minimum) or early night (from sunset to midnight) was carried out by a calibration on the value of the ratio between daily thermal range ( $DTR_d$ ) and the climatic monthly averages ( $DTR_m$ ):

$$k = \frac{DTR_d}{DTR_m} \quad (7)$$

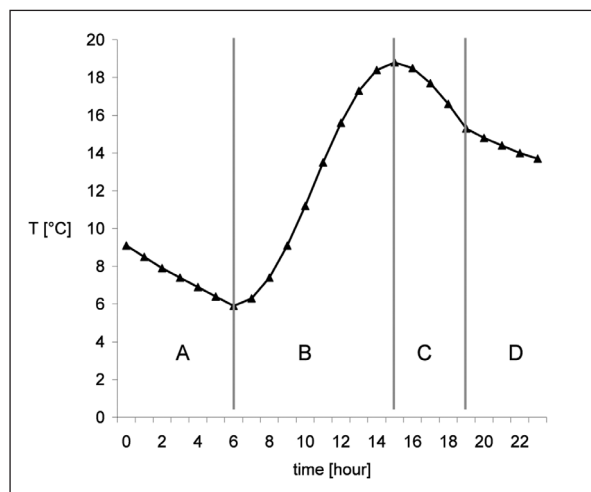


**Fig. 1** – Example of hourly temperature interpolation. A: parabola/line I. B: sinusoid I. C: sinusoid II. D: parabola/line II (see equations in the text).

*Fig. 1 – Esempio di interpolazione oraria delle temperature. A: parabola/retta I. B: sinusoida I. C: sinusoida II. D: parabola/retta II (equazioni nel testo).*

	$H_{min}$		$H_{max}$		$H_s$		C	
	S. Michele	Cles	S. Michele	Cles	S. Michele	Cles	S. Michele mean: 0.39	Cles mean: 0.38
JAN	8	<b>8</b>	15	<b>15</b>	17	<b>17</b>	0.36	0.36
FEB	8	<b>8</b>	16	<b>15</b>	18	<b>18</b>	0.37	0.38
MAR	7	<b>7</b>	15	<b>15</b>	18	<b>18</b>	0.26	0.28
APR	6	<b>6</b>	15	<b>15</b>	19	<b>19</b>	0.36	0.37
MAY	5	<b>5</b>	15	<b>15</b>	20	<b>19</b>	0.46	0.36
JUN	5	<b>5</b>	15	<b>15</b>	20	<b>20</b>	0.45	0.46
JUL	5	<b>5</b>	15	<b>15</b>	20	<b>20</b>	0.44	0.47
AUG	6	<b>6</b>	15	<b>15</b>	19	<b>19</b>	0.35	0.39
SEP	6	<b>6</b>	15	<b>15</b>	18	<b>18</b>	0.30	0.34
OCT	7	<b>7</b>	15	<b>15</b>	18	<b>17</b>	0.49	0.30
NOV	8	<b>7</b>	<b>15</b>	14	<b>17</b>	<b>17</b>	0.41	0.40
DEC	8	<b>8</b>	15	<b>15</b>	<b>17</b>	<b>17</b>	0.41	0.47

**Tab. 1** – Calibration of parameters for TM model.  $H_{min}$ : hour of minimum temperature;  $H_{max}$ : hour of maximum temperature;  $H_s$ : hour of sunset;  $c$ : coefficient for the determination of  $T_s$  (sunset temperature – see equation 5). Values used in the “unified” setting are highlighted.

*Tab. 1 – Calibrazione dei parametri per il modello TM.  $H_{min}$ : ora della temperatura minima;  $H_{max}$ : ora della temperatura massima;  $H_s$ : ora del tramonto;  $c$ : coefficiente per la determinazione di  $T_s$  (temperatura al tramonto – vedi formula 5). I valori impiegati nell’impostazione “unificata” sono evidenziati.*

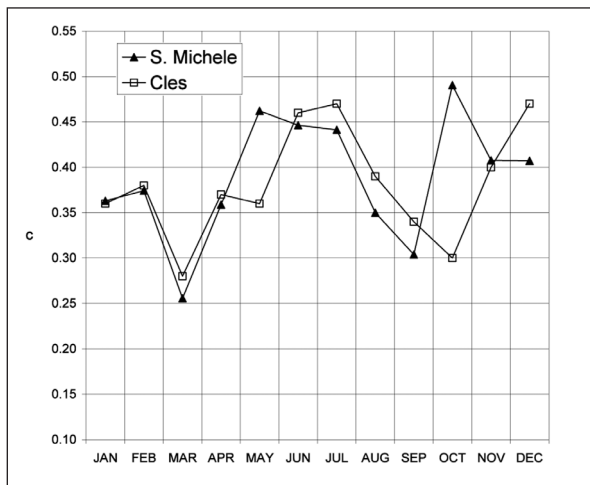


**Fig. 2** – Values of the coefficient “c” for the assessment of sunset temperature – see equation 5 - calibrated monthly over a 27-year period (1983 – 2009), stations of S. Michele and Cles.

*Fig. 2 – Valori del coefficiente “c” per la stima della temperatura al tramonto - vedi formula 5 - calibrato mensilmente su un periodo di 27 anni (1983 – 2009), stazioni di S. Michele e Cles.*

which gave for both stations and for both cases (“late night” and “early night”) an optimal value of 1.5: for lower values the linear equation allows for better interpolation than the parabolic one.

A monthly differentiation is important for times of minimum (“dawn”) and for times of change of

the equation from sinusoid II to parabola/line II (“sunset”), secondarily for the time of maximum, which, for mean hourly recordings, peaks in frequency (with few exceptions) at 3 PM (that is, in the previous 60 minutes).  $H_s$  was calibrated as the time of the day more frequently associated to the largest temperature fall in the afternoon. Also the parameter “c”, necessary for the definition of the sunset temperature  $T_s$ , can be easily calibrated on a monthly basis. The authors of the TM model proposed a mean value for “c” of 0.39, which is fully confirmed by the calibration carried out on the two 27-year long series of S. Michele (210 m a.s.l., valley bottom), and Cles (650 m a.s.l., hill side), in Trentino (Tab. 1 and Fig. 2). With the exception of a couple of months, a good agreement can be observed for the calibration of “c” between the two stations. As regards the calibration of timing, in general, a difference of one hour is not dramatic, corresponding to shifts in the discontinuities of the curve type at a time when either the rate of temperature change is at its minimum ( $H_{\min}$  and  $H_{\max}$  times), or both curves are decreasing ( $H_s$  time), resulting in limited errors.

The introduction of linear interpolation of night values as alternative to the parabolic one allows for an improvement of both mean and absolute errors, thanks to the calibration of the parameter k (eq. 7). Indeed, when night radiation loss is

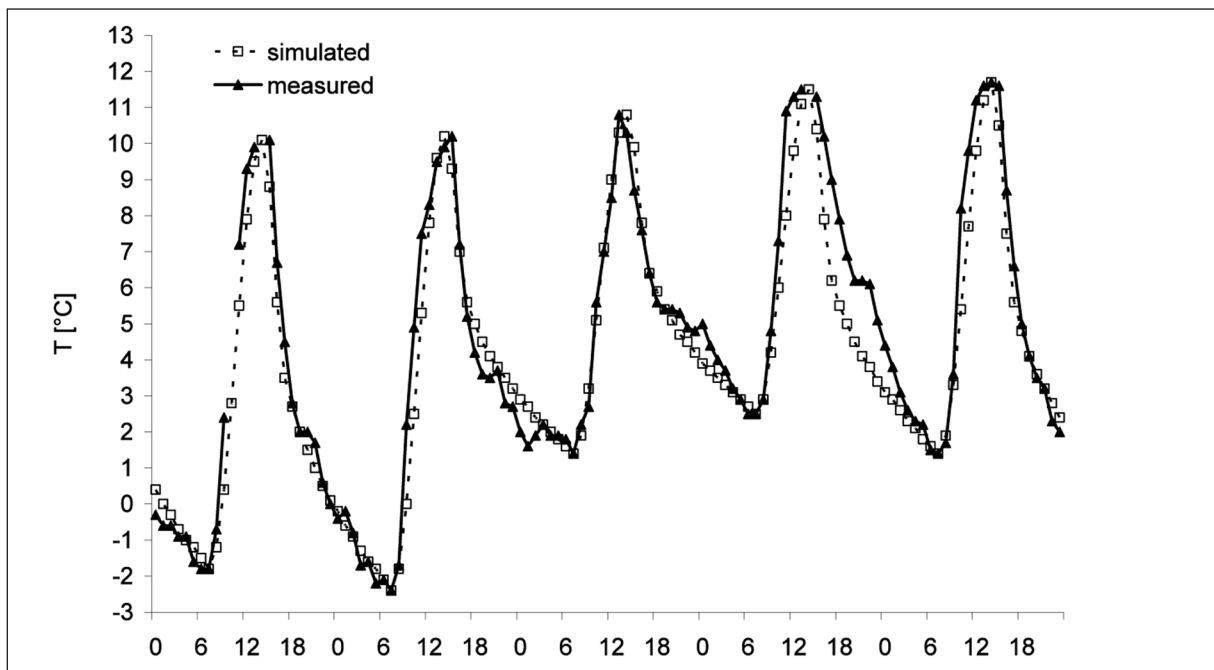


**Fig. 3** – Example of hourly interpolation, compared with measured values (S. Michele, 24<sup>th</sup> – 28<sup>th</sup> January 1983).

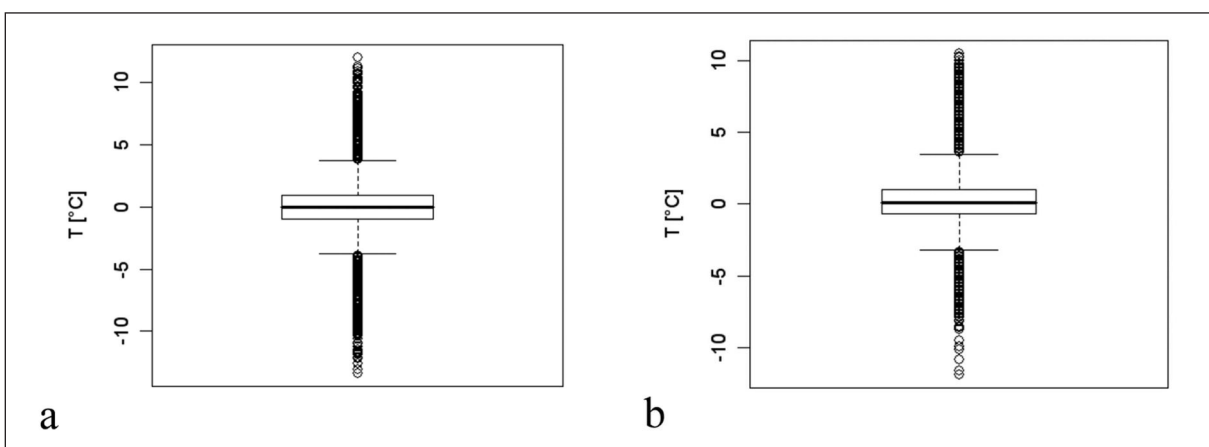


**Fig. 4 – Boxplots of estimation errors of hourly temperature (estimated – measured), 1983-2009. a) S. Michele; b) Cles.**  
**Fig. 4 – Boxplot dell'errore di stima della temperatura oraria (stimata – misurata), 1983-2009. a) S. Michele; b) Cles**

inhibited (as in the case of overcast or just cloudy sky), the temperature decrease is irregular and, in general, there is no clear sign of a concavity in the corresponding line.

For simulating the case of unavailability of hourly series, a “unified” set of parameters was chosen. It can be seen that there are no large differences in the two series between  $H_{\min}$ ,  $H_{\max}$  and  $H_s$ , so the

“smoothest” set of monthly  $H_{\min}$  and  $H_s$  was chosen (see Tab. 1), while  $H_{\max}$  was fixed to the constant value of 15 (3 PM) and  $c$  to the constant value of 0.39.

The application of the interpolation algorithm (excerpt in Fig. 3) yields a mean error of -0.01 / +0.04 °C and a mean absolute error of 1.29 / 1.14 °C, for S. Michele and Cles, respectively. There

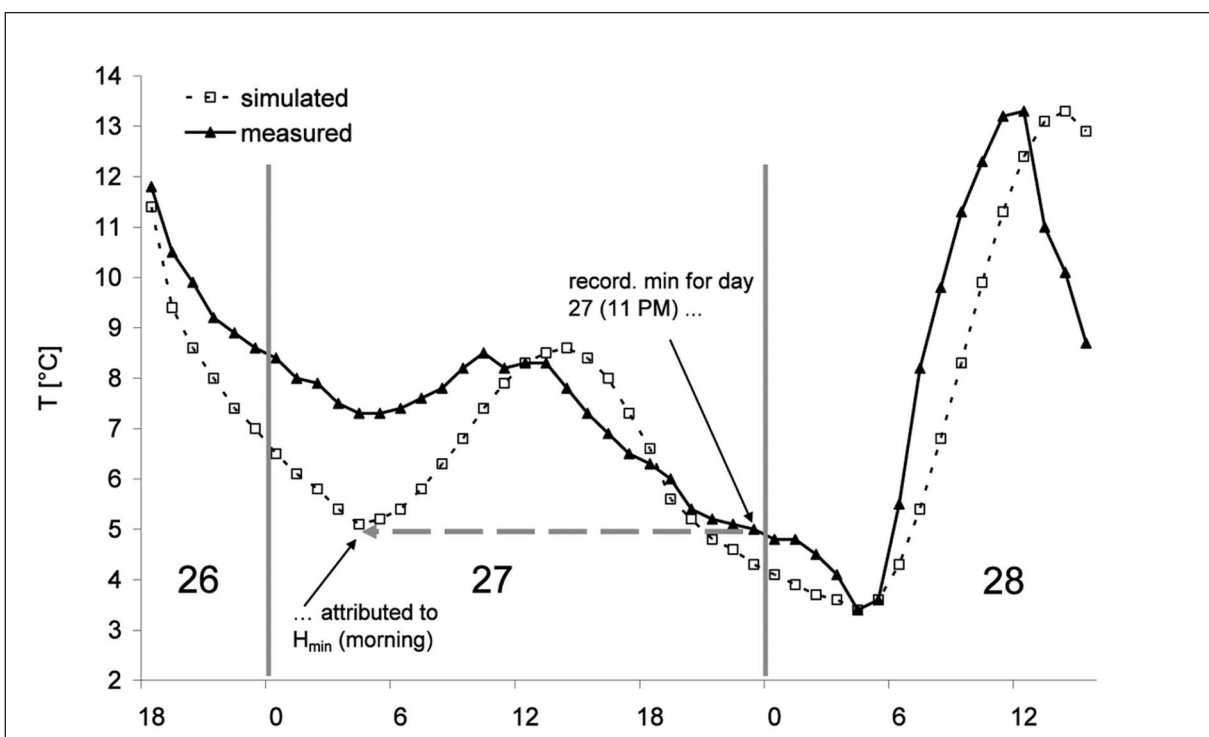


**Fig. 5 – Example of interpolation error due to the erroneous attribution of the time of minimum temperature by the interpolation algorithm, when no restriction is applied to the possible timing of occurrence of minima. Cles, 26th – 28th May 1984.**  
**Fig. 5 – Esempio di errore di interpolazione dovuto all’erronea attribuzione dell’ora della temperatura minima, quando non è applicata alcuna restrizione sugli orari possibili di occorrenza delle minime. Cles, 26 – 28 maggio 1984.**

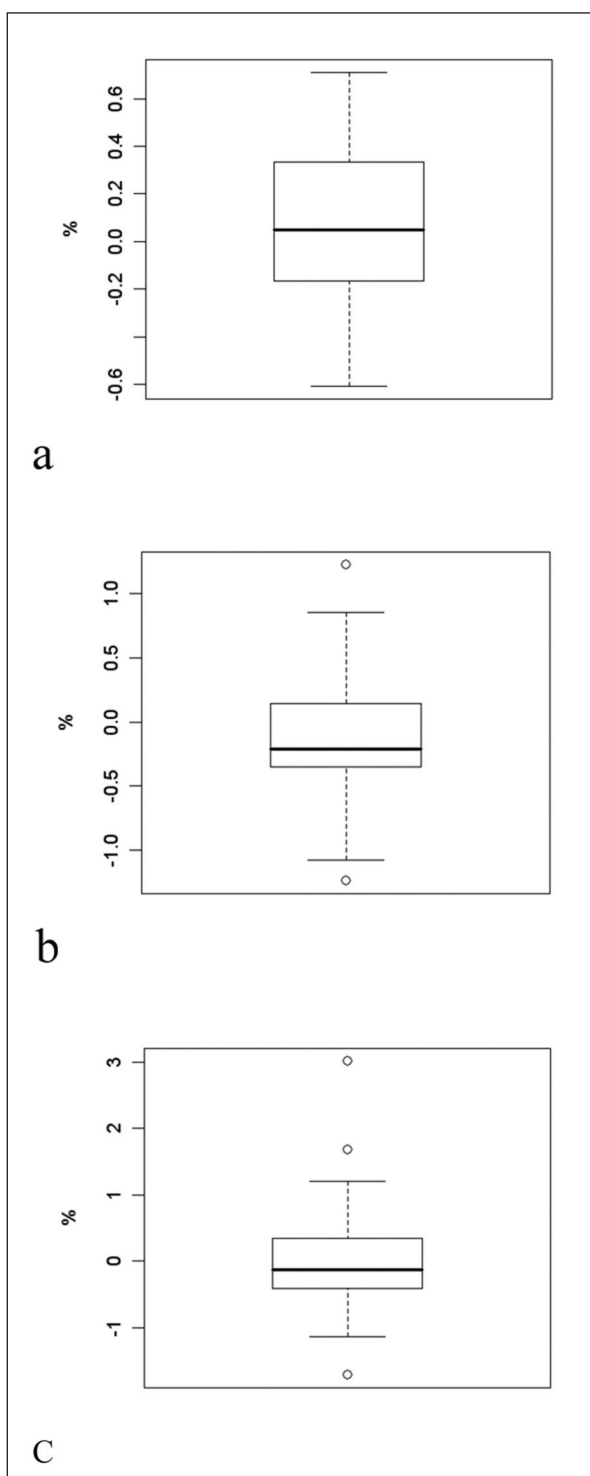


**Fig. 6** – Boxplots of percentages of errors of the hourly thermal sums (1<sup>st</sup> Jan – 31<sup>st</sup> Dec., 1983 – 2009), from the comparison with measured hourly values – Station of Cles. a)  $T_{\text{soglia}} = 0^{\circ}\text{C}$ . b)  $T_{\text{soglia}} = 5^{\circ}\text{C}$ . c)  $T_{\text{soglia}} = 10^{\circ}\text{C}$ .

*Fig. 6 – Boxplot degli errori percentuali di stima delle somme termiche orarie (1° genn. – 31 dic., 1983 – 2009) determinate dal confronto con i valori orari misurati – Stazione di Cles.*  
 a)  $T_{\text{threshold}} = 0^{\circ}\text{C}$ . b)  $T_{\text{threshold}} = 5^{\circ}\text{C}$ . c)  $T_{\text{threshold}} = 10^{\circ}\text{C}$ .

are also single major errors, as can be seen from fig. 4, but the Inter-Quantile Range (IQR) remains narrow. During the trials, a few considerable errors in the records have been detected and corrected, but it is highly probable that still a few cases of disagreement between modelled and measured temperatures could be attributed to errors in the database, rather than to the interpolation itself. The introduction of the “linear” option in eqs. 1 and 4 allows the removal of a non-negligible negative bias of estimation, which would have required an offset of the interpolation curves in the range of 0.5 – 0.6 °C.

The interpolation algorithm is intrinsically unbiased in the reproduction of both minimum and maximum daily values. Indeed, it functions pretty well, but it rather strictly reproduces the same pattern of temperature trend for every day, even with the timings of curve discontinuity ( $H_{\min}$ ,  $H_{\max}$  and  $H_s$ ) changing from month to month and the night-time curve type changing according to the case. One assumption is that the time of minimum falls in a time band ranging from 5 to 8 AM, according to the month. The ideal minimum series should be built by calculating minimum temperature in that period of the day, so temperature strongly decreasing after sunset would not contribute to the search for minimum of that day (a well-known problem, see e.g. Parton and Logan, 1981, and Wann *et al.*, 1985). This has its physical grounds; however, in most meteorological databases, this is not the case, minimum temperatures being just the lowest measured in each day from 0 AM to 12 PM. In the first part of this investigation, Eccel (2010) calculated that days when minimum temperatures fall after midday account for, roughly, one-fifth of the total. Now, the results above refer to “blind” daily series, whose corresponding hourly series were not considered in building minimum and maximum series. A check on the major interpolation errors shows that many of them are due to the wrong attribution of the time of occurrence of maximum and, above all, of minimum daily temperature (the mechanism is exemplified in Fig. 5). The absolute error of the interpolation could be reduced further by using maximum and minimum series created with the abovementioned “filter” on the time bands for the search of minima.

It may be argued that the mean absolute error of the interpolation, larger than 1 °C, is still non-negligible. In order to assess the cumulative error that can arise from the use of an hourly series, a

test was carried out to compare values of thermal sums originated by interpolated data with the true ones, calculated with measures. In many agrometeorological applications (especially vegetal and parasite developmental models), the use of hourly series is associated to the calculation of thermal sums, so this control is particularly delicate and useful. Three thresholds were considered: 0°C, 5°C, and 10°C. Results show that errors increase with the threshold, but they remain fully acceptable, mean values being as low as  $-0.13\% \pm 0.51\%$  (period: 1983-2009) for a threshold temperature of 10°C (Fig. 6).

Finally, it may be interesting to assess the improvement of the creation of simulated hourly temperature in a series to the correct estimation of mean daily temperature. In absence of other information, mean temperature is usually calculated as the average between minimum and maximum daily values. But, when the average can be calculated from hourly values, the error committed when averaging  $T_{\min}$  and  $T_{\max}$  is evident: a mean absolute error of  $0.85 \pm 0.73 / 0.72 \pm 0.52^\circ\text{C}$ , respectively for S. Michele and Cles (for the usual period 1983-2009), and (remarkable) biases of, respectively,  $+0.61 \pm 0.94 / +0.57 \pm 0.68^\circ\text{C}$ . On the other hand, the production of the hourly interpolation can lower such high biases of one order of magnitude, as reported above, even if it cannot decrease the standard deviation of daily errors ( $0.79 / 0.58^\circ\text{C}$ , respectively for S. Michele and Cles).

The reported results can be certainly refined, by taking into consideration more than two stations, possibly displaying more pronounced differences in climatic features. This investigation, and the analyses of possible differences from one site to another, make up the core of future development of this work. Nevertheless, the similarity in the results of the calibration trials of the two analysed series encourages its generalization and the extension to sites where no hourly records are available. So evident are the advantages coming from the use of simulated hourly series, and so easy the application of interpolation algorithms, that we warmly feel to encourage their use.

## ACKNOWLEDGMENT

This study was carried out in the frame of the project ENVIROCHANGE, funded by the Autonomous Province of Trento.

Thanks to Piero Cau for his suggestions.

*Note: the R codes for hourly interpolation are available on demand.*

## REFERENCES

- Ashcroft L.G., Richardson E.A., Schuyler D.S., 1977. A statistical method of determining chill unit and growing degree hour requirements for deciduous fruit trees. Horticultural Science, 12: 347-348.
- Blaeser M., Weltzien H.C., 1979. Epidemiological studies to improve the control of grapevine downy mildew (*Plasmopara viticola*). Journal of Plant Diseases and Protection, 86: 489-498.
- Cesaraccio C., Spano D., Duce P., Snyder, R.L., 2001. An improved model for determining degree-day values from daily temperature data. Int. J. Biometeorol, 45: 161-169.
- Eccel E., 2010. What we can ask to hourly temperature recording. Part I: statistical vs. meteorological meaning of minimum temperature. Italian Journal of Agrometeorology, anno 15, (2): 41-43.
- Gleason M.L., Taylor S.E., Loughin T.M., Koehler K.J., 1994. Development and validation of an empirical model to estimate the duration of dewperiods. Plant Dis., 78: 1011-1016.
- Parton W.J., and Logan J.A., 1981. A model for diurnal variation in soil and air temperature. Agricultural Meteorology, 23: 205-216.
- Rea R., Eccel E., 2006. Phenological models for blooming of apple in a mountainous region. International Journal of Biometeorology, Volume 51: 1-16.
- Rossi V., Caffi T., Giosuè S., Bugiani R., 2008. A mechanistic model simulating primary infections of downy mildew in grapevine. Ecological modelling, 212: 480-491.
- Wann M., Yen D., and Gold H.J., 1985. Evaluation and calibration of three models for daily cycle of air temperature. Agricultural and Forest Meteorology, 34: 121-128.
- Worner S., 1988. Evaluation of diurnal temperature models and thermal summation in New Zealand. Journal of Economic Entomology, 81: 9-13.



See discussions, stats, and author profiles for this publication at: <https://www.researchgate.net/publication/293186245>

# What we can ask to hourly temperature recording. Part II: Hourly interpolation of temperatures for climatology and modelling

Article in *Italian Journal of Agrometeorology* · August 2010

---

CITATIONS

14

READS

298

1 author:



Emanuele Eccel

Fondazione Edmund Mach - Istituto Agrario San Michele All'Adige

67 PUBLICATIONS 1,362 CITATIONS

[SEE PROFILE](#)

# What we can ask to hourly temperature recording.

## Part II: hourly interpolation of temperatures for climatology and modelling

Emanuele Eccel<sup>\*1</sup>

**Abstract:** Several applications in agrometeorology and in biological modelling make use of hourly time series. However, some difficulties arise in finding hourly series of acceptable length, resulting in a limited application of hourly models. In this work, an interpolation model is described which makes use of linear, parabolic and sinusoidal functions between daily maximum and minimum temperatures. Benefits coming from the use of simulated time series are discussed. The errors due to the reconstructed hourly series are small, especially when applications like thermal sums are considered, in which a compensation of single hourly errors takes place. The generation of hourly series allows a good correction of the error committed in mean temperature estimation, when it is calculated by the simple arithmetic average of daily maximum and minimum.

**Keywords:** temperature, interpolation

**Riassunto:** Le serie temporali orarie hanno diverse applicazioni in agrometeorologia e nella modellistica biologica. Esistono tuttavia difficoltà nel reperire serie orarie di sufficiente lunghezza, tanto che l'uso ne è limitato. Nel lavoro viene descritto un modello che impiega funzioni lineari, paraboliche e sinusoidali per interpolare valori orari a partire dai valori giornalieri di temperatura massima e minima. Vengono quindi discussi i benefici dell'uso delle serie orarie simulate. Gli errori determinati dall'uso di serie orarie ricostruite sono piccoli, specialmente quando si valutano applicazioni come le somme termiche, che consentono una compensazione dei singoli errori orari. La generazione di serie orarie permette anche di correggere in gran parte l'errore che si commette nella stima delle temperature medie effettuata con la semplice media algebrica di massime e minime giornaliere.

**Parole chiave:** temperatura, interpolazione

In spite of a widespread use of models that make use of daily meteorological values, there are many situations in which hourly resolution is advisable, or even required. This is the case of modelling infection precursors (for example: Rossi *et al.*, 2008; Gleason *et al.*, 1994; Blaeser and Weltzien, 1979); traditionally, chill requirements in phenological models has been expressed in (normalised) chill hours (Ashcroft and Richardson, 1977); Rea and Eccel (2006) found that phenological hourly models based on thermal sums performed better than the equivalent daily ones, even when hourly temperature series were artificially produced from daily maximum and minimum values. Worner (1988) warns about the errors coming from the use of daily values for thermal summations, instead of hourly ones; the author also presents a review of hourly interpolation algorithms developed starting from the sixties.

One problem with the use of hourly temperatures, at least in climate applications, is the limited availability of hourly series, often shorter than the period in which series of minima and maxima are available. In climatic

projections, hourly resolution is unavailable from both direct and downscaled model outputs. The present work shows the usefulness of implementing hourly interpolation models, proposing a simple and rapid algorithm. Equations were adapted from the "TM model" (Cesaraccio *et al.*, 2001); in particular, equation (2) was changed and equations (1) and (4) were split to account for possible linear interpolation stretches in the corresponding time bands.

The protocol consists of a first (optional) part of calibration, for the setting of monthly dawn times, hour of minimum, hour of maximum, and sunset times, and of the parameters "c" and "z". Hourly interpolation is carried out with four portions of curves (Fig. 1): parabola/line I, from 0 AM to dawn (same equation of the previous day, from sunset to 11 PM); sinusoid I, from dawn to time of maximum; sinusoid II, from maximum to sunset time; parabola/line II, from sunset to midnight (and continuing till dawn of the following day).

The four equations used are the following:

parab./line I:

$$T(t) = T_{s-1} + \Delta_I \cdot (t + 24 - H_s)^2 \quad (1)$$

$$0 \leq t \leq H_{\min}$$

<sup>\*</sup> Corresponding author: emanuele.eccel@iasma.it  
<sup>1</sup> IASMA Research and Innovation Centre - Fondazione Edmund Mach - Environment and Natural Resources Area - S. Michele all'Adige (TN) - Italy



sinus I:

$$T(t) = T_{min} + \frac{(T_{max} - T_{min})}{2} \cdot \left[ 1 + \sin\left(\pi \frac{t - H_{min}}{H_{max} - H_{min}} - \frac{\pi}{2}\right) \right] \quad (2)$$

$H_{min} \leq t \leq H_{max}$

sinus. II:

$$T(t) = T_s + (T_{max} - T_s) \cdot \sin\left\{ \frac{\pi}{2} \cdot \left[ 1 + \frac{(t - H_{max})}{(H_s - H_{max})} \right] \right\} \quad (3)$$

$H_{max} \leq t \leq H_s$

parab./line II:

$$T(t) = T_s + \Delta_{II} \cdot (t - H_s)^z \quad (4)$$

$H_s \leq t \leq 23$

with

$$T_s = T_{max} - c(T_{max} - T_{min+1}) \quad (5)$$

$$\Delta_I = \frac{T_{min} - T_{s-1}}{(H_{min} + 24 - H_s)^z} \quad (6a)$$

$$\Delta_{II} = \frac{T_{min+1} - T_s}{(H_{min} + 24 - H_s)^z} \quad (6b)$$

where  $H_{max}$ ,  $H_{min}$ ,  $H_s$  = times of maximum and minimum temperature and time of sunset, respectively;  $T_{max}$ ,  $T_{min}$ ,  $T_s$  = maximum, minimum and sunset temperature, respectively;  $c$ : coefficient;  $z$  = either 0.5 (parabola - case of “clear late/early

night”) or 1 (line - case of “cloudy late/early night”). Subscript “-1”: day before; subscript “+1”: day after. The discrimination between clear and cloudy late night (from midnight to the hour of morning minimum) or early night (from sunset to midnight) was carried out by a calibration on the value of the ratio between daily thermal range ( $DTR_d$ ) and the climatic monthly averages ( $DTR_m$ ):

$$k = \frac{DTR_d}{DTR_m} \quad (7)$$

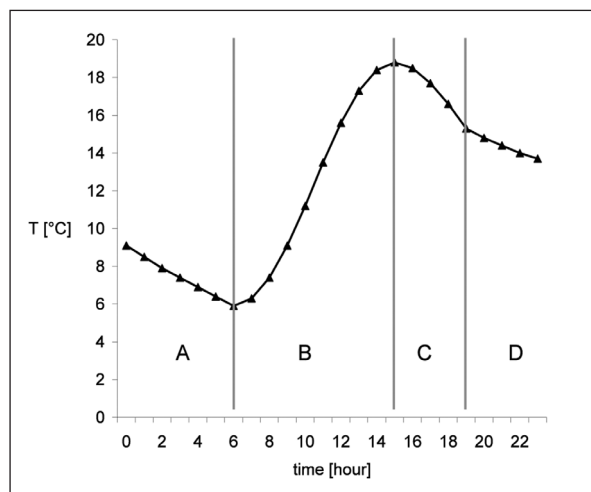


**Fig. 1** – Example of hourly temperature interpolation. A: parabola/line I. B: sinusoid I. C: sinusoid II. D: parabola/line II (see equations in the text).

*Fig. 1 – Esempio di interpolazione oraria delle temperature. A: parabola/retta I. B: sinusoida I. C: sinusoida II. D: parabola/retta II (equazioni nel testo).*

	$H_{min}$		$H_{max}$		$H_s$		C	
	S. Michele	Cles	S. Michele	Cles	S. Michele	Cles	S. Michele mean: 0.39	Cles mean: 0.38
JAN	8	<b>8</b>	15	<b>15</b>	17	<b>17</b>	0.36	0.36
FEB	8	<b>8</b>	16	<b>15</b>	18	<b>18</b>	0.37	0.38
MAR	7	<b>7</b>	15	<b>15</b>	18	<b>18</b>	0.26	0.28
APR	6	<b>6</b>	15	<b>15</b>	19	<b>19</b>	0.36	0.37
MAY	5	<b>5</b>	15	<b>15</b>	20	<b>19</b>	0.46	0.36
JUN	5	<b>5</b>	15	<b>15</b>	20	<b>20</b>	0.45	0.46
JUL	5	<b>5</b>	15	<b>15</b>	20	<b>20</b>	0.44	0.47
AUG	6	<b>6</b>	15	<b>15</b>	19	<b>19</b>	0.35	0.39
SEP	6	<b>6</b>	15	<b>15</b>	18	<b>18</b>	0.30	0.34
OCT	7	<b>7</b>	15	<b>15</b>	18	<b>17</b>	0.49	0.30
NOV	8	<b>7</b>	<b>15</b>	14	<b>17</b>	<b>17</b>	0.41	0.40
DEC	8	<b>8</b>	15	<b>15</b>	<b>17</b>	<b>17</b>	0.41	0.47

**Tab. 1** – Calibration of parameters for TM model.  $H_{min}$ : hour of minimum temperature;  $H_{max}$ : hour of maximum temperature;  $H_s$ : hour of sunset;  $c$ : coefficient for the determination of  $T_s$  (sunset temperature – see equation 5). Values used in the “unified” setting are highlighted.

*Tab. 1 – Calibrazione dei parametri per il modello TM.  $H_{min}$ : ora della temperatura minima;  $H_{max}$ : ora della temperatura massima;  $H_s$ : ora del tramonto;  $c$ : coefficiente per la determinazione di  $T_s$  (temperatura al tramonto – vedi formula 5). I valori impiegati nell’impostazione “unificata” sono evidenziati.*

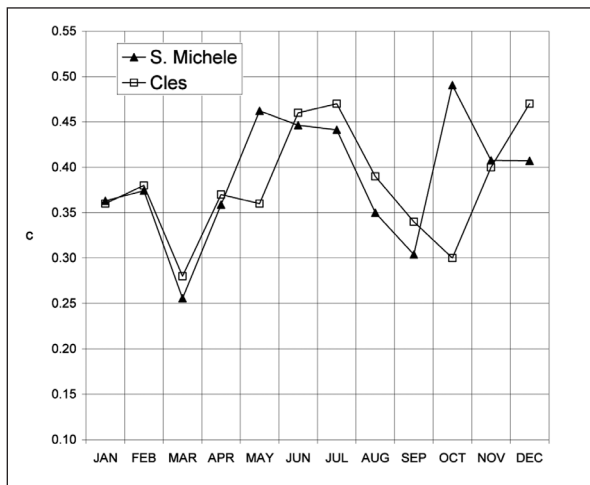


**Fig. 2** – Values of the coefficient “c” for the assessment of sunset temperature – see equation 5 - calibrated monthly over a 27-year period (1983 – 2009), stations of S. Michele and Cles.

*Fig. 2 – Valori del coefficiente “c” per la stima della temperatura al tramonto - vedi formula 5 - calibrato mensilmente su un periodo di 27 anni (1983 – 2009), stazioni di S. Michele e Cles.*

which gave for both stations and for both cases (“late night” and “early night”) an optimal value of 1.5: for lower values the linear equation allows for better interpolation than the parabolic one.

A monthly differentiation is important for times of minimum (“dawn”) and for times of change of

the equation from sinusoid II to parabola/line II (“sunset”), secondarily for the time of maximum, which, for mean hourly recordings, peaks in frequency (with few exceptions) at 3 PM (that is, in the previous 60 minutes).  $H_s$  was calibrated as the time of the day more frequently associated to the largest temperature fall in the afternoon. Also the parameter “c”, necessary for the definition of the sunset temperature  $T_s$ , can be easily calibrated on a monthly basis. The authors of the TM model proposed a mean value for “c” of 0.39, which is fully confirmed by the calibration carried out on the two 27-year long series of S. Michele (210 m a.s.l., valley bottom), and Cles (650 m a.s.l., hill side), in Trentino (Tab. 1 and Fig. 2). With the exception of a couple of months, a good agreement can be observed for the calibration of “c” between the two stations. As regards the calibration of timing, in general, a difference of one hour is not dramatic, corresponding to shifts in the discontinuities of the curve type at a time when either the rate of temperature change is at its minimum ( $H_{\min}$  and  $H_{\max}$  times), or both curves are decreasing ( $H_s$  time), resulting in limited errors.

The introduction of linear interpolation of night values as alternative to the parabolic one allows for an improvement of both mean and absolute errors, thanks to the calibration of the parameter k (eq. 7). Indeed, when night radiation loss is

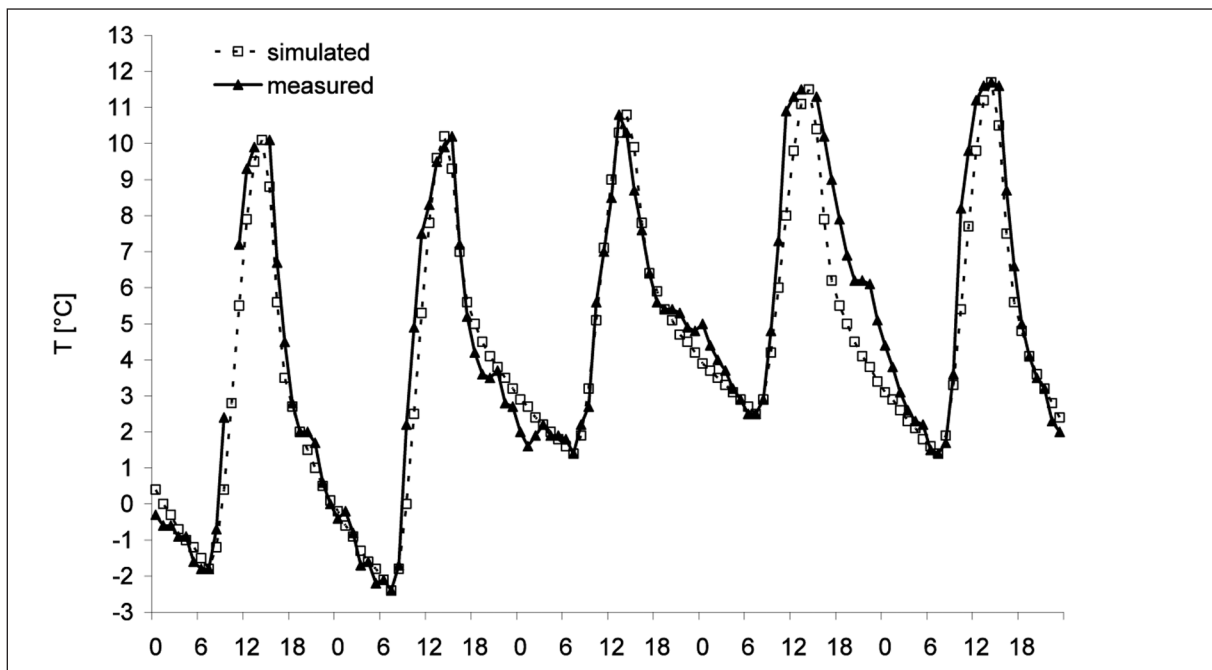


**Fig. 3** – Example of hourly interpolation, compared with measured values (S. Michele, 24<sup>th</sup> – 28<sup>th</sup> January 1983).

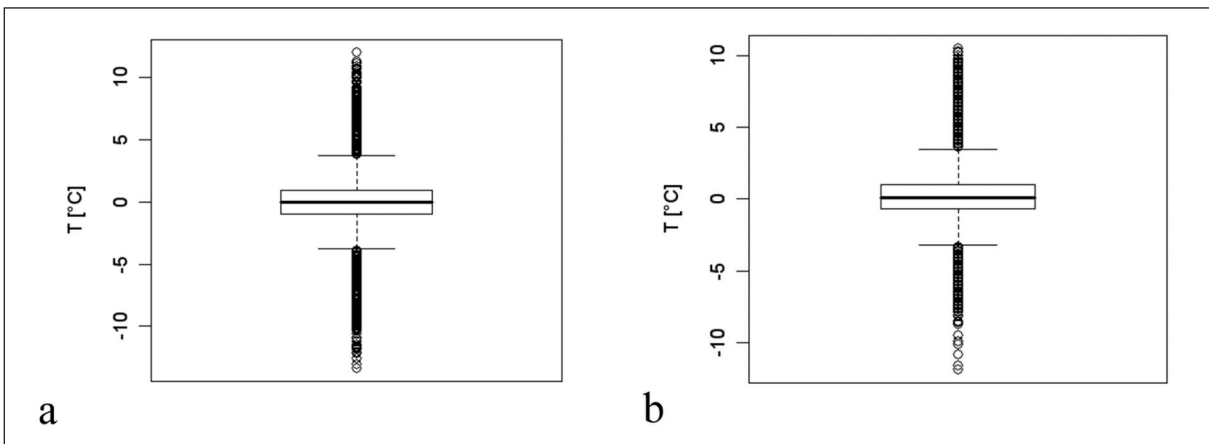


**Fig. 4 – Boxplots of estimation errors of hourly temperature (estimated – measured), 1983-2009. a) S. Michele; b) Cles.**  
**Fig. 4 – Boxplot dell'errore di stima della temperatura oraria (stimata – misurata), 1983-2009. a) S. Michele; b) Cles**

inhibited (as in the case of overcast or just cloudy sky), the temperature decrease is irregular and, in general, there is no clear sign of a concavity in the corresponding line.

For simulating the case of unavailability of hourly series, a “unified” set of parameters was chosen. It can be seen that there are no large differences in the two series between  $H_{\min}$ ,  $H_{\max}$  and  $H_s$ , so the

“smoothest” set of monthly  $H_{\min}$  and  $H_s$  was chosen (see Tab. 1), while  $H_{\max}$  was fixed to the constant value of 15 (3 PM) and  $c$  to the constant value of 0.39.

The application of the interpolation algorithm (excerpt in Fig. 3) yields a mean error of -0.01 / +0.04 °C and a mean absolute error of 1.29 / 1.14 °C, for S. Michele and Cles, respectively. There

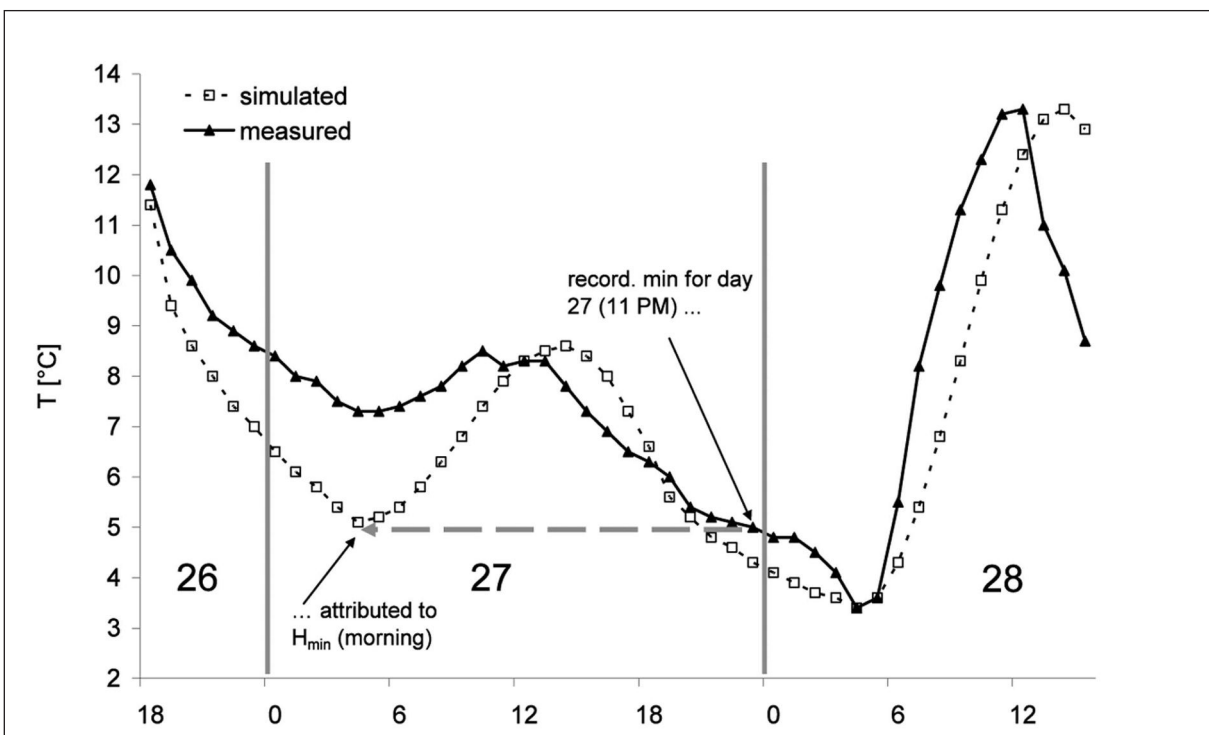


**Fig. 5 – Example of interpolation error due to the erroneous attribution of the time of minimum temperature by the interpolation algorithm, when no restriction is applied to the possible timing of occurrence of minima. Cles, 26th – 28th May 1984.**  
**Fig. 5 – Esempio di errore di interpolazione dovuto all'erronea attribuzione dell'ora della temperatura minima, quando non è applicata alcuna restrizione sugli orari possibili di occorrenza delle minime. Cles, 26 – 28 maggio 1984.**

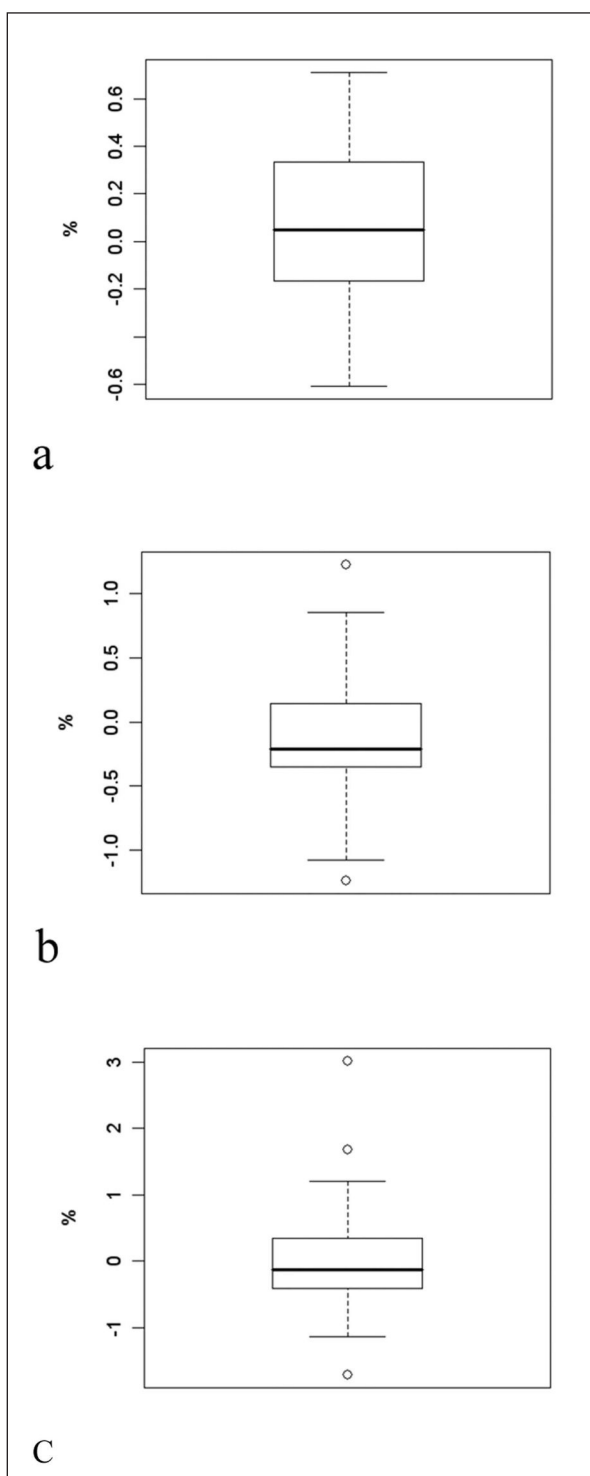


**Fig. 6** – Boxplots of percentages of errors of the hourly thermal sums (1<sup>st</sup> Jan – 31<sup>st</sup> Dec., 1983 – 2009), from the comparison with measured hourly values – Station of Cles. a)  $T_{\text{soglia}} = 0^{\circ}\text{C}$ . b)  $T_{\text{soglia}} = 5^{\circ}\text{C}$ . c)  $T_{\text{soglia}} = 10^{\circ}\text{C}$ .

*Fig. 6 – Boxplot degli errori percentuali di stima delle somme termiche orarie (1° genn. – 31 dic., 1983 – 2009) determinate dal confronto con i valori orari misurati – Stazione di Cles.*  
 a)  $T_{\text{threshold}} = 0^{\circ}\text{C}$ . b)  $T_{\text{threshold}} = 5^{\circ}\text{C}$ . c)  $T_{\text{threshold}} = 10^{\circ}\text{C}$ .

are also single major errors, as can be seen from fig. 4, but the Inter-Quantile Range (IQR) remains narrow. During the trials, a few considerable errors in the records have been detected and corrected, but it is highly probable that still a few cases of disagreement between modelled and measured temperatures could be attributed to errors in the database, rather than to the interpolation itself. The introduction of the “linear” option in eqs. 1 and 4 allows the removal of a non-negligible negative bias of estimation, which would have required an offset of the interpolation curves in the range of 0.5 – 0.6 °C.

The interpolation algorithm is intrinsically unbiased in the reproduction of both minimum and maximum daily values. Indeed, it functions pretty well, but it rather strictly reproduces the same pattern of temperature trend for every day, even with the timings of curve discontinuity ( $H_{\min}$ ,  $H_{\max}$  and  $H_s$ ) changing from month to month and the night-time curve type changing according to the case. One assumption is that the time of minimum falls in a time band ranging from 5 to 8 AM, according to the month. The ideal minimum series should be built by calculating minimum temperature in that period of the day, so temperature strongly decreasing after sunset would not contribute to the search for minimum of that day (a well-known problem, see e.g. Parton and Logan, 1981, and Wann *et al.*, 1985). This has its physical grounds; however, in most meteorological databases, this is not the case, minimum temperatures being just the lowest measured in each day from 0 AM to 12 PM. In the first part of this investigation, Eccel (2010) calculated that days when minimum temperatures fall after midday account for, roughly, one-fifth of the total. Now, the results above refer to “blind” daily series, whose corresponding hourly series were not considered in building minimum and maximum series. A check on the major interpolation errors shows that many of them are due to the wrong attribution of the time of occurrence of maximum and, above all, of minimum daily temperature (the mechanism is exemplified in Fig. 5). The absolute error of the interpolation could be reduced further by using maximum and minimum series created with the abovementioned “filter” on the time bands for the search of minima.

It may be argued that the mean absolute error of the interpolation, larger than 1 °C, is still non-negligible. In order to assess the cumulative error that can arise from the use of an hourly series, a

test was carried out to compare values of thermal sums originated by interpolated data with the true ones, calculated with measures. In many agrometeorological applications (especially vegetal and parasite developmental models), the use of hourly series is associated to the calculation of thermal sums, so this control is particularly delicate and useful. Three thresholds were considered: 0°C, 5°C, and 10°C. Results show that errors increase with the threshold, but they remain fully acceptable, mean values being as low as  $-0.13\% \pm 0.51\%$  (period: 1983-2009) for a threshold temperature of 10°C (Fig. 6).

Finally, it may be interesting to assess the improvement of the creation of simulated hourly temperature in a series to the correct estimation of mean daily temperature. In absence of other information, mean temperature is usually calculated as the average between minimum and maximum daily values. But, when the average can be calculated from hourly values, the error committed when averaging  $T_{\min}$  and  $T_{\max}$  is evident: a mean absolute error of  $0.85 \pm 0.73 / 0.72 \pm 0.52^\circ\text{C}$ , respectively for S. Michele and Cles (for the usual period 1983-2009), and (remarkable) biases of, respectively,  $+0.61 \pm 0.94 / +0.57 \pm 0.68^\circ\text{C}$ . On the other hand, the production of the hourly interpolation can lower such high biases of one order of magnitude, as reported above, even if it cannot decrease the standard deviation of daily errors ( $0.79 / 0.58^\circ\text{C}$ , respectively for S. Michele and Cles).

The reported results can be certainly refined, by taking into consideration more than two stations, possibly displaying more pronounced differences in climatic features. This investigation, and the analyses of possible differences from one site to another, make up the core of future development of this work. Nevertheless, the similarity in the results of the calibration trials of the two analysed series encourages its generalization and the extension to sites where no hourly records are available. So evident are the advantages coming from the use of simulated hourly series, and so easy the application of interpolation algorithms, that we warmly feel to encourage their use.

## ACKNOWLEDGMENT

This study was carried out in the frame of the project ENVIROCHANGE, funded by the Autonomous Province of Trento.

Thanks to Piero Cau for his suggestions.

*Note: the R codes for hourly interpolation are available on demand.*

## REFERENCES

- Ashcroft L.G., Richardson E.A., Schuyler D.S., 1977. A statistical method of determining chill unit and growing degree hour requirements for deciduous fruit trees. Horticultural Science, 12: 347-348.
- Blaeser M., Weltzien H.C., 1979. Epidemiological studies to improve the control of grapevine downy mildew (*Plasmopara viticola*). Journal of Plant Diseases and Protection, 86: 489-498.
- Cesaraccio C., Spano D., Duce P., Snyder, R.L., 2001. An improved model for determining degree-day values from daily temperature data. Int. J. Biometeorol, 45: 161-169.
- Eccel E., 2010. What we can ask to hourly temperature recording. Part I: statistical vs. meteorological meaning of minimum temperature. Italian Journal of Agrometeorology, anno 15, (2): 41-43.
- Gleason M.L., Taylor S.E., Loughin T.M., Koehler K.J., 1994. Development and validation of an empirical model to estimate the duration of dewperiods. Plant Dis., 78: 1011-1016.
- Parton W.J., and Logan J.A., 1981. A model for diurnal variation in soil and air temperature. Agricultural Meteorology, 23: 205-216.
- Rea R., Eccel E., 2006. Phenological models for blooming of apple in a mountainous region. International Journal of Biometeorology, Volume 51: 1-16.
- Rossi V., Caffi T., Giosuè S., Bugiani R., 2008. A mechanistic model simulating primary infections of downy mildew in grapevine. Ecological modelling, 212: 480-491.
- Wann M., Yen D., and Gold H.J., 1985. Evaluation and calibration of three models for daily cycle of air temperature. Agricultural and Forest Meteorology, 34: 121-128.
- Worner S., 1988. Evaluation of diurnal temperature models and thermal summation in New Zealand. Journal of Economic Entomology, 81: 9-13.



# Triticum Aestivum L. Phenological response to air temperature in Greece

Athanasiou Kamoutsis<sup>\*1</sup>, Aristidis Matsoukis and Aikaterini Chronopoulou-Sereli<sup>1</sup>

**Abstract:** In this research, the winter wheat (*Triticum aestivum L.*) response to air temperature was investigated in Greece. Phenological observations were taken in order to evaluate the emergence (C0), heading (C1), anthesis (C2), fruit development (C3), and ripening (C4) phenophases of *Triticum aestivum L. cv. Yecora* at the sites (from Northern to Southern Greece) of Xanthi, Kozani, Karditsa, Thives and Araxos, during the period 1985-1990. Also, sowing dates and air temperature data were recorded at the same period. The warmer temperature conditions at the sites of Karditsa, Thives and Araxos promoted the reproductive growth phenophases of wheat (C1, C2, C3 and C4) compared to the respective conditions in Xanthi and Kozani. The C1 phenophase was influenced by the air temperature of the spring months (April and May) at the sites of Xanthi and Araxos. Air temperature during April and May plays an important role, to a different degree, for the C2 phenophase at the sites of the Central (Karditsa) and Southern (Thives, Araxos) part of Greece.

**Keywords:** phenology, reproductive growth, winter wheat

**Riassunto:** In questa ricerca si è studiato il riscontro del frumento invernale alla temperatura dell'aria in Grecia. Sono state effettuate osservazioni fenologiche per valutare l'emersione (C0), la spigatura (C1), la fioritura (C2), la formazione dei frutti (C3) e la maturazione dei frutti (C4) del *Triticum aestivum L. cv. Yecora* nelle regioni (dalla Grecia settentrionale a quella meridionale) di: Xanthi, Kozani, Karditsa, Tebe e Araxos nell'arco di tempo 1985-1990. Inoltre, sono state registrate le date della semina e della temperatura dell'aria durante lo stesso periodo. Le temperature più elevate nelle zone di Karditsa, Tebe e Araxos contribuiscono ad accelerare i tempi delle fasi fenologiche di crescita riproduttiva del frumento (C1, C2, C3, C4) in comparazione con le rispettive condizioni di Xanthi e Kozani. La data d'inizio della C1 fu influenzata dalla temperatura dell'aria dei mesi primaverili (aprile e maggio) nelle regioni di Xanthi e Araxos. La temperatura dell'aria durante i mesi di aprile e maggio ha un ruolo rilevante, a differenti gradi, per le date d'inizio della fase C2 nelle regioni della zona centrale della Grecia (Karditsa) ed in quelle meridionali (Tebe, Araxos).

**Parole chiave:** fenologia, crescita riproduttiva, frumento invernale

## INTRODUCTION

Phenology, the sequence of plant life events in the various ecosystems, as expressed by the timing of various plant stages, is influenced by the environment, especially temperature (Schwartz, 2003).

Air temperature has been strongly correlated with the seasonal timing of plant phenophases, such as anthesis, in mid- and high- latitudes (Chmielewski, 2003; Menzel, 2003; Tao *et al.*, 2006; Estrella *et al.*, 2007; Pudas *et al.*, 2008). Higher values of temperature than a certain value, result in a greater rate of plant development and thus an earlier appearance of phenophases (Hu *et al.*, 2005). It has been reported that the rise of air temperature by 1 °C led to an earlier onset of various phenophases of fruit trees and annual crops by 4-17 days (Sparks *et al.*, 2000; Chmielewski *et al.*, 2004; Doi, 2007). The knowledge of the onset

of plant phenophases could provide valuable information for the evaluation of climate variation at a local scale (Aono and Kazui, 2008). Also, long series of phenological observations may be used for the detection of climate variability and can facilitate the understanding of climate changes (Ventura *et al.*, 2006; Bonamano, 2008).

Changes in the appearance of fruit trees and field crops phenophases have a great economic importance because of their impact on the quality of agricultural products and crop yield (Chmielewski *et al.*, 2004). Winter wheat (*Triticum aestivum L.*), one of the most important small-grain cereal crops for human nutrition (Lithourgidis *et al.*, 2006) is an important crop grown in many Mediterranean climate zones around the world (Schillinger *et al.*, 2008), playing a noticeable role in the development of civilization (Martin *et al.*, 1976). This crop is of major importance for the agricultural production in Greece (Lithourgidis *et al.*, 2006). The phenological behavior of winter wheat is strongly influenced by air temperature (Dalezios *et al.*,

<sup>\*</sup> Corresponding author: email: akamoutsis@hua.gr

<sup>1</sup> Laboratory of General and Agricultural Meteorology, Department of General Sciences, Agricultural University of Athens, Athens, Greece.



2002; Sadras and Monzon, 2006; Wang *et al.*, 2008). The analysis of the phenological data of a particular wheat cultivar in several locations could provide a measure for their temperature changes (Hu *et al.*, 2005). Global warming is expected to cause shorter growing seasons for wheat in the Mediterranean basin (Rosenzweig and Tubiello, 1997; Harrison *et al.*, 2000; Ferrara *et al.*, 2010). This would lead to an earlier occurrence of the spring phenophases of wheat, resulting in a shorter grain-filling period and consequently in the reduction of yields (Harrison and Butterfield, 1996). According to the climate change scenarios, an increase of 2 °C during the period of 2031-2060 is expected to cause a crop growing cycle reduction of cereals by 9.0 days on average, in the European Mediterranean countries (Bindi and Moriondo, 2005; Moriondo and Bindi, 2007). The purpose of this study is to investigate the response of winter wheat (*Triticum aestivum* L. cv. Yecora) phenophases to air temperature at representative cultivated sites in Greece.

## MATERIALS AND METHODS

Research was conducted at five representative wheat cultivation sites in Greece (Tab. 1), based mainly on the latitude, altitude and distance from the sea during a 5-year cultivation period from 1985/86 to 1989/90.

Phenological observation data for winter wheat (*Triticum aestivum* L. cv. Yecora) were collected weekly, from a cultivated area of about 4000 m<sup>2</sup> in each site, in order to evaluate the starting dates of wheat stages (named 'phenophases') based on a

recommended scale (BBCH) for phenological observations according to Meier (2003): emergence - coleoptile breaks through soil surface – BBCH 09 - appearance of the planting lines (C0), heading of about 10% of plants - BBCH 51 (C1), anthesis when 10% of the flowers has opened - BBCH 61 (C2), fruit development when the caryopsis is watery ripe and 10% of the grains has reached final size - BBCH 71 (C3) and ripening or fruit coloration - BBCH - 81 (C4). In addition, the dates of sowing (D2) were recorded. At the same time, air temperature data were provided by the meteorological stations of the Hellenic National Meteorological Service which covered the study sites. The mean distance between the phenological observation sites and the meteorological stations was 10.4 km and the maximum distance did not exceed 12.3 km. From the air temperature data, average values were calculated during each cultivation period (November – July) at each study site. A Pearson's correlation analysis was conducted between the examined wheat phenophases and the average air temperature during the period of their appearance. For the statistical analysis, SPSS 11.0 and MS Excel were used with a significance level (*p*) ≤ 0.05.

## RESULTS AND DISCUSSION

The *Triticum aestivum* L. phenophases at the study sites in Greece from 1985 to 1990 are presented in Tab. 2. During the reproductive growth phenophases of wheat from April to June, the average temperature for the years 1986-1990, was higher by 2.3 °C, 3.1 °C and 3.4 °C, at the sites of Araxos, Thives and Karditsa,

Site	Region	Latitude	Longitude	Altitude (m)	Distance from the sea (km)	AvgT (°C)	MAT (°C)	base period
Xanthi (Xa)	East Macedonia and Thrace	40° 54' N	24° 36' E	5	3	18.9	14.9	1984-97
Kozani (Kz)	West Macedonia	40° 17' N	21° 46' E	627	42	17.1	12.9	1955-97
Karditsa (Kard)	Thessaly	39° 33' N	21° 46' E	109	70	20.5	16.1	1973-97
Thives (Th)	Central Greece	38° 19' N	23° 31' E	140	19	20.2	16.8	1957-97
Araxos (Arx)	West Greece (Peloponnese Peninsula)	38° 08' N	21° 25' E	15	4	19.4	17.8	1955-97

**Tab. 1** - Phenological observation sites of *Triticum aestivum* L. cv. Yecora in Greece and respective average temperature values (AvgT) from April to June during the period 1986-90 in these sites. MAT: Climatic values of mean annual temperature (Source: Hellenic National Meteorological Service, 1999).

*Tab. 1 - Regioni di osservazioni fenologiche del Triticum aestivum L. cv. Yecora in Grecia e rispettivi valori medi della temperatura (AvgT) per il periodo aprile-giugno nell'arco di tempo 1986-90 nelle zone in oggetto. MAT: Valori climatici della temperatura annuale media. (Sorgente: Hellenico Nationale Servizio Meteorologico, 1999).*

	<b>X<sub>Xa</sub></b>	<b>SE<sub>Xa</sub></b>	<b>X<sub>Kz</sub></b>	<b>SE<sub>Kz</sub></b>	<b>X<sub>Kard</sub></b>	<b>SE<sub>Kard</sub></b>	<b>X<sub>Th</sub></b>	<b>SE<sub>Th</sub></b>	<b>X<sub>Arx</sub></b>	<b>SE<sub>Arx</sub></b>
<b>D2</b>	321.2	3.7	304.4	3.0	321.0	0.9	319.2	6.2	312.8	3.0
<b>C0</b>	353.4	5.8	335.2	4.8	338.2	2.9	333.0	3.3	322.0	3.6
<b>C1</b>	118.2	3.8	118.4	5.8	107.2	4.8	103.0	4.0	111.6	3.6
<b>C2</b>	135.2	1.1	142.2	2.0	123.0	9.0	117.0	2.7	118.2	3.7
<b>C3</b>	149.2	3.4	152.0	3.2	135.2	5.8	129.6	3.4	142.0	2.9
<b>C4</b>	169.6	5.5	170.2	2.9	165.8	4.0	164.0	4.9	161.8	4.8

**Tab. 2** - Mean values in Julian days (X) and Standard error (SE) of the mean of the sowing dates and of the studied phenophases of *Triticum aestivum* L. cv. Yecora at the sites of Xanthi, Kozani, Karditsa, Thives and Araxos during the period 1985-90.

*Tab. 2 - Valori medi, in giorni giuliani (X) ed Errore standard (SE) della media delle date della semina e delle fasi fenologiche studiate del Triticum aestivum L. cv. Yecora nelle zone di Xanthi, Kozani, Karditsa, Tebe e Araxos durante il periodo 1985-90.*

respectively, than in Kozani. Similarly, the site of Xanthi was warmer than Kozani by 1.8 °C (Tab. 1). Thus, during the study period, in the northern part of Greece (Kozani, Xanthi) cooler temperature conditions dominated, compared to the sites of Karditsa, Thives and Araxos (Central and Southern part of Greece). We can assume that the warmer temperature conditions in the sites of Karditsa, Thives and Araxos promoted the reproductive growth phenophases (C1, C2, C3 and C4) compared to the respective ones in Xanthi and Kozani (Tab. 2). The results of the correlation analysis (Tab. 3) between air temperature and the reproductive growth phenophases indicated that the C1 phenophase correlated negatively with the average air temperature in April in Xanthi and Araxos. Also, at this site, a negative correlation was observed at a higher degree between C1 and air temperature for the period April-May, compared to the temperature in both April and May. These findings showed that the C1 phenophase was influenced by the air temperature in April and May in the coastal sites of Araxos and Xanthi which are characterized by lower altitudes (Tab. 1).

A negative correlation (Pearson) between the C2 phenophase and the average air temperature in April-May was observed at the sites of Karditsa, Thives and Araxos (Tab. 3). In addition, a higher correlation between the above mentioned phenophase and the air temperature in April compared to the April-May period was observed in Thives. On the other hand, a lower correlation between C2 and the air temperature in both April and May, compared to the April-May period was observed in Araxos. These findings indicated that the temperature during the above months is a crucial factor, to a different degree, for the C2 phenophase at the sites of the Central and

Southern part of Greece. The correlation between the air temperature of the April-May period and C2 gets slightly stronger from Central (Karditsa) to Southern Greece (Thives, Araxos).

The C3 phenophase correlated negatively with the average air temperature of the April-June period in Karditsa and of May in Kozani (Tab. 3). Thus, this phenophase is influenced by the air temperature in spring and early summer months at the continental sites of Central (Karditsa) and Northern Greece (Kozani), depending on the latitude. Generally, higher air temperatures in spring accelerate the developmental process and consequently lead to an advanced timing (Chmielewski and Rötzer, 2001; Chmielewski *et al.*, 2004) of the reproductive growth phenophases. The results of our work are at accordance with those of Tao *et al.* (2006) on winter wheat in China as well as with those of Estrella *et al.* (2007) on winter wheat, barley and rye in Germany. An earlier heading or flowering of wheat at the Great Plains of the United States indicated warmer spring season temperature conditions (Hu *et al.*, 2005). A negative correlation between the milk stage-ripening time period of wheat and air temperature was found by Wang *et al.* (2008) in China. Similarly, a negative correlation between the air temperature and vegetative or reproductive growth phenophases has been observed recently on other crops like cotton, maize, rice and sugar beet (Chmielewski *et al.*, 2004; Tao *et al.*, 2006; Estrella *et al.*, 2007; Wang *et al.*, 2008). On the contrary, the C0 phenophase of vegetative growth did not correlate with air temperature (data not shown), in the vast majority of the cases at the study sites, due to a weaker response of the vegetative growth phenophases of wheat than of the reproductive ones (Porter and Gavith, 1999), in accordance to Estrella *et al.* (2007)

	$T_4$	$T_5$	$T_6$	$T_7$	$T_{45}$	$T_{46}$	$T_{56}$	$T_{67}$
XANTHI								
C1	-0.869*	0.821			0.486			
C2		0.613						
C3		0.759	0.786			0.831		
C4			0.277	0.317			0.351	
KOZANI								
C1	-0.211	0.214			-0.182			
C2		0.820						
C3		-0.964*	0.666			0.824		
C4			0.163					
KARDITSASA								
C1	-0.668							
C2	-0.792	-0.334			-0.923*			
C3	-0.435	-0.620	-0.430		-0.722	-0.931*	-0.577	
C4		-0.524	-0.174				-0.387	
THIVES								
C1	-0.386							
C2	-0.957*	-0.373			-0.930*			
C3	-0.569	-0.241			-0.563			
C4		-0.651	-0.587			0.807		
ARAXOS								
C1	-0.872*	-0.900*			-0.960**			
C2	-0.890*	-0.895*			-0.966*			
C3		-0.779	0.547			0.807		
C4		-0.367	-0.736			-0.608		

\*, \*\*, \*\*\*: significant at  $p \leq 0.05$ , 0.01 and 0.001, respectively.

\*, \*\*, \*\*\*: significativo  $p \leq 0.05$ , 0.01 e 0.001, rispettivamente.

**Tab. 3** - Pearson's correlation coefficients between air temperature (from April to July) and reproductive growth phenophases of wheat (*Triticum aestivum* L. cv. Yecora) in the sites of Xanthi, Kozani, Karditsa, Thives and Araxos, in Greece from 1985/86 to 1989/90.  $T_4$ ,  $T_5$ ,  $T_6$ ,  $T_7$ : average monthly air temperature for April, May, June and July, respectively.  $T_{45}$ ,  $T_{56}$ ,  $T_{46}$ ,  $T_{67}$ : average air temperature from April to May, May to June, April to June and June to July, respectively.

*Tab. 3 - Coefficienti di correlazione di Pearson fra la temperatura d'aria (da aprile fino a luglio) e le date d'inizio delle fasi feonologiche della crescita riproduttiva delle coltivazioni di grano nelle zone di Xanthi, Kozani, Karditsa, Tebe e Araxos in Grecia dal 1985/86 fino al 1989/90.  $T_4$ ,  $T_5$ ,  $T_6$ ,  $T_7$ : temperatura mensile media dell'aria nei mesi di aprile, maggio, giugno e luglio, rispettivamente.  $T_{45}$ ,  $T_{56}$ ,  $T_{46}$ ,  $T_{67}$ : temperatura media dell'aria da aprile fino a maggio, da maggio fino a giugno, da aprile fino a giugno e da giugno fino a luglio, rispettivamente.*

who reported that the phenophase 'emergence' (C0) of *Triticum aestivum* L. was much less influenced by air temperature than the subsequent phenophases.

## CONCLUSIONS

The most important results of this study can be summed up as follows:

The warmer temperature conditions at the sites of Karditsa, Thives and Araxos promoted the

reproductive growth phenophases of wheat (C1, C2, C3 and C4) compared to the respective ones in Xanthi and Kozani.

The heading was influenced by air temperature in the spring months (April and May) at the coastal sites of Xanthi (Northern Greece) and Araxos (Southern Greece).

Air temperature during April and May plays an important role, to a different degree, in anthesis at the studied sites of the Central (Karditsa) and



Southern (Thives, Araxos) parts of Greece. The fruit development correlated with the air temperature in May and in the April-June period at the continental sites of the Northern (Kozani) and Central (Karditsa) parts of Greece, respectively. This work is one of the first steps of a research concerning the effect of meteorological parameters on the phenological behavior of winter wheat in Greece. In the future, the research will focus on other cultivated plants for better understanding of the interaction between weather and phenology in Greece.

#### ACKNOWLEDGEMENTS

Many thanks are due to the observers of the Hellenic Ministry of Rural Development and Food for their valuable work, to the agronomist L. Katafygiotis of the Agrometeorology Research and Environment Department of the above mentioned Ministry for providing the phenological data and to the Assistant Professor of Statistics of Agricultural University of Athens G. Papadopoulos for his helpful comments.

#### REFERENCES

- Aono Y. and Kazui K., 2008. *Int. J. Climatol.*: 28, 905-914.
- Bonamano A., 2008. An application of agrometeorology: irrigation water management in maize. Ph.D Thesis, University of Padova, Doctorate School in Crop Science, Padova, Italy, p. 122.
- Bindi M. and Moriondo M., 2005. In: C. Giannakopoulos, M. Bindi, M. Moriondo, P. LeSager and T. Tin, Climate change impacts in the Mediterranean resulting from a 2°C global temperature rise. A WWF Report. WWF, Gland, Switzerland: 54-66.
- Chmielewski F.M. and Rötzer T., 2001. *Agric. For. Meteor.*, 108: 101-112.
- Chmielewski F.M., 2003. In: M.D. Schwartz, (Ed.), Phenology: An integrative Environmental Science. Kluwer Academic Publishers, Dordrecht, the Netherlands: 505-522.
- Chmielewski F.M., Müller A. and Bruns E., 2004. *Agric. For. Meteor.*, 121: 69-78.
- Dalezios N.R., Loukas A. and Bampzelis D., *J. Phys.* 2002. *Chem. Earth*, 27: 1019-1023.
- Doi H., 2007. *Clim. Res.*, 34: 99-104.
- Estrella N., Sparks T.H. and Menzel A., 2007. *Glob. Change Biol.*, 13: 1737-1747.
- Ferrara R.M., Trevisiol P., Acutis M., Rana G., Richter G.M. and Baggaley N., 2010. *Theor. Appl. Climatol.*, 99: 53-65.
- Harrison P.A. and Butterfield R.E., 1996. *Clim. Res.*, 7: 225-241.
- Harrison P.A., Porter J.R and Downing T.E., 2000. *Agric. For. Meteor.*, 101: 167-186.
- Hellenic National Meteorological Service (H.N.M.S.), 1999. Climate data of the stations of H.N.M.S., Years 1955-1997. Direction of Climatology, H.N.M.S., Athens, Greece (in Greek): p. 260.
- Hu Q., Weiss A., Feng S. and Baenzinger P.S., 2005. *Agric. For. Meteor.*, 135: 284-290.
- Lithourgidis A.S., Damalas C.A. and A.A. Gagianas, 2006. *Eur. J. Agron.*, 25: 208-214.
- Martin J.H., Warren H.L. and Stamp D.L., 1976. Principles of Field Crop Production, Macmillan Publishing Co., Inc., N.Y., U.S.A.: 1130 pp.
- Meier U., In: M.D. Schwartz, (Ed.), 2003. Phenology: An integrative Environmental Science. Kluwer Academic Publishers, Dordrecht, the Netherlands: 269-283.
- Menzel A., 2003. *Clim. Change*, 57: 243-263.
- Moriondo M. and Bindi M., 2007. *Rivista Italiana di Agrometeorologia*, 12: 5-12.
- Porter J.R. and Gawith M., 1999. *Eur. J. Agron.*, 10: 23-36.
- Pudas E., Leppälä M., Tolvanen A., Poikolainen J., Venäläinen A. and Kubin E., 2008. *Int. J. Biometerol.*, 52: 251-259.
- Rosenzweig C. and Tubiello F.N., 1997. *Clim. Change*, 1: 219-232.
- Sadras V.O. and Monzon J.P., 2006. *Field Crops Res.*, 99: 136-146.
- Schillinger W.F., Shofstall S.E., Alldredge J.R., 2008. *Field Crop Research*, 109: 45-49.
- Schwartz M.D., 2003. In: M.D. Schwartz, (Ed.), Phenology: An integrative Environmental Science. Kluwer Academic Publishers, Dordrecht, the Netherlands: 3-7.
- Sparks T.H., Jeffree E.P. and Jeffree C.E., 2000. *Int. J. Biometerol.*, 44: 82-87.
- Tao F., Yokozawa M., Xu Y., Hayashi Y. and Zhang Z., 2006. *Agric. For. Meteor.*, 138: 82-92.
- Ventura F., Traini S., Gaspari N., and Rossi P., 2006. *Rivista Italiana di Agrometeorologia*, 12: 41-45.
- Wang H.L., Gan H.T., Wang R.Y., Niu J.Y., Zhao H., Yang Q.G. and Li G.C., 2008. *Agric. Forest Meteorol.*, 148: 1242-1251.

